DEVELOPMENT OF SITE SPECIFIC VERTICAL DESIGN SPECTRUM FOR TURKEY

A THESIS SUBMITTED TO
THE GRADUATE SCHOOL OF NATURAL AND APPLIED SCIENCES
OF
MIDDLE EAST TECHNICAL UNIVERSITY

BY

EMRE AKYÜZ

IN PARTIAL FULFILLMENT OF THE REQUIREMENTS
FOR
THE DEGREE OF THE MASTER OF SCIENCE
IN
CIVIL ENGINEERING

JANUARY 2013

Approval of the thesis:

DEVELOPMENT OF SITE SPECIFIC VERTICAL DESIGN SPECTRUM FOR TURKEY

submitted by **EMRE AKYÜZ** in partial fulfillment of the requirements for the degree of **Master of Science in Civil Engineering Department, Middle East Technical University** by,

Prof. Dr. Canan Özgen _____
Dean, Graduate School of **Natural and Applied Science**

Prof. Dr. Ahmet Cevdet Yalçıner _____
Head of Department, **Civil Engineering**

Asst. Prof. Dr. Zeynep Gülerce _____
Supervisor, **Civil Engineering Dept., METU**

Examining Committee Members:

Prof. Dr. Kemal Önder Çetin _____
Civil Engineering Dept., METU

Asst. Prof. Dr. Zeynep Gülerce _____
Civil Engineering Dept., METU

Prof. Dr. Bilge Siyahi _____
Earthquake and Structural Engineering Dept., Gebze Institute of Technology

Assoc. Prof. Dr. Ayşegül Askan Gündoğan _____
Civil Engineering Dept., METU

Inst. Dr. Onur Pekcan _____
Civil Engineering Dept., METU

Date: **28.01.2013**

I hereby declare that all information in this document has been obtained and presented in accordance with academic rules and ethical conduct. I also declare that, as required by these rules and conduct, I have fully cited and referenced all material and results that are not original to this work.

Name, Last name : Emre AKYÜZ

Signature :

ABSTRACT

DEVELOPMENT OF SITE SPECIFIC VERTICAL DESIGN SPECTRUM FOR TURKEY

Akyüz, Emre
M.S., Department of Civil Engineering
Supervisor: Asst. Prof. Dr. Zeynep Gülerce

January 2013, 70 pages

Vertical design spectra may be developed in a probabilistic seismic hazard assessment (PSHA) by computing the hazard using vertical ground motion prediction equations (GMPEs), or using a vertical-to-horizontal spectral acceleration (V/H) ratio GMPEs to scale the horizontal spectrum that was developed using the results of horizontal component PSHA. The objective of this study is to provide GMPEs that are compatible with regional ground motion characteristics to perform both alternatives. GMPEs for the V/H ratio were developed recently by Gülerce and Abrahamson (2011) using NGA-W1 database. A strong motion dataset consistent with the V/H ratio model parameters is developed by including strong motion data from earthquakes occurred in Turkey with at least three recordings per earthquake. The compatibility of GA2011 V/H ratio model with the magnitude, distance, and site amplification scaling of Turkish ground motion dataset is evaluated by using inter-event and intra-event residual plots and necessary coefficients of the model is adjusted to reflect the regional characteristics. Analysis of the model performance in the recent moderate-to-large magnitude earthquakes occurred in Turkey shows that the Turkey-Adjusted GA2011 model is a suitable candidate V/H ratio model for PSHA studies conducted in Turkey. Using the same dataset, a preliminary vertical ground motion prediction equation for Turkey consistent with the preliminary vertical model based on NGA-W1 dataset is developed. Proposed preliminary model is applicable to magnitudes 5-8.5, distances 0-200 km, and spectral periods of 0-10 seconds and offers an up-to-date alternative to the regional vertical GMPEs proposed by Kalkan and Gülkan (2004).

.

Keywords: NGA, GMPE, V/H ratio, Turkish ground motion database, probabilistic seismic hazard assessment, regionalization of global GMPEs, vertical ground motion component.

ÖZ

TÜRKİYE'DE SAHAYA ÖZEL DİKEY TASARIM EĞRİLERİNİN GELİŞTİRİLMESİ

Akyüz, Emre
Yüksek Lisans, İnşaat Mühendisliği Bölümü
Tez Yöneticisi: Yrd. Doç. Dr. Zeynep Gülerce

Ocak 2013, 70 sayfa

Olasılıksal Sismik Tehlike Analizlerinde (OSTA) sahaya özel dikey tasarım spektrumu, dikey yer hareketi tahmin denklemleri yardımıyla ya da OSTA'dan elde edilen yatay yer ivmesi için tasarım spektrumunu dikey – yatay oranı tahmin denklemleri (YHTD) ile orantılayarak bulunabilir. Bu çalışmanın amacı, her iki alternatifi de uygulayabilecek ve bölgesel tektonik karakteristikleri ile uyumlu yer hareketi tahmin denklemlerinin oluşturulmasıdır. Dikey – Yatay (D/Y) spektral ivme oranını veren yer hareketi tahmin modelleri, Gülerce ve Abrahamson (2011) tarafından yeni nesil azalım projesi (NGA-W1) veritabanı kullanılarak üretilmiştir. D/Y oranı model parametreleri ile tutarlı kuvvetli yer hareketi veri seti, Türkiye'de yaşanan ve her deprem için en az üç kayıt alınarak oluşturulan kuvvetli yer hareketi verileri ilave edilerek hazırlanmıştır. GA2011 D/Y oranı tahmin modelinin, Türk kuvvetli yer hareketi veri setindeki deprem büyüklüğü, uzaklık ve zemin büyütmesi ölçeklendirmeleri ile uygunluğu, olay-içi ve olaylar-arası farklılıkları grafikleri ile değerlendirilmiş ve modeldeki gerekli katsayılarda, bölgesel karakteristikleri yansıtması için düzeltmeler yapılmıştır. Yakın zamanda Türkiye'de olmuş orta ve büyük depremlerde uyarlanmış modelin tahmin performansını ölçmek için yapılan analizler, Türkiye'ye uyarlanmış GA2011 modelinin, Türkiye'de yapılacak OSTA çalışmalarında kullanılmaya uygun bir D/Y modeli olduğunu göstermiştir. Aynı veri seti kullanılarak, Türkiye için, NGA-W1 veri setini temel alan öncül dikey model ile tutarlı bir öncül dikey yer hareketi tahmin denklemi de üretilmiştir. Önerilen öncül model, deprem büyüklüğü için 5-8.5, uzaklık için 0-200 km ve 0-10 saniye spectral ivme değer aralıkları için uygulanabilir ve Kalkan ve Gülkan (2004) tarafından önerilen bölgesel dikey YHTD'i için güncel bir alternatif sunmaktadır.

Anahtar Kelimeler: Türk Kuvvetli Yer Hareketi Veritabanı, olasılıksal sismik tehlike analizi, Global YHTD'nin bölgeselleştirilmesi, D/Y oranı, yeni nesil kuvvetli yer hareketi tahmin denklemleri, dikey depremj ivmeleri.

to my beloved wife...

ACKNOWLEDGEMENTS

I would like to express sincere appreciation to my supervisor, Asst. Prof. Dr. Zeynep Gülerce for her guidance, continuous understanding, invaluable patience and support throughout this research. I would also like to thank Dr. Norman Abrahamson, for his invaluable guidance.

I would like to acknowledge my friends R.Soner Ocak, Bahadır Kargıoğlu, Onur Balal, Umut Akın and Okan Bozkurt for their helpful suggestions and encouragements during this study.

Finally, I express my sincere thanks to my family members for their endless supports throughout my life.

TABLE OF CONTENTS

LIST OF TABLES

TABLES

LIST OF FIGURES

FIGURES

LIST OF ABBREVIATIONS

VGM: Vertical Ground Motion
GMPE's: Ground Motion Prediction Equations
PSHA: Probabilistic Seismic Hazard Assesment
V/H: Vertical to Horizontal Ratio
NGA: Next Generation Attenuation Relationships
PGA: Peak Ground Acceleration
PGV: Peak Ground Velocity
PGD: Peak Ground Displacement
SR: Site Response
EC8 : Eurocode 8
TEC2007: Turkish Earthquake Code revised at 2007

CHAPTER 1

INTRODUCTION

On the overall seismic response of structures the influence of the vertical component of an earthquake is usually not considered. After the Northridge Earthquake in 1994, the vertical component was much larger than is usually considered as “normal” and interest in the effects of vertical ground motion increased. Many steel structures suffered a considerable amount of damage during this earthquake and prompted a discussion about whether the large vertical accelerations may have caused the damage.

Several codes like Federal Emergency Management Agency (FEMA), European Building Code (EC8) and Uniform Building Code (UBC), tried to address the effect of vertical earthquake component. Some engineering guidelines in the United States recommend the use of a constant value of vertical to horizontal response ratio over the entire period range of engineering interest which is adopted initially from the study of Newmark and Hall (1978) as V/H=2/3. In 1993, the Commission of the European Communities allowed V/H to vary with period in the European Building Code (EC8). The 1997 Uniform Building Code (UBC-97) recognized the fact that V/H is dependent on source-to-site distance at relatively short distances and recommended using site-specific vertical response spectra for sites located close to active faults; however, neither the UBC-97 nor the 2000 International Building Code (IBC-2000) offers guidance on how a general vertical design spectrum should be developed. Despite the lack of evaluation of vertical motions in the current practice, it is necessary to examine the characteristics of vertical ground motions and their effects on the response of engineering structures. The key question is under what conditions the vertical component need to be considered in structural design of critical structures such as nuclear power plants, highway bridges and dams.

In the probabilistic seismic hazard assessment (PSHA) environment, site-specific vertical design spectra may be developed by computing the hazard independently for the vertical ground motion component, which in fact requires accurate prediction of vertical component ground motion intensity measures. However; new and updated vertical ground motion prediction equations (GMPEs) are not available for Western US or other active tectonic regions like Turkey. Along with the increase in the national strong motion network and acceleometric data after the 1999 Kocaeli and Düzce events, several researchers attempted to develop regional attenuation models of horizontal ground motion component for Turkey (Gülkan and Kalkan 2002, Ulusay et al. 2004, Özbey et al. 2004, Akkar and Cagnan 2010). Only one of these studies, the Gülkan and Kalkan (2004) model, has a consistent set of empirical attenuation relationships for predicting the vertical component and the V/H ratio. Kalkan and Gülkan (2004) developed their V/H ratio and vertical model based on the directly calculated vertical ground motion predictions and V/H ratios from 100 ground motions recorded during 47 events occurred in Turkey between years 1976 and 2002. Even after the comprehensive efforts on compiling the Turkish Strong Motion Database (details will be provided in the next Chapter), Kalkan and Gülkan (2004) model was not updated by its developers or any alternative regional vertical and V/H ratio model were not proposed for Turkey.

1.1 Research Statement

The objective of this study is to evaluate the conditions that lead to the vertical component to have a significant effect on the response of critical structures by evaluating the compatibility of preliminary vertical ground motion equation developed by Yılmaz (2008) and V/H ratio prediction equation developed by Gülerce and Abrahamson (2011) with Turkish strong ground motions using the comparison dataset of Gülerce et al. (2013) and to offer an up-to-date alternative to the Vertical ground motion prediction equation model and V/H ratio model proposed by Kalkan and Gülkan (2004).

Implementation of global GMPEs, especially the NGA-W1 models developed mainly for California in the other shallow crustal and active tectonic regions is a topic of ongoing discussion (e.g. Stafford et al. 2008 and Scasserra et al. 2009). Gülerce et al. (2013) modified and used the recently developed Turkish Strong Motion Database (TSMD, Akkar et al., 2010) to check the compatibility of the magnitude, distance, and site amplification scaling of NGA-W1 vertical to horizontal ratio prediction models with the ground motions recorded in Turkey and adjusted necessary coefficients of these models to reflect the regional characteristics for the PSHA applications in Turkey. The preferred methodology for evaluating the differences between the model predictions and actual data is the analysis of model residuals. Using the random-effects regression with a constant term, model residuals between the actual strong motion data and NGA-W1 vertical to horizontal ratio (V/H ratio) model predictions are calculated for each recording in the comparison dataset. Plots of the residuals are used to evaluate the differences in the magnitude, distance, and site amplification scaling between the Turkish data set and the NGA-W1 V/H ratio models. Analysis results showed that model residuals relative to distance and magnitude measures plots suggest no trend but the GA2011 model slightly miscalculates the ground motions in the Turkey comparison dataset at stiff soil/engineering rock sites (where Vs30 > 550 m/s). The misfit between the actual data and model predictions are corrected with adjustments functions.

In addition to the regionalized V/H ratio model, a preliminary vertical ground motion prediction equation for Turkey consistent with the preliminary vertical model based on NGA-W1 dataset developed by Yılmaz (2008) is developed. Same dataset used for regionalized V/H ratio model utilized; however the magnitudes are tentatively restricted to Mw ≥ 5.0 to emphasize the ground motions of engineering interests for the vertical ground motion component. Nonlinear site effects were not observed in the NGA-W1 vertical ground motion dataset (Yılmaz, 2008); therefore only linear site amplification is included for this preliminary effort. The standard deviation is magnitude dependent with smaller magnitudes leading to larger standard deviations. Within the contents of this chapter, the functional form of the attenuation model and the regression analysis are described in parallel to preliminary vertical model based on NGA-W1 dataset developed by Yılmaz (2008). Median predictions of the current model are compared the predictions of the only regional vertical model available, Kalkan and Gulkan (2004), in this chapter.

Finally, the vertical design spectra constructed by the models proposed in Chapter 3 and Chapter 4 is compared. To develop the TR-Adjusted vertical curves, the Adjusted V/H median predictions are multiplied by the median predictions of equally weighted TR-Adjusted horizontal NGA-W1 models (Gulerce et al., 2013)

1.2 Scope

The scope of this thesis can be summarized as follows;

In the first chapter general information about the concepts reviewed in this study are reviewed. Research statement and the scope of this study is presented.

In Chapter 2, the previous vertical ground motion prediction modeling efforts in global and regional scale are reviewed in terms of datasets, functional forms and validity range.

In Chapter 3, regionalization of the NGA-W1 Vertical to Horizontal Spectral Acceleration Ratio prediction equations is presented. Also, a comprehensive summary of the dataset used for evaluating the adjusted model introduced. In addition a test case, including recent events in 2010 and 2011, for adjusting models is presented.

In Chapter 4, the preliminary regional vertical ground motion prediction equations for Turkey are presented by checking the compatibility of magnitude scaling, distance scaling and site effects scaling by using the Turkish strong motion comparison dataset.

In Chapter 5 the thesis is enclosed by presenting the final forms of the Regional vertical ground motion prediction equations for Turkey and Turkey-Adjusted V/H GMPEs model and comparing them in terms of different scenarios.

CHAPTER 2

GLOBAL AND REGIONAL PREDICTIVE MODELS FOR THE VERTICAL GROUND MOTION COMPONENT

Vertical ground motions are considered in the seismic design of critical structures such as nuclear power plants and dams. Results of a recent study revealed that the effect of vertical component ground motion on seismic response of ordinary highway bridges is also significant, especially in the near-fault regions (Gülerce et al., 2012; Gülerce and Abrahamson, 2010). In the probabilistic seismic hazard assessment (PSHA) environment, site-specific vertical design spectra may be developed by computing the hazard independently for the vertical ground motion component, which in fact requires accurate prediction of vertical component ground motion intensity measures. However; new and updated vertical ground motion prediction equations (GMPEs) are not available for Western US or other active tectonic regions like Turkey. Within the contents of this chapter, fundamental background on the datasets and functional forms of early-stage global vertical GMPEs is provided. Only one vertical model, Yılmaz (2008), which provides a basis for the proposed vertical GMPE will be elaborately discussed in Chapter 4.

Conducting separate vertical and horizontal component PSHAs may lead to inconsistent horizontal and vertical spectra due to the different distance and magnitude scaling and different standard deviation values of vertical GMPEs compared to horizontal GMPEs. The alternative approach is to use empirical vertical-to-horizontal spectral acceleration ratio (V/H ratio) prediction models to scale the horizontal spectrum that was developed using the results of horizontal component PSHA. Recent empirical V/H ratio predictive models in the literature are summarized in the second part of this chapter.

Finally, regional attenuation models for the vertical component and V/H ratio developed by Kalkan and Gülkan (2004) will be presented.

2.1 Early-Stage Global GMPEs for the Vertical Ground Motion Component

Although a large number of researchers have developed GMPEs for the horizontal ground motion component, vertical component equations have not been included except for a few cases: Abrahamson and Silva (1997), Campbell (1997), Ambraseys and Douglas (2003), Bozorgnia and Campbell (2004), and Ambraseys et al. (2005). The recently developed PEER NGA models (Abrahamson and Silva, 2008; Boore and Atkinson, 2008; Campbell and Bozorgnia, 2008; Chiou and Youngs 2008; and Idriss 2008) provide improved horizontal GMPEs that include recent large magnitude earthquakes, but new GMPEs for the vertical components of the NGA models are currently not available.

Abrahamson and Silva (1997) used 655 recordings obtained from 58 earthquakes occurred mainly in Western US. Moment magnitude and closest distance to the rupture (Rrup) were used in the basic model for strike-slip earthquakes. To characterize the site effects, Geomatrix site class definitions were modified and reduced it into 2 different site categories: rock site and deep soil site. Random effects model proposed by Abrahamson and Youngs

(1992) was employed in regression. In addition to the basic model (f1 in Equation 2.1), style-of-faulting, hanging wall and site response effects were included using dummy variables as:

$$\ln \mathrm{Sa} = \mathrm{f}_1 + \mathrm{F}\,\mathrm{f}_3 + \mathrm{HW} * \mathrm{f}_{\mathrm{HW}}(\mathrm{M}) * \mathrm{f}_{\mathrm{HW}}\left(\mathrm{R}_{\mathrm{rup}}\right) + \mathrm{S}\,\mathrm{f}_5 \qquad 2.1$$

where Sa is spectral acceleration, M is moment magnitude, $\mathrm{R}_{\mathrm{rup}}$ is rupture distance, F is style of faulting, HW is dummy for hanging wall site, S is dummy for site class, f_1 is the basic functional form of attenuation relation, $\mathrm{f}_3 \mathrm{and}\ \mathrm{f}_5$ represent the functional form for style of faulting and site effects, $\mathrm{f}_{\mathrm{HW}}(\mathrm{M})$ and $\mathrm{f}_{\mathrm{HW}}\left(\mathrm{R}_{\mathrm{rup}}\right)$ are the models to account for the systematic increase in the ground motions recorded over the hanging wall.

Campbell and Bozorgnia (2003) updated the **Campbell (1997)** model using 960 unprocessed recordings obtained from 49 earthquakes and 443 processed recordings obtained from 36 earthquakes. Four different categories were used for local site classification: firm soil, very firm soil, soft rock and firm rock. Moment magnitude (Mw) was used for defining the size of earthquake and shortest distance between the station and zone of seismogenic energy release (R_{seis}) was used for defining source-to-site distance. Recordings were included in the database only if their R_{seis} was less than 60 km to avoid the complications related to arrival of multiple reflections from lower crust. Non-linear least squares method was used to determine the coefficients of the equation. Similar to horizontal ground motion, vertical ground motion is given as;

$$\ln \mathrm{Y} = \mathrm{c}_1 + \mathrm{f}_1(\mathrm{M_w}) + \mathrm{c}_4 \ln\sqrt{\mathrm{f}_2(\mathrm{M_w}, \mathrm{r_{seis}}, \mathrm{S}} + \mathrm{f}_3(\mathrm{F}) + \mathrm{f}_4(\mathrm{S}) + \mathrm{f}_5(\mathrm{HW}, \mathrm{F}, \mathrm{M_w}, \mathrm{r_{seis}}) \qquad 2.2$$

where Y is vertical spectral acceleration, $\mathrm{M_w}$ is moment magnitude, $\mathrm{r_{seis}}$ is the closest distance to seismogenic rupture in kilometers, F is dummy term for faulting style, S is dummy term for local site conditions, c_1 and c_4 are regression coefficients, f_1 is functional form defining magnitude scaling, f_2 is functional form for source to site distance effects, f_3 is functional form for faulting style, f_4 is functional form for local site effects and f_5 is functional form for hanging wall effects. The hanging wall model of this model was adopted from Abrahamson and Silva (1997) model with a few modifications.

Ambraseys and Douglas (2003) developed both vertical and horizontal predictive models using a worldwide dataset of 186 strong-motion records. Later in 2005, these models were updated by **Ambraseys et al. (2005)** using a larger dataset. Dataset of Ambraseys et al. (2005) was composed of 595 strong-motion records from 135 earthquakes occurred in Europe and the Middle East. The majority of records come from four countries: Italy, 174 (29%), Turkey, 128 (22%), Greece, 112 (19%) and Iceland, 69 (12%). The relatively strict criteria adopted in this study limited the number of ground motions included although the total number of recordings from earthquakes with Ms >4 from Europe and the Middle East has more than doubled in the last ten years (Ambraseys et al., 2005). Additionally, there are few records available at long periods due to filtering applied; therefore they limited the regression analysis at 2.5s spectral period. To determine the coefficients of equation they used a two-step regression analysis. Firstly, the regression analysis was performed with all terms included some coefficients were significantly different than zero at certain periods. In order to improve the accuracy of those terms, the analysis was repeated constraining the non-significant terms to zero. Final adopted functional form was:

$$\ln \mathrm{Y} = \mathrm{a}_1 + \mathrm{a}_2(\mathrm{M_w}) + \left(\mathrm{a}_3 + \mathrm{a}_4(\mathrm{M_w})\right)\log\sqrt{d^2 + {\mathrm{a}_5}^2} + \mathrm{a}_6\mathrm{S_S} + \mathrm{a}_7\mathrm{S_A} + \mathrm{a}_8\mathrm{F_N} + \mathrm{a}_9\mathrm{F_T} + \mathrm{a}_{10}\mathrm{F_O} \qquad 2.3$$

where S_S =1 for soft soil sites and 0 otherwise, S_A =1 for stiff soil sites and 0 otherwise, F_N =1 for normal faulting earthquakes and 0 otherwise, F_T =1 for thrust faulting earthquakes and 0 otherwise and F_O =1 for odd faulting earthquakes and 0 otherwise.

Figure 2.1 shows the vertical response spectra from all four relations (Campbell and Bozorgnia (2004), Abrahamson and Silva (1997), Campbell (1997) and Sadigh et al. (1997)) for a magnitude 7 earthquake within 10 km from the rupture for generic soil and generic rock site conditions. For generic soil conditions, the results from all three relations are similar except for the period shift of Abrahamson and Silva (1997) curve. The differences in generic rock spectra from different relations may be a result of differences in the datasets and the definitions of engineering rock of each study.

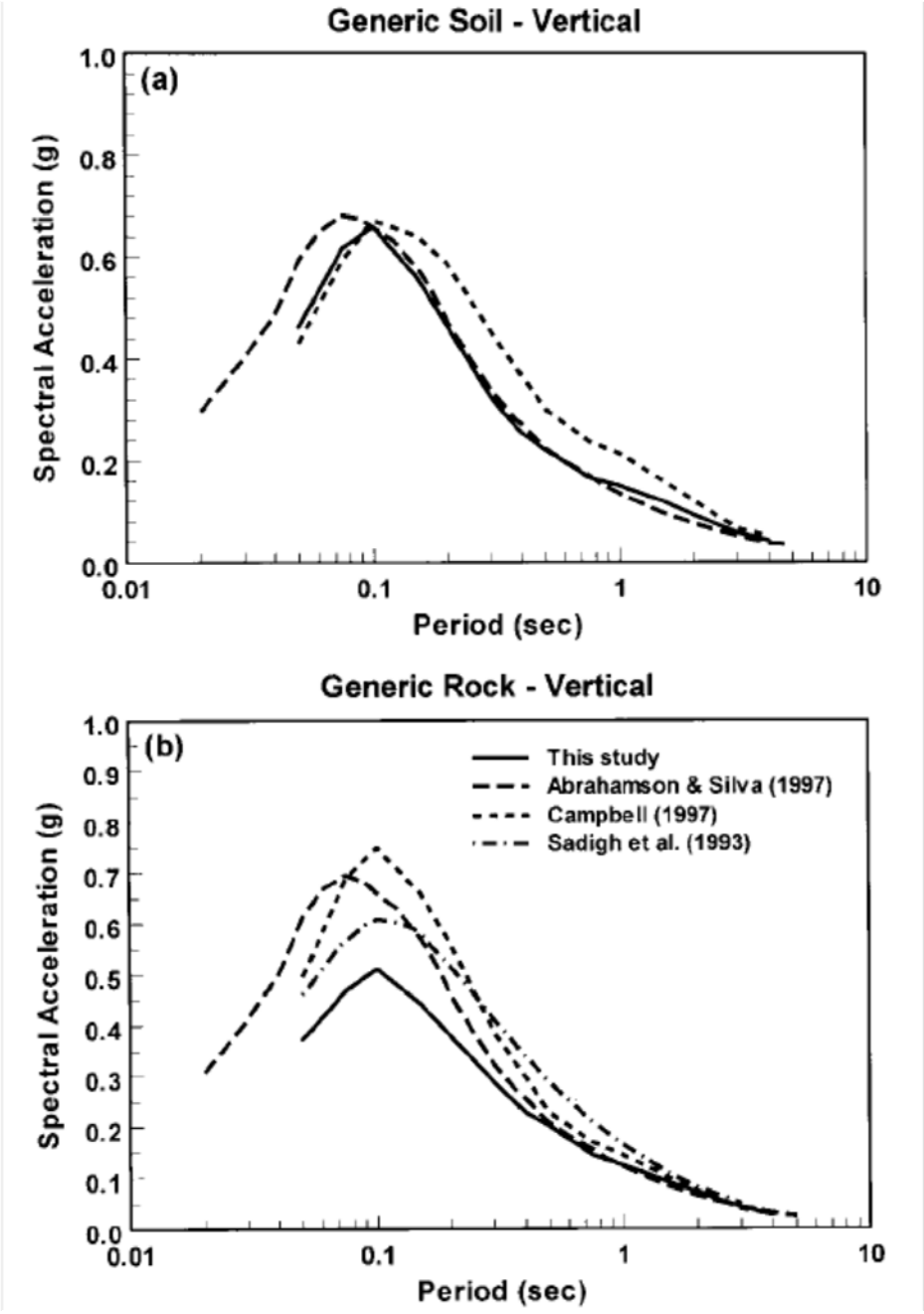

Figure 2.1 Comparison of predicted PSA (5%damping) from the vertical ground motion relations mentioned above for: (a) generic soil, (b) generic rock (After Campbell and Bozorgnia, 2003).

2.2 Global GMPEs for the V/H Ratio

Empirical V/H ratio predictive models may be built by developing separate vertical and horizontal GMPEs and then computing the ratio for a given magnitude and distance. In their studies, both **Campbell and Bozorgnia (2003) and Bindi et al. (2009)** used this approach on different sets of ground motion data. Database of Campbell and Bozorgnia (2003) model includes 1380 recordings from 80 earthquakes that were mainly occurred in California with a moment magnitude range of 4.7 to 7.7. Bindi et al. (2009) used the Italian Acceleometric Archive (ITACA) database, which is composed of 107 earthquakes occurred in Italy from year 1972 to 2007 with magnitudes 4.0 to 6.9. Both site conditions and style of faulting effects are represented by dummy variables in Campbell and Bozorgnia (2003) and Bindi et al. (2009) models. Magnitude and distance scaling of the models are also quite similar ensuing consistent results in the range of applicability of the models.

In their recent studies, **Bommer et al. (2011), Edwards et al. (2011), and Gülerce and Abrahamson (2011)** used datasets consist of the directly calculated V/H ratios of ground motions to develop the prediction equations. The datasets used by the authors, functional forms and range of applicability of each model is considerably different. Database of Bommer et al. (2011) model includes 1267 ground motions from 392 earthquakes occurred in Europe and surrounding regions with the magnitude range of 4.5 to 7.6 and Joyner-Boore distances up to 100 km. Edwards et al. (2011) combined two datasets; small magnitude data from Switzerland was enriched with moderate-to-large magnitude data from Japan, therefore the model covers a large magnitude range from magnitude 2 to 7.3. Gülerce and Abrahamson (2011) used the horizontal-component PEER-NGA-W1 dataset of Abrahamson and Silva (2008) horizontal model with small changes due to exclusion of recordings with missing vertical components. The dataset consists of 2,636 recordings from 126 shallow crustal earthquakes from active tectonic regions around the world. The magnitude range of the events is $4.3 \leq Mw \leq 7.9$ with rupture distances up to 200 km.

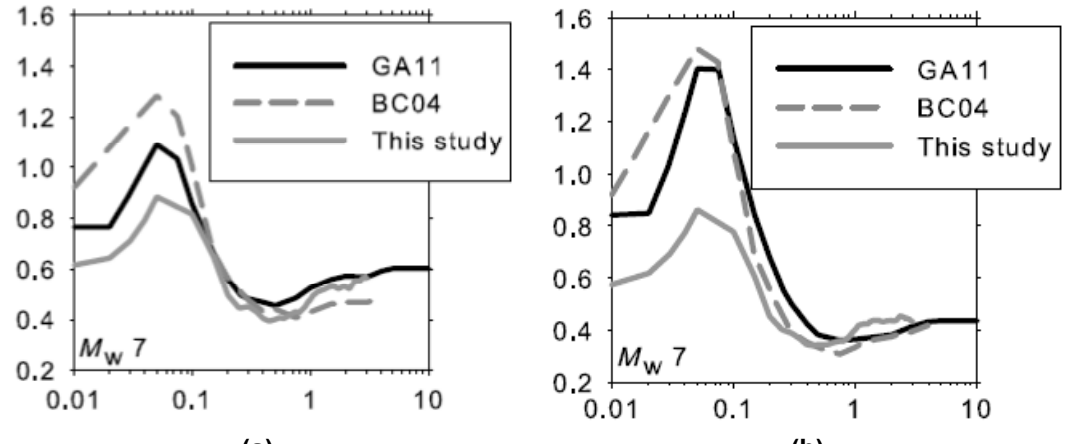

Figure 2.2 Comparison of the median predictions of V/H ratio models for a strike slip earthquake with M_w=7, R_{rup}=10 for: (a) generic soil, (b) generic rock (After Bommer et al., 2011)

Edwards et al. (2011) modeled the V/H ratio at rock with a single site parameter sites independent of the earthquake magnitude, the average quarter-wavelength velocity, but the

residuals of the model were corrected by a distance term for short distances. Bommer et al. (2011) and Gulerce and Abrahamson (2011) models define the V/H ratios as function of magnitude, distance and dummy style-of-faulting variables (reverse, normal, strike-slip) with different functional forms. However, the main divergence of the models lays in the definition of the site response effects. While Bommer et al. (2011) model used dummy variables for site class (rock, stiff soil, soft soil); Gulerce and Abrahamson (2011) classified the sites as a continuous function of VS30 and included the soil non-linearity, which leads to higher V/H ratios then the other two models at soft soil sites as shown in Figure 2.2.

2.3 Turkish Practice for Vertical Component

Along with the increase in the national strong motion network and acceleometric data after the 1999 Kocaeli and Düzce events, several researchers attempted to develop regional attenuation models of horizontal ground motion component for Turkey (Gülkan and Kalkan 2002, Ulusay et al. 2004, Özbey et al. 2004, Akkar and Cagnan 2010). Only one of these studies, the Gülkan and Kalkan (2002) model, has a consistent set of empirical attenuation relationships for predicting the vertical component and the V/H ratio (Kalkan and Gülkan 2004). Kalkan and Gülkan (2004) developed their V/H ratio model based on the directly calculated V/H ratios from 100 ground motions recorded during 47 events obtained from 65 permanent stations occurred in Turkey between years 1976 and 2002. Table 2.1 shows earthquakes and number of recordings used in their analysis. Their dataset consisted of 33 strike-slip, 12 normal, and 2 reverse-fault mechanism earthquakes with 27 rock, 26 soil, and 47 soft-soil ground motion measurements.

Kalkan and Gülkan (2004) limited the number of recordings included to the closer distances to minimize the complex propagation effects for longer distances. Particularly, based on the USGS, PEER, and COSMOS broadcasted information some correction and fine-tuning were done on the distance and local-site condition parameters of the Kocaeli and Düzce events. For the source distance (r_{cl}), they have adopted the closest horizontal distance (or Joyner and Boore distance) between the recording station and a point on the horizontal projection of the rupture. The magnitudes were restricted to about M_W>4.5. Only Burdur earthquake, the 3 April 2002, M_W=4.2, was not subjected to that limitation because of its high vertical acceleration (31 mg) recorded. The epicenters of earthquakes and recording locations were marked in Figure 2.3 along with active faults.

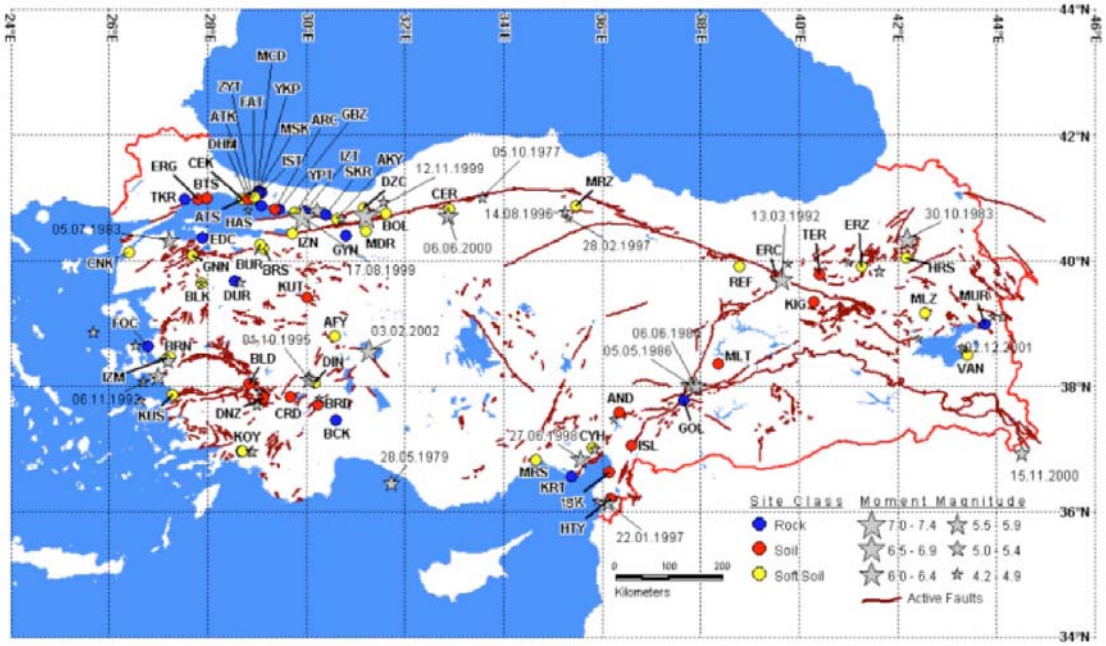

Figure 2.3 Epicenters of earthquakes and locations of strong motion recording stations on active faulting map of Turkey (After Kalkan and Gulkan, 2004).

Table 2.1 Earthquakes and number of recordings in Kalkan and Gulkan (2004) dataset

Event No	Date (dd.mm.yy)	Event	Faulting Type *	M_W	Depth (km) *	Epicenter Coordinates *	Number of Recordings Rock	Soil	Soft Soil
1	19.08.1976	DENİZLİ	Normal	5.3	20.0	37.7100N - 29.0000E		1	
2	05.10.1977	ÇERKEŞ	Strike-Slip	5.4	10.0	41.0200N - 33.5700E			1
3	16.12.1977	İZMİR	Normal	5.5	24.0	38.4100N - 27.1900E			1
4	11.04.1979	MURADİYE	Strike-Slip	4.9	44.0	39.1200N - 43.9100E	1		
5	28.05.1979	BUCAK	Normal	5.8	111.0	36.4600N - 31.7200E	1		
6	18.07.1979	DURSUNBEY	Strike-Slip	5.3	7.0	39.6600N - 28.6500E	1		
7	30.06.1981	HATAY	Strike-Slip	4.7	63.0	36.1700N - 35.8900E		1	
8	05.07.1983	BİGA	Reverse	6.1	7.0	40.3300N - 27.2100E	2		1
9	30.10.1983	HORASAN-NARMAN	Strike-Slip	6.5	16.0	40.3500N - 42.1800E			2
10	29.03.1984	BALİKESİR	Strike-Slip	4.5	0.0	39.6400N - 27.8700E			1
11	17.06.1984	FOÇA	Normal	5.0	0.0	38.8700N - 25.6800E	1		
12	12.08.1985	KİĞI	Strike-Slip	4.9	29.0	39.9500N - 39.7700E		1	
13	06.12.1985	KÖYCEĞİZ	Strike-Slip	4.6	0.0	36.9700N - 28.8500E			1
14	05.05.1986	MALATYA	Strike-Slip	6.0	4.0	38.0200N - 37.7900E	1		
15	06.06.1986	SÜRGÜ (MALATYA)	Strike-Slip	6.0	11.0	38.0100N - 37.9100E	1	1	
16	20.04.1988	MURADİYE	Strike-Slip	5.0	55.0	39.1100N - 44.1200E	1		
17	12.02.1991	İSTANBUL	Strike-Slip	4.8	10.0	40.8000N - 28.8200E	1		
18	13.03.1992	ERZİNCAN	Strike-Slip	6.9	27.0	39.7200N - 39.6300E		1	1
19	06.11.1992	SİVRİHİSAR	Normal	6.1	17.0	38.1600N - 26.9900E			1
20	03.01.1994	ISLAHİYE	Strike-Slip	5.0	26.0	37.0000N - 35.8400E		1	
21	24.05.1994	GİRİT	Normal	5.0	17.0	38.6600N - 26.5400E	1		
22	13.11.1994	KÖYCEĞİZ	Strike-Slip	5.2	10.0	36.9700N - 28.8090E			1
23	29.01.1995	TERCAN	Strike-Slip	4.8	31.0	39.9008N - 40.9900E		1	
24	26.02.1995	VAN	Strike-Slip	4.7	N/A	38.6000N - 43.3300E			1
25	01.10.1995	DİNAR	Normal	6.4	5.0	38.1100N - 30.0500E		1	1
26	02.04.1996	KUŞADASI	Normal	4.9	33.0	37.7800N - 26.6400E			1
27	14.08.1996	MERZİFON	Strike-Slip	5.4	10.0	40.7900N - 35.2300E			1
28	21.01.1997	BULDAN	Normal	4.8	9.0	38.1200N - 28.9200E		1	
29	22.01.1997	HATAY	Strike-Slip	5.5	23.0	36.1400N - 36.1200E		2	
30	28.02.1997	MERZİFON	Strike-Slip	4.7	5.0	40.6800N - 35.3000E			1
31	03.11.1997	MALAZGİRT	Strike-Slip	4.9	N/A	38.7600N - 42.4000E			1
32	04.04.1998	DİNAR	Normal	4.6	7.0	38.1400N - 30.0400E		1	1
33	27.06.1998	ADANA-CEYHAN	Strike-Slip	6.3	18.0	36.8500N - 35.5500E	1	3	2
34	09.07.1998	BORNOVA	Normal	5.1	21.0	38.0800N - 26.6800E			1
35	17.08.1999	KOCAELİ	Strike-Slip	7.4	18.0	40.7000N - 29.9100E	9	6	11
36	11.11.1999	SAPANCA-ADAPAZARI	Strike-Slip	5.7	8.9	40.8100N - 30.2000E	1		
37	12.11.1999	DÜZCE	Strike-Slip	7.2	10.0	40.7400N - 31.2100E	4	1	7
38	06.06.2000	ÇANKIRI-ORTA	Strike-Slip	6.1	10.0	40.7200N - 32.8700E			1
39	23.08.2000	HENDEK-AKYAZI	Strike-Slip	5.1	15.3	40.6800N - 30.7100E	1		3
40	04.10.2000	DENİZLİ	Normal	4.7	8.4	37.9100N - 29.0400E		1	
41	15.11.2000	TATVAN-VAN	Strike-Slip	5.5	10.0	36.9300N - 44.5100E			1
42	10.07.2001	ERZURUM-PASİNLER	Strike-Slip	5.4	5.0	39.8273N - 41.6200E			1
43	26.08.2001	YIĞILCA-DÜZCE	Strike-Slip	5.4	7.8	40.9455N - 31.5728E			1
44	02.12.2001	VAN	Strike-Slip	4.5	5.0	38.6170N - 43.2940E			1
45	03.02.2002	SULTANDAĞI-ÇAY	Reverse	6.5	5.0	38.5733N - 31.2715E		1	1
46	03.04.2002	BURDUR	Strike-Slip	4.2	5.0	37.8128N - 30.2572E		1	
47	14.12.2002	ANDIRIN-K. MARAŞ	Strike-Slip	4.8	13.6	37.4720N - 36.2210E		1	
						Total	27	26	47

Functional form of Kalkan and Gülkan (2004) vertical model were developed from the general form of the equation proposed by Spudich et al. (1999). The general form of the equation is:

$$\ln \mathrm{Yv} = \mathrm{C}_1 + \mathrm{C}_2(\mathrm{M}-6) + \mathrm{C}_3(\mathrm{M}-6)^2 + \mathrm{C}_4(\mathrm{M}-6)^3 + \mathrm{C}_5 \ln r + \mathrm{C}_6\Gamma_1 + \mathrm{C}_7\Gamma_2 + \mathrm{P}\sigma \qquad 2.4$$

$$\mathrm{r} = \sqrt{h^2 + \mathrm{r_{cl}}^2} \qquad 2.5$$

where Y_V is the vertical ground motion parameter (vertical PGA in g), M is the moment magnitude, r_{cl} is the Joyner-Boore distance from the station to a site of interest in km, and C_1, C_2 , C_3 , C_4 , C_5 , and h are the regression parameters used in two-stage multivariate nonlinear regression. C_6 and C_7 are soil and soft-soil amplification parameters with respect to rock. In this equation, h is a fictitious depth, and Γ is an index variable controlling the local geological conditions. For rock sites Γ_1=Γ_2=0; for soil sites Γ_1=1 and Γ_2= 0; for soft soil sites Γ_1= 0 and Γ_2=1. The additional cubical term for magnitude was introduced in equation 2.4 to

compensate for the controversial effects of sparsity of the Turkish earthquakes, and consequently resulted in a better fit to the actual data. In this equation, distance term shows the geometrical attenuation, whereas the terms of magnitude and site conditions represent an elastic attenuation. The standard deviation of $\ln Y_V$ is s, and the P takes a value of 0 for mean values and 1 for 84-percentile of $\ln Y_V$.

Considerable exploratory analyses for obtaining simultaneously the best estimates and least standard error justified the use of two-stage multivariate nonlinear regression analysis for determining the coefficients in the median attenuation equation via decoupling the site effects from magnitude and distance dependence. Thus the entire data was regressed in the first stage disregarding the local-site effects, yielding the parameters C_1 to C_5 and h. In this stage, magnitude and distance are the only independent parameters. Local-site effects were determined in the next stage, thereby constraining the initially estimated parameters (C_1 to C_5 and h). Thereafter, the rock data was first regressed to update the value of offset factor C_1 using a transferring parameter C_8. Then the soil amplification factors, C_6 and C_7, were derived by performing separate regression analyses on soil and soft soil data constraining the aforementioned parameters and using updated C_1 (Kalkan and Gülkan, 2004).

A consistent set of equations for predicting the V/H spectral ratios for Turkey was developed by Kalkan and Gulkan (2004) utilizing the same data set. The general form of the equation is:

$$\mathrm{SAv}/\mathrm{SAh} = \mathrm{C}_1 + \mathrm{C}_2(\mathrm{M}) + \mathrm{C}_3 r_{\mathrm{cl}} + \mathrm{C}_4\Gamma_1 + \mathrm{C}_5\Gamma_2 + \mathrm{P}\sigma \qquad 2.6$$

where *M* is the moment magnitude, *rcl* is the closest horizontal distance (or Joyner-Boore distance) from the station to a site of interest in km, and *C*1 , *C*2 , and *C*3 are the regression parameters. *C*4 and *C*5 are soil and soft soil amplification (or de-amplification) parameters with respect to rock. Γ is an index variable controlling the local-site effects. For rock sites $\Gamma_1=\Gamma_2=0$; for soil sites $\Gamma_1=1$ and $\Gamma_2= 0$; for soft soil sites $\Gamma_1= 0$ and $\Gamma_2=1$.The standard deviation of *R* is σ, and the *P* takes a value of 0 for mean values and 1 for 84-percentile of *R*.

Even after the comprehensive efforts on compiling the Turkish Strong Motion Database (details will be provided in the next section), Kalkan and Gülkan (2004) model was not updated by its developers or any alternative regional V/H ratio or vertical model was proposed for Turkey.

CHAPTER 3

REGIONALIZATION OF THE NGA-W1 VERTICAL TO HORIZONTAL SPECTRAL ACCELERATION RATIO PREDICTION EQUATIONS

Implementation of global GMPEs, especially the NGA-W1 models developed mainly for California in the other shallow crustal and active tectonic regions is a topic of ongoing discussion (e.g. Stafford et al. 2008 and Scasserra et al. 2009). Gülerce et al. (2013) modified and used the recently developed Turkish Strong Motion Database (TSMD, Akkar et al., 2010) to check the compatibility of the magnitude, distance, and site amplification scaling of NGA-W1 horizontal prediction models with the ground motions recorded in Turkey and adjusted necessary coefficients of these models to reflect the regional characteristics for the PSHA applications in Turkey. Analysis results showed that the horizontal NGA-W1 models over predict the ground motions from the earthquakes occurred in Turkey, especially the small magnitude events recorded on stiff soil-rock sites, suggesting the possibility of similar trends in NGA-W1 V/H ratio predictive models.

One of the objectives of this study is to evaluate the compatibility of Gülerce and Abrahamson (2011) (this model is denoted by GA2011 from now on) model predictions with Turkish strong ground motions using the comparison dataset of Gülerce et al. (2013) and to offer an up-to-date alternative to the regional V/H ratio model proposed by Kalkan and Gülkan (2004). A brief summary of the Gülerce et al. (2013) dataset is provided in the following section with the emphasis on V/H spectral acceleration ratios. Evaluation of the model residuals and the adjustments made on the original model are presented in the subsequent sections. Turkey-Adjusted GA2011 model predictions are compared to the original GA2011, Kalkan and Gülkan (2004) and Bommer et al. (2011) model predictions for different scenarios. Finally, the performance of the Turkey-Adjusted GA2011 predictions in recent large magnitude events occurred in Turkey (2010 Elazığ and 2011 Van Earthquakes) is evaluated. This study complements the findings of Gülerce et al. (2013) on NGA-W1 horizontal GMPEs and these two studies will collectively provide an insight on application of NGA-W1 models in PSHA studies performed in other active and shallow crustal tectonic regions.

3.1 Summary of the Comparison Dataset

Strong motion data recorded by the Turkish national strong motion network had been compiled and processed together with detailed geophysical and geotechnical site measurements for recording stations by Akkar et al. (2010). The Turkish strong motion database (TSMD) including 4067 sets of recordings from 2996 events occurred between years 1976-2007 is disseminated through the Web at http://daphne.deprem.gov.tr. Gülerce et al. (2013) used TSMD as a starting point for the regionalization of global NGA-W1 models for Turkey. A comprehensive review of the changes on the initial TSMD, efforts on estimating the missing parameters required for comparison with the NGA-W1 predictive models, calculation of the orientation-independent intensity measures and final comparison dataset can be found in Gülerce et al. (2013), but a brief summary is given below:

- Only 173 earthquakes (approximately 6% of the total number of recorded events) were magnitude 5 or bigger and during these events 685 recordings were taken. To preserve all valuable data, all of these recordings were added to the comparison dataset.

- The recordings from small magnitude (M_w<5) events were included in the comparison dataset only if 3 or more recordings were available in the database.
- The moment magnitude values for 119 of earthquakes were not available, so they were estimated from local magnitude (M_L) using recently proposed magnitude conversion relationships by Akkar et al. (2010).
- No site information (V_{s30} or any site classification) could be found for 431 of remaining recordings. The V_{S30} values of 49 recordings were estimated from the NGA-W1 dataset and rest of the recordings were removed. In Figure 3.1(a), number of recordings with estimated and measured (taken from TSDM database) V_{S30} in each NEHRP site class is presented. The number of recordings from stations with estimated V_{S30} is quite small (10%) within the whole set.
- The style of faulting for 47 events was estimated using the mechanisms of other earthquakes in the sequence or the dominant mechanism of the region.
- 118 records with rupture distance (R_{RUP}) or Joyner-Boore distance (R_{JB}) larger than 200 km were discarded from the dataset. Source-to-site distance metrics for 96 records were missing. Fortunately, these ground motions were recorded during small magnitude earthquakes, therefore the R_{RUP} and R_{JB} were estimated from the hypocentral distance and epicentral distance, respectively. Distribution of recordings with respect to R_{JB} is shown in Figure 3.1(b).
- Majority of the recordings in the remaining dataset were processed by Akkar et al., (2010). With the intention of preserving as much data as possible to obtain a representative dataset, 284 unfiltered recordings were included to the database along with processed data. The number of filtered and unfiltered recordings in each magnitude range is presented in Figure 3.1(c).
- The waveform data of all remaining ground motions were checked for data quality and 37 unfiltered recordings were eliminated from the dataset due to spike, insufficient digitizer resolution, multi-event or S-wave trigger problems. A sample waveform from the discarded recordings with North - South, East –West and Vertical ground motion components is shown in Figure 3.2.
- Final dataset used in the comparison includes 1142 recordings from 288 events with the earthquake metadata (moment magnitude, style of faulting, rake and dip angles, etc.), distance metrics for the recordings (R_{RUP} and R_{JB}), V_{s30} values for the recording stations, horizontal component spectral values in terms on GMRotI50, vertical spectral accelerations and V/H ratios for 22 spectral periods (0.01, 0.02, 0.03, 0.04, 0.05, 0.075, 0.10, 0.15, 0.20, 0.25, 0.30, 0.40, 0.50, 0.75, 1.0, 1.5, 2.0, 3.0, 4.0, 5.0, 7.5, 10.0 seconds).

GA2011 model is based on the NGA-W1 project database, in which the strong ground motions from the earthquakes occurred in Turkey was poorly represented. Table 3.1 shows that only 19 recordings, mostly from two major earthquakes occurred in 1999 (Kocaeli and Düzce Earthquakes), were included in the GA2011 dataset. Consistency of the V/H ratios in the comparison dataset and NGA-W1 database is evaluated in Figure 3.3 for mutual recordings from these events available in both datasets. Figure 3.3 implies that the distance measures of the mutual recordings are generally consistent in both datasets; however some discrepancies may occur in the spectral values due to different filtering procedures employed.

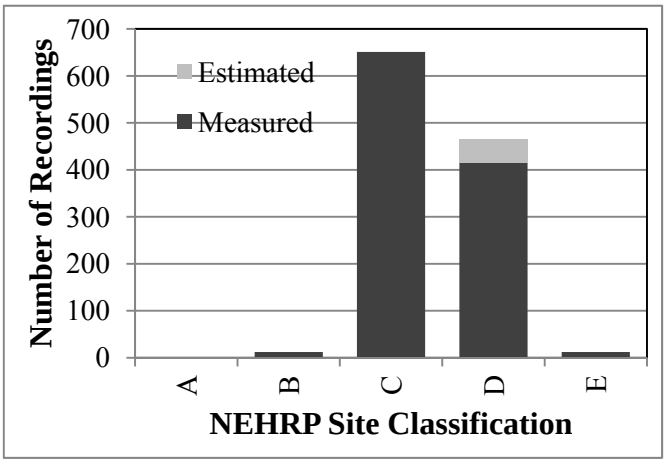

(a)

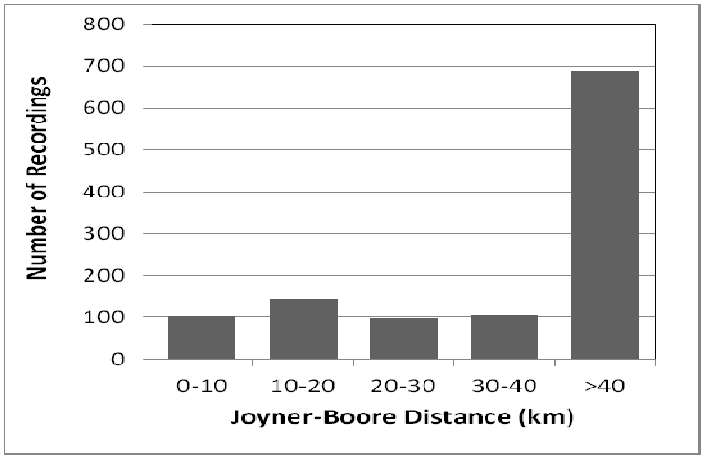

(b)

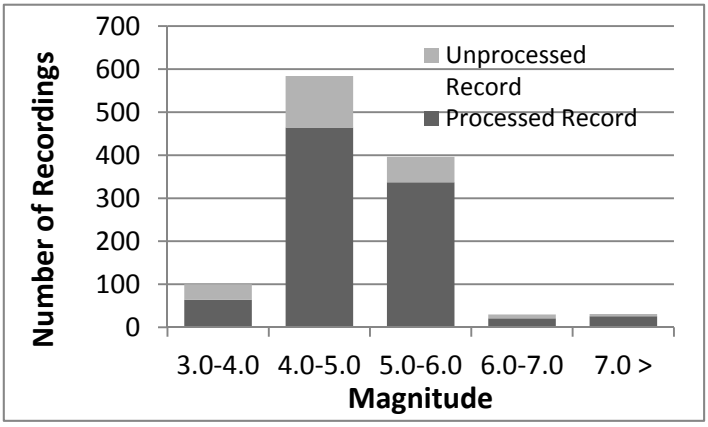

(c)

Figure 3.1 Distribution of the recordings in the comparison dataset with respect to (a) NEHRP site classification, (b) Joyner-Boore distance, and (c) magnitude.

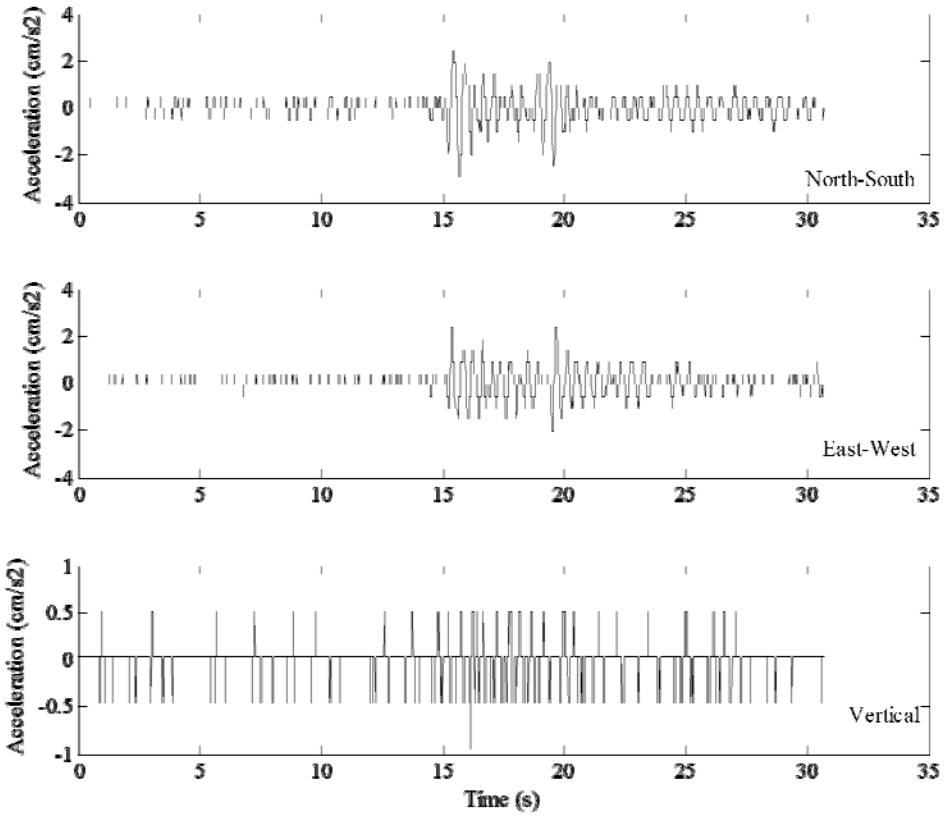

Figure 3.2 A sample record with (NS, EW and vertical components) that was discarded due to low digitizer resolution (record name: 19981008204912_ 2401).

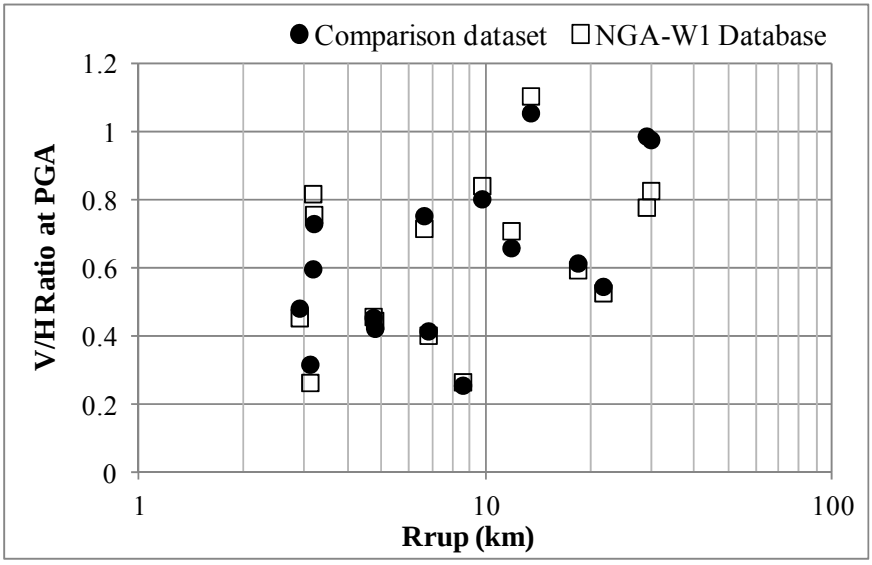

Figure 3.3 V/H ratio values at PGA and rupture distances of the mutual recordings from 1999 Kocaeli and Düzce Earthquakes in the comparison dataset and NGA-W1 database.

Table 3.1 Ground motions recorded from the earthquakes occurred in Turkey in the GA2011 model dataset.

Year-Event	NGA-W1 Database Record ID	TSMD Record ID	M_w	R_{RUP} (km)	V_{S30} (m/s)
1995 - Dinar	1141	120	6.4	2.89	198.1
1995 - Dinar	1137	117	6.4	28.97	334.6
1999 - Kocaeli	1162	1107	7.51	29.82	347.7
1999 - Kocaeli	1165	1110	7.51	6.61	826.1
1999 - Kocaeli	1161	1106	7.51	13.42	701.1
1999 - Kocaeli	1158	1104	7.51	11.79	282
1999 – Kocaeli	1171	1112	7.51	7.08	412
1999 - Düzce	1611	1581	7.14	3.18	719.3
1999 - Düzce	1617	1594	7.14	3.1	481.3
1999 - Düzce	1618	1595	7.14	4.72	448.2
1999 - Düzce	1612	1585	7.14	3.16	439.5
1999 - Düzce	1615	1584	7.14	4.77	316
1999 - Düzce	1614	1591	7.14	6.8	455.7
1999 - Düzce	1616	1582	7.14	18.36	454.8
1999 - Düzce	1613	1580	7.14	21.71	616.4
1999 - Düzce	1605	1583	7.14	9.71	282
1999 - Düzce	1602	1578	7.14	8.55	293.6

3.2 Evaluation of Model Residuals

The preferred methodology for evaluating the misfit between the model predictions and actual ground motion data is the analysis of model residuals. The actual V/H ratio and GA2011 model prediction for each recording (i) from each event (j) at each period (k) are denoted by a_{ijk} and p_{ijk}, respectively. Total model residuals are calculated and separated into three components: the mean offset representing the average bias of the actual data relative to the model predictions (c_k), the event terms (or inter-event residuals, φ_{jk}), and the intra-event residuals (τ_{ijk}) using random effects regression as given in Equation 3.1:

$$R_{ijk} = \ln(a_{ijk}) - \ln(p_{ijk}) = c_k + \phi_{jk} + \tau_{ijk} \quad (3.1)$$

As the first step towards checking the compatibility of GA2011 model predictions with the comparison dataset, total inter-event residuals ($c_k+\varphi_{jk}$) are plotted with respect to moment magnitude for PGA, 0.2 second and 1 second spectral periods as shown in Figure 3.4.

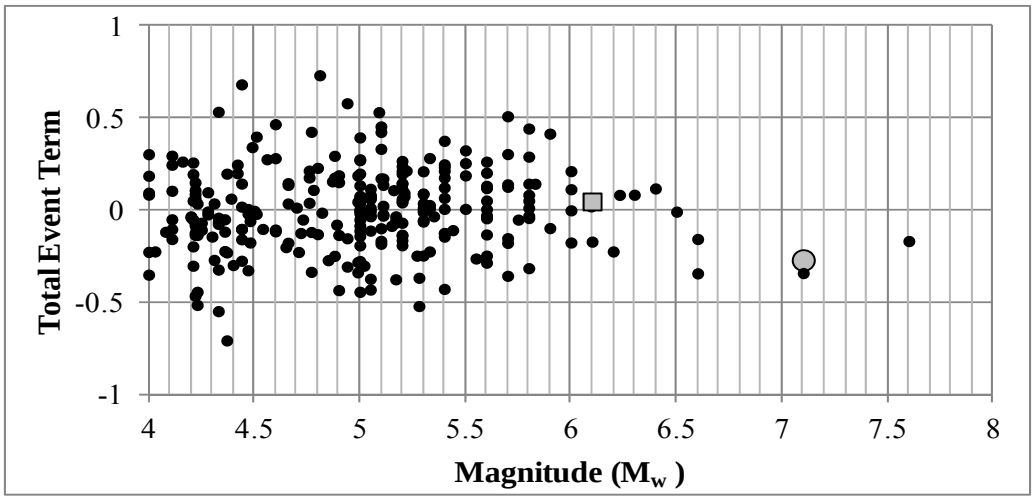

(a)

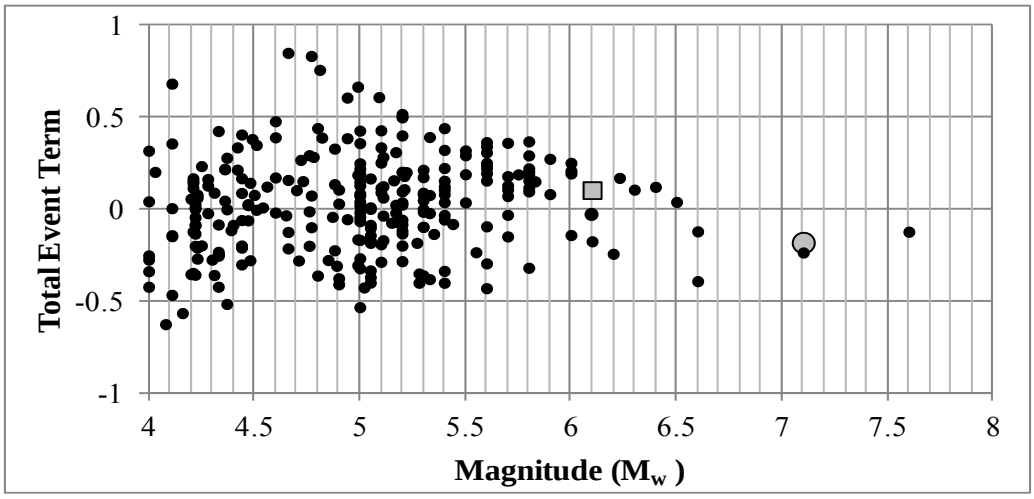

(b)

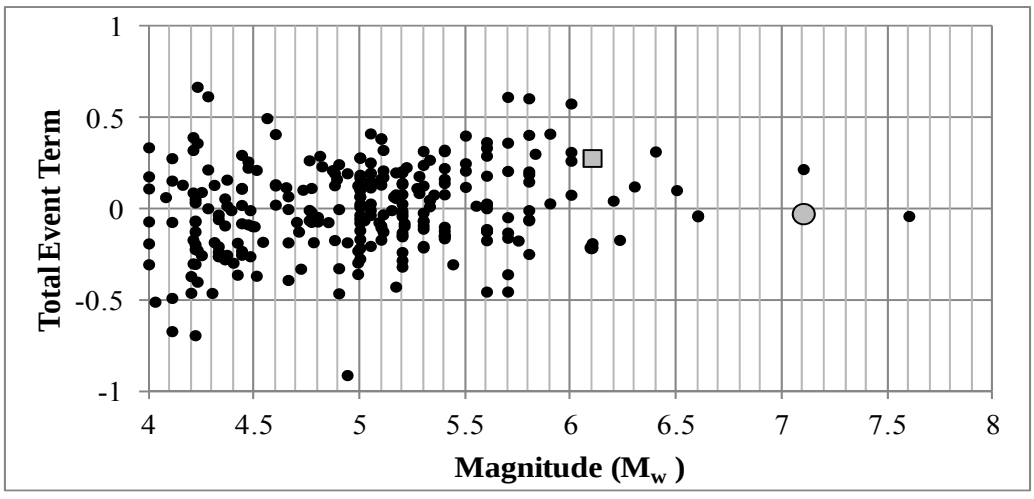

(c)

Figure 3.4. The total inter-event residuals in natural log units with respect to magnitude (Mw) (a) for PGA, (b) for 0.2 second spectral period, and (c) for 1 second spectral period. In each figure gray square represents the event term of 2010 Elazığ Earthquake and gray dot represents the event term of 2011 Van Earthquake.

Figure 3.4(a), Figure 3.4(b), and Figure 3.4(c) show that the total event terms are evenly distributed along the zero-line indicating no bias in the magnitude scaling of the prediction model. NGA-W1 models for the horizontal ground motion component significantly overestimated the ground motions in the same comparison dataset (especially for small-to-moderate magnitudes) and those features of the NGA-W1 models had to be adjusted for the Turkey dataset (Gülerce et al., 2013). However, since the V/H ratio is less dependent on the earthquake magnitude then the horizontal component itself (Edwards et al., 2011), a significant difference in the magnitude scaling of the model and the dataset was not expected for V/H ratio case. A consequence of large overestimation in horizontal component is later observed in the mean offset plot (Figure 3.11) which in terms reflected by an increase in the model predictions of the Turkey-Adjusted GA2011 model when compared to GA2011 model.

Next, the intra-event residuals are plotted with respect to rupture distance in Figure 3.5 for PGA, T=0.2, and T=1 second spectral periods, suggesting no trend within the applicability range of the GA2011 model for tectonic regions other than Western US (up to 100 kilometers where the vertical ground motions are critical for engineering design). Same behavior was observed in the distance scaling of horizontal model by Gülerce et al. (2013). Therefore, the distance scaling of the model does not require any adjustments for the Turkish dataset. The distribution of intra-event residuals with respect to V_{s30} for PGA, 0.2 second and 1 second spectral periods are given in Figure 3.6(a), Figure 3.6(b), and Figure 3.6(c), respectively. It is observed from Figures 3.6(b) and 3.6(c) that the GA2011 model slightly miscalculates the ground motions in the Turkey comparison dataset at stiff soil/engineering rock sites (where V_{s30} > 550 m/s) but this effect diminishes as V_{s30} decreases.

This observation should be expected since approximately 40% of the GA2011 model dataset consist of data from Taiwan (1999 Chi-Chi Earthquake) and the deeper shear wave velocity profiles of the recording stations in Taiwan and Western US were found to be different (Abrahamson, 2012). The trend is visible between 0.4 sec. and 3 sec. spectral period residual plots but weakens for shorter and longer periods. The site amplification scaling of GA2011 model includes both linear (depends on only V_{s30}) and non-linear (depends on V_{s30} and PGA_{1100}) terms as given in Equation 3.2:

$$f_5(P\hat{G}A_{1100}, V^*_{S30}) = a_{10}\ln\left(\frac{V^*_{S30}}{V_{LIN}}\right) - \begin{cases} -b\ln\left(P\hat{G}A_{1100}+c\right)+b\ln\left(P\hat{G}A_{1100}+c\left(\frac{V^*_{S30}}{V_{LIN}}\right)^n\right) & for\, V^*_{S30} < V_{LIN} \\ (bn)\ln\left(\frac{V^*_{S30}}{V_{LIN}}\right) & for\, V^*_{S30} \geq V_{LIN} \end{cases} \quad (3.2)$$

where b, c, and n are the non-linear site amplification coefficients that were constrained outside the regression analysis, V_{LIN} is the period dependent cut-off shear wave velocity above which the site response is linear, and a_{10} is the linear site amplification coefficient. Distribution of intra-event residuals for the ground motions recorded at soft soil sites (V_{s30} < 270 m/s) are evaluated to check the compatibility of the non-linear site amplification term through Figures 3.7(a), 3.7(b) and 3.7(c).

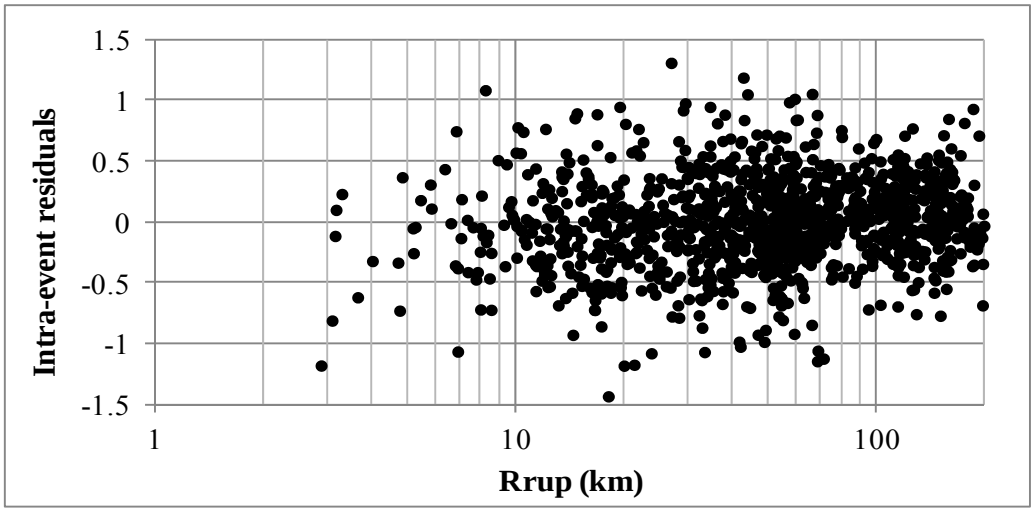

(a)

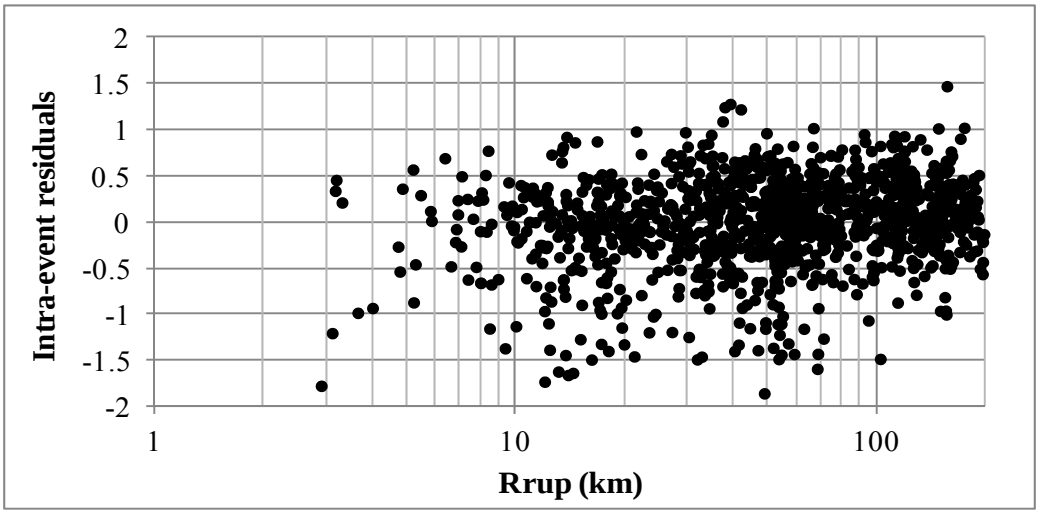

(b)

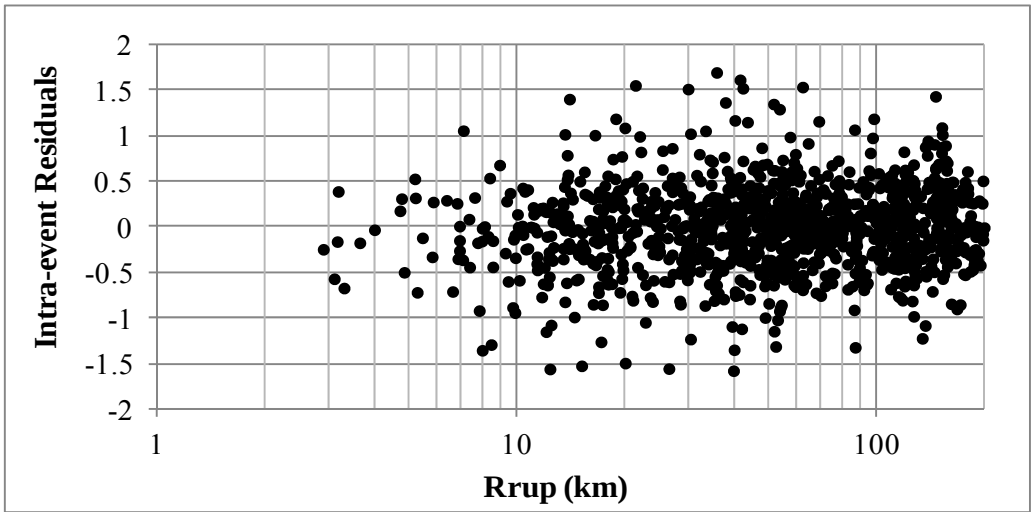

(c)

Figure 3.5. The intra-event residuals in natural log units with respect to rupture distance (a) for PGA, (b) for 0.2 second spectral period, and (c) for 1 second spectral period.

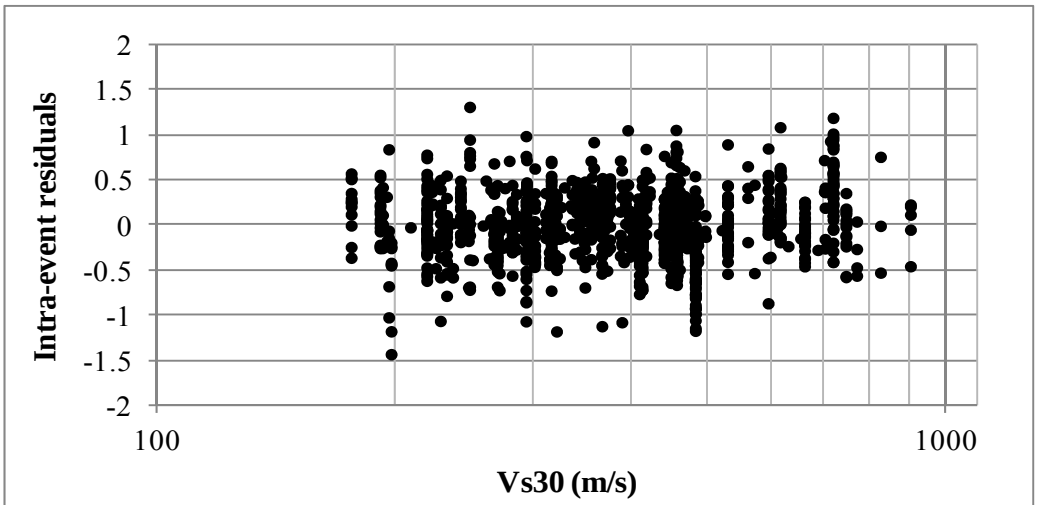

(a)

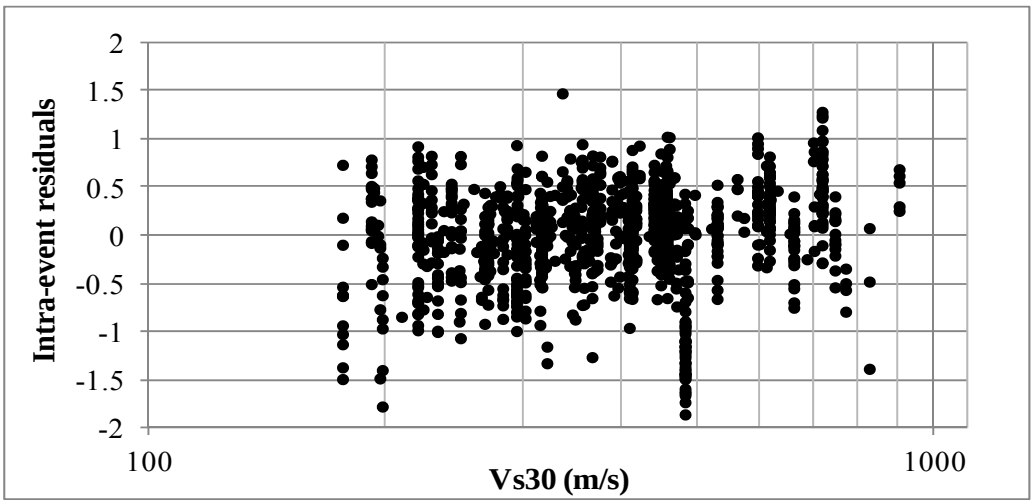

(b)

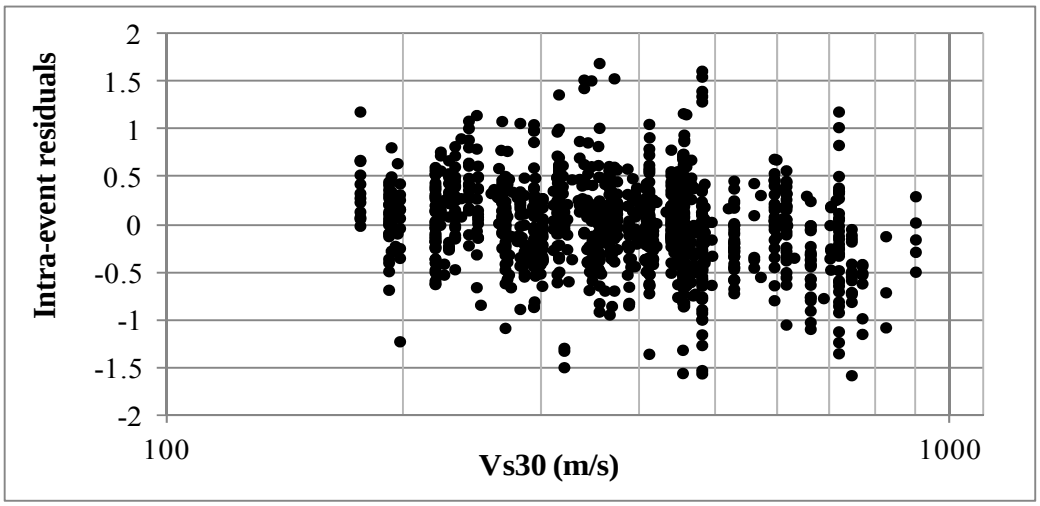

(c)

Figure 3.6. The intra-event residuals in natural log units with respect to Vs30 (a) for PGA, (b) for 0.2 second spectral period, and (c) for 1 second spectral period.

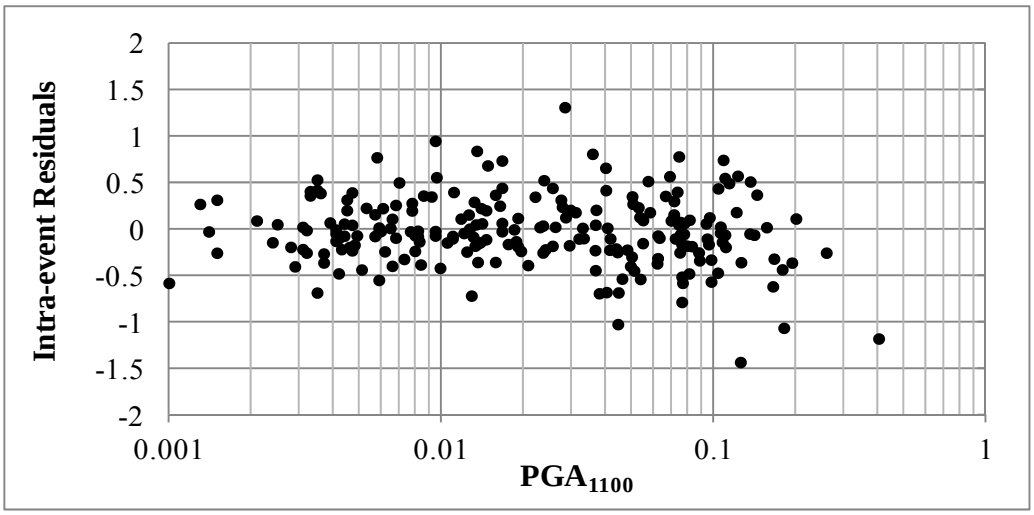

(a)

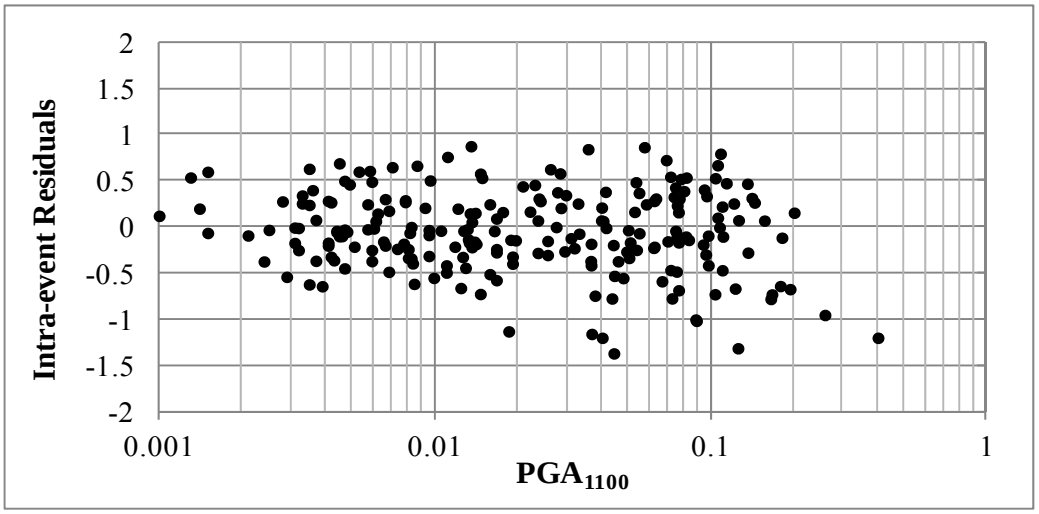

(b)

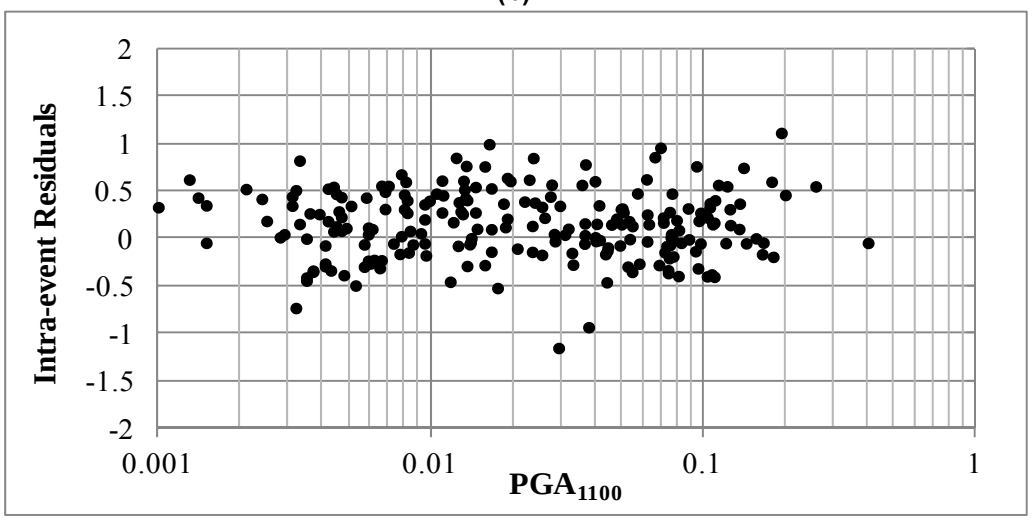

(c)

Figure 3.7. The intra-event residuals of strong motions recorded in soft soil sites (Vs30 < 270 m/s) in natural log units with respect to median PGA1100 (a) for PGA, (b) for 0.2 second spectral period, and (c) for 1 second spectral period.

Figures 3.6 and 3.7 indicate that the incompetency of the model predictions with the comparison dataset mainly depends on the linear site amplification term and may be corrected with an adjustment function:

$$f_{5,TR}(V^*_{S30},T)=\begin{cases}\alpha_{10}(T)\times\ln\left(\frac{V^*_{S30}}{V_{S30,cut-off}(T)}\right)\rightarrow V^*_{S30}>V_{S30,cut-off}(T)\\ 0\rightarrow else\end{cases} \quad (3.3)$$

where $V_{s30,cut\text{-}off}(T)$ is the cut-off shear wave velocity value for a particular period T, below which no trend is observed in the residuals, V_{S30}* is the shear wave velocity value used in GA2011 model and α_{10} is the regression coefficient. For each period, the $V_{s30,cut\text{-}off}(T)$ value is determined statistically as the beginning point of the curvature for the 3rd degree polynomial fit to the residuals (as shown in Figure 3.8). $V_{s30,cut\text{-}off}(T)$ values across the periods are presented in Figure 3.9, along with the V_{LIN} values that represent the end of non-linear site effects in GA2011 model.

These two hinge shear wave velocity values are found to be very close to each other, therefore Equation 3.3 is simplified into Equation 3.4 and site amplification term of the Turkey-Adjusted GA2011 model is defined as given in Equation 3.5:

$$f_{5,TR}(V^*_{S30},T)=\begin{cases}\alpha_{10}(T)\times\ln\left(\frac{V^*_{S30}}{V_{LIN}(T)}\right)\rightarrow V^*_{S30}>V_{V_{LIN}}(T)\\ 0\rightarrow else\end{cases} \quad (3.4)$$

$$f_5(P\hat{G}A_{1100},V^*_{S30})=a_{10}*\ln\left(\frac{V^*_{S30}}{V_{LIN}}\right)-\begin{cases}-b\ln\left(P\hat{G}A_{1100}+c\right)+b\ln\left(P\hat{G}A_{1100}+c\left(\frac{V^*_{S30}}{V_{LIN}}\right)^n\right) & forV^*_{S30}<V_{LIN}\\ (bn)\ln\left(\frac{V^*_{S30}}{V_{LIN}}\right) & forV^*_{S30}\geq V_{LIN}\end{cases} \quad (3.5)$$

where $a_{10}* = a_{10} + \alpha_{10}$. After the adjustment, the intra-event residuals are re-calculated using the modified form of GA2011 model. Intra-event residuals of the modified model are plotted with respect to V_{s30} for PGA, T=0.2, and T=1 second spectral periods in Figure 3.10, indicating that the modified site amplification scaling of the model is now compatible with the comparison dataset.

The mean offset (c_k) values across the periods before and after the V_{s30} adjustment are presented in Figure 3.11. The mean offsets from 0.3 to 2 second spectral periods were improved with the V_{s30} adjustment, however in the small and large frequency bands, mean offsets between ±0.3 natural log units are still observed. As mentioned above, these relatively large mean offsets are a consequence of significant overestimation by the NGA-W1 horizontal models and indicate that a similar but smaller overestimation should be expected in the vertical component. This effect cannot be quantified since the vertical components of the NGA-W1 models are not yet available. Constant term in the base GA2011 model (denoted by a_1) is calibrated using the remaining mean offset values. Figure 3.12 and Figure 3.13 show the distribution of the constant terms, a_1 and a_{10}, across the periods before (a_1, a_{10}) and after calibration (a_1*, a_{10}*), respectively.

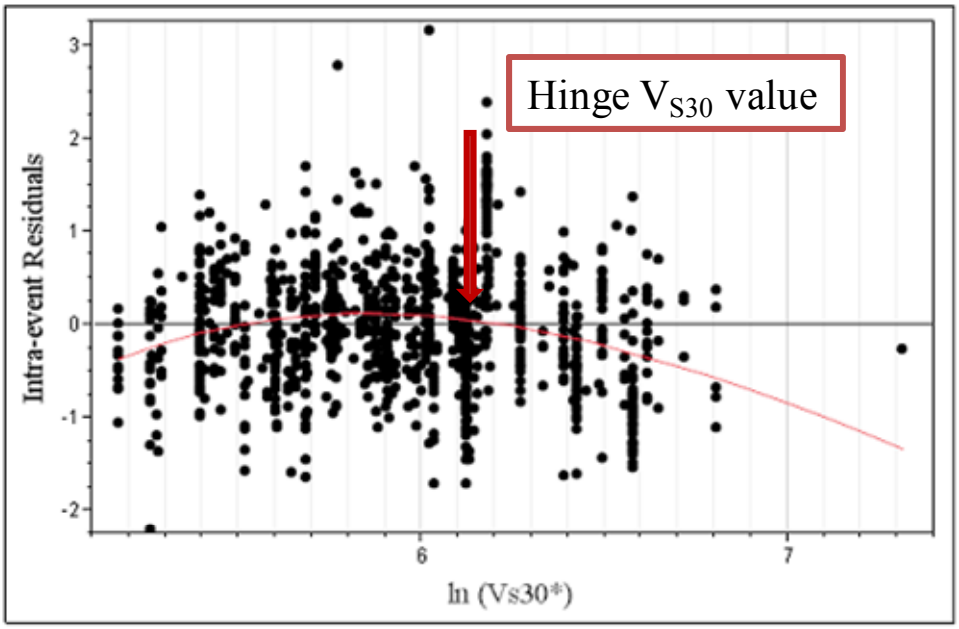

Figure 3.8 Choosing the cut-off shear wave velocity value over which the trend in the intra-event residuals are observed using the 3rd degree polynomial fit to the intra-event residuals.

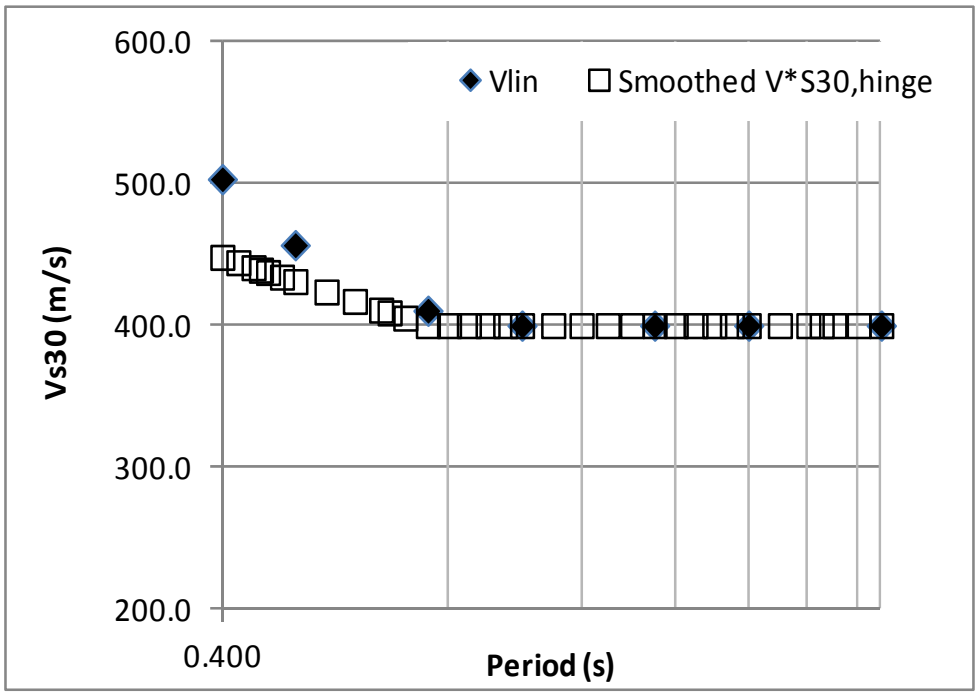

Figure 3.9 The cut-off shear wave velocity value below which no trend is observed in the residuals and V_{LIN} values that represent the end of non-linear site effects in GA2011 model across the periods.

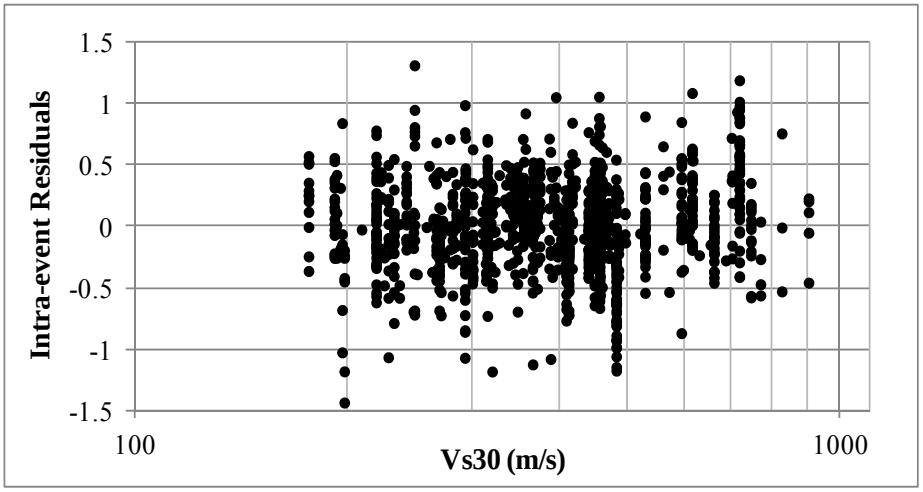

(a)

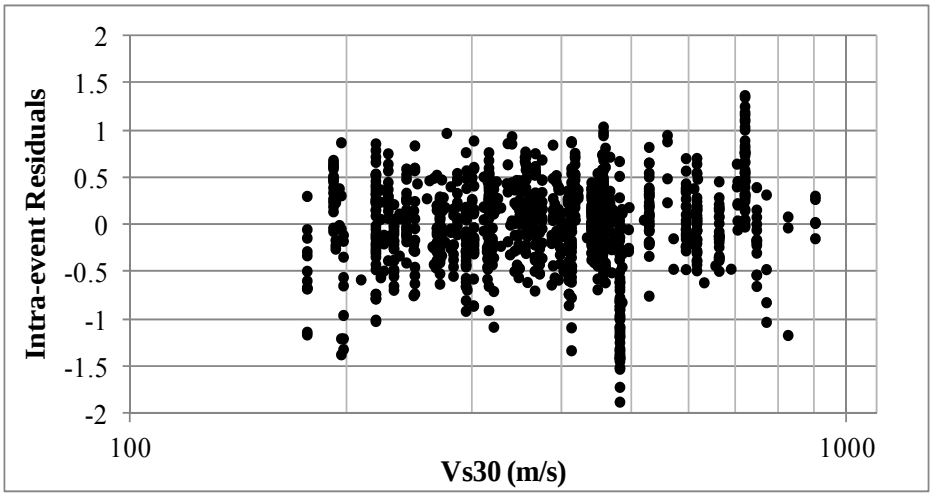

(b)

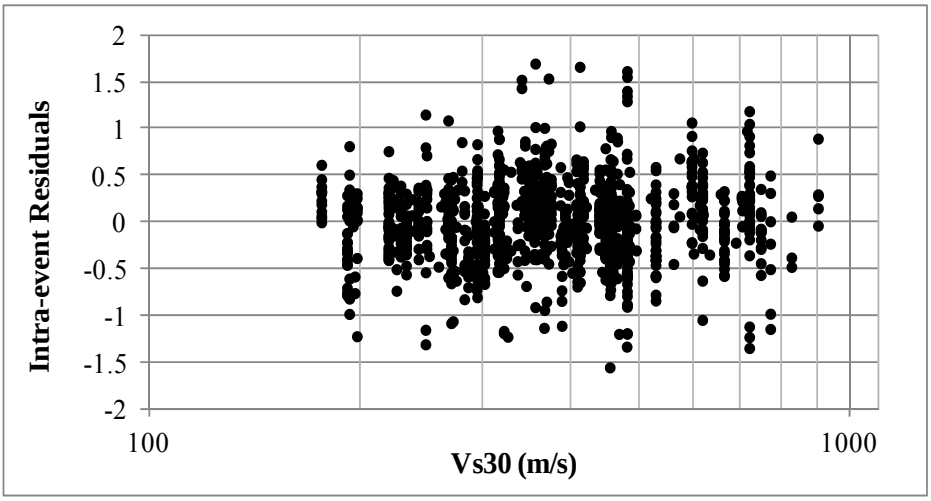

(c)

Figure 3.10 The intra-event residuals in natural log units after the VS30 adjustment with respect to VS30 (a) for PGA, (b) for 0.2 sec spectral period, and (c) for 1 sec spectral period.

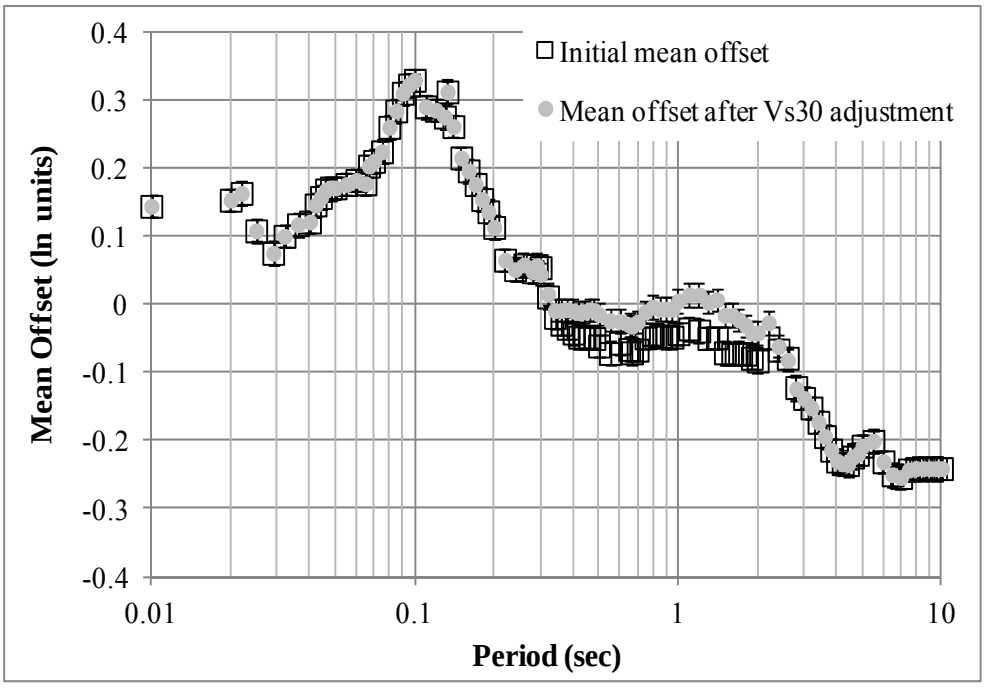

Figure 3.11 The mean offset values across the periods before and after the adjustment of the site amplification scaling of the GA2011 model.

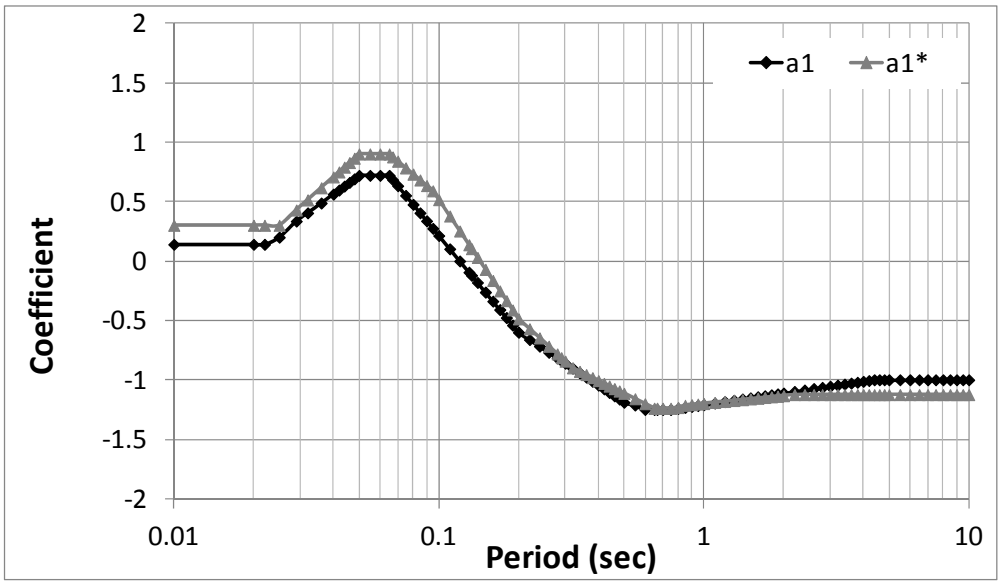

Figure 3.12 The constant a_1 term of the model across the periods before (a_1) and after (a_1*) the adjustment.

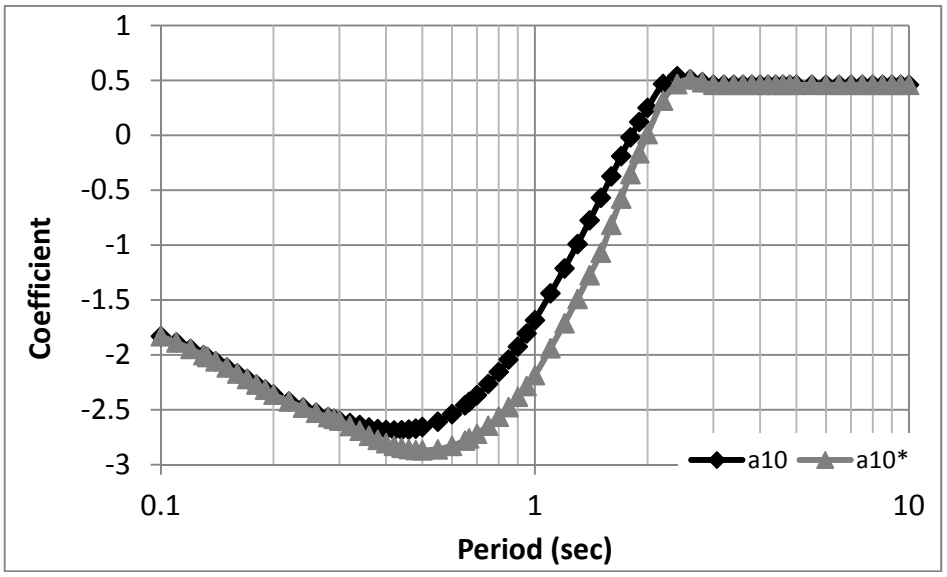

Figure 3.13 The linear site amplification a_{10} term of the model across the periods before (a_{10}) and after (a_{10}*) the adjustment.

New form of the Turkey-Adjusted GA2011 base model is given by Equation 3.6:

$$f_1(M, R_{rup}) = \begin{cases} a_1 * + a_4(M - c_1) + a_8(8.5 - M)^2 + \left[a_2 + a_3(M - c_1)\right]\ln(R) \rightarrow for(M \le c_1) \\ a_1 * + a_5(M - c_1) + a_8(8.5 - M)^2 + \left[a_2 + a_3(M - c_1)\right]\ln(R) \rightarrow for(M > c_1) \end{cases} \quad (3.6)$$

where a_2-a_8 are the coefficients of original GA2011 model and a_1* is the modified constant term. Modified coefficients of the Turkey-Adjusted GA2011 model (a_1* and a_{10}*) are provided in Table 3.2.

Table 3.2 Modified coefficients for the Turkey-Adjusted GA2011 model

Period	a_1*	a_{10}*	Period	a_1*	a_{10}*
0.01	0.300	-1.230	0.75	-1.270	-2.645
0.02	0.300	-1.268	1.0	-1.219	-2.185
0.05	0.900	-1.533	1.5	-1.171	-1.070
0.075	0.787	-1.706	2.0	-1.136	0.012
0.10	0.525	-1.831	2.5	-1.125	0.510
0.15	-0.069	-2.114	3.0	-1.125	0.460
0.20	-0.490	-2.362	4.0	-1.125	0.460
0.26	-0.713	-2.527	5.0	-1.125	0.460
0.30	-0.835	-2.598	6.0	-1.125	0.460
0.40	-1.010	-2.804	7.5	-1.125	0.460
0.50	-1.129	-2.869	10.0	-1.125	0.460
0.60	-1.227	-2.828			

A magnitude-dependent standard deviation model was used for GA2011 model as given in Equations 3.7-3.9:

$$\sigma_0 = \begin{cases} s_1 & for M < 5 \\ s_1 + (\frac{s_2 - s_1}{2})(M - 5) & for\ 5 \le M \le 7 \\ s_2 & for M > 7 \end{cases} \quad (3.7)$$

$$\tau_0 = \begin{cases} s_3 & for M < 5 \\ s_3 + (\frac{s_4 - s_3}{2})(M - 5) & for\ 5 \le M \le 7 \\ s_4 & for M > 7 \end{cases} \quad (3.8)$$

$$\sigma = \sqrt{\sigma_0^{\,2} + \tau_0^{\,2}} \quad (3.9)$$

where s_1 to s_4 are the regression coefficients. The standard deviations of the Turkey-Adjusted GA2011 model predictions are compared with the standard deviation model coefficients of the original GA2011 in Figures 3.14 (a) and 3.14(b). Regressed coefficients of GA 2011 model, s_1 to s_4, are generally well-suited to the standard deviations of the TR-Adjusted model with minor differences observed in s_2 and s_4 at longer periods (larger than 3 seconds). These differences are expected since the number of data points used in the regression decreases significantly after 2.6 seconds due to the usable period range of filtered records in the comparison dataset (Gülerce at al., 2013). NGA-W1 dataset is better constrained in the large magnitude range than the Turkish dataset, therefore standard deviation values of the original model is preserved.

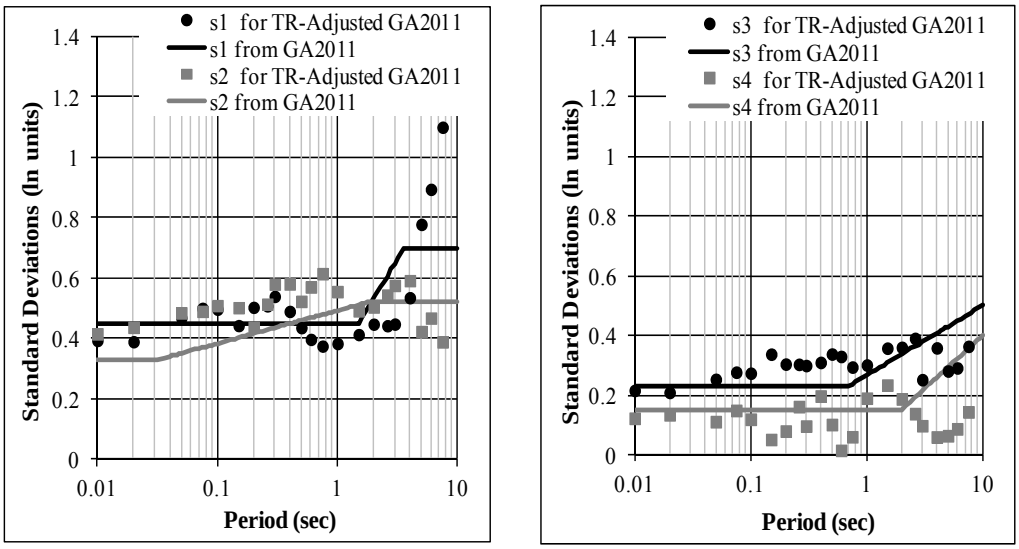

(a) **(b)**

Figure 3.14 The standard deviations of the Turkey-Adjusted GA2011 model predictions (in grey squares and black dots) compared to the standard deviation model coefficients of the original GA2011 model (in gray and black lines). The intra-event standard deviations (σ) are given in Part (a) and the inter-event standard deviations (τ) are given in Part (b).

3.3 Median Predictions of Turkey-Adjusted GA2011 Model

The median response spectra of the TR-Adjusted GA2011 model and the original GA2011 model for magnitudes 5 and 7 for rock and soil sites at the rupture distance of 5 and 30 kilometers are compared through Figures 3.15 and 3.16, respectively.

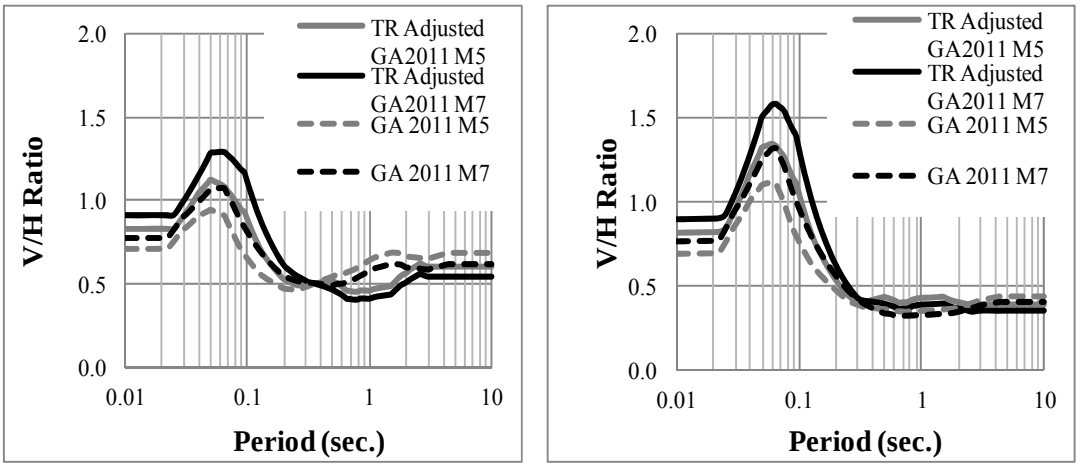

Figure 3.15 Comparison of median spectral acceleration from the proposed model with the median spectral acceleration from the GA2011 model for vertical strike-slip earthquakes for R_{rup}=5 km (a) for rock sites (V_{s30}=760 m/s), and (b) for soil sites (V_{s30}=270 m/s).

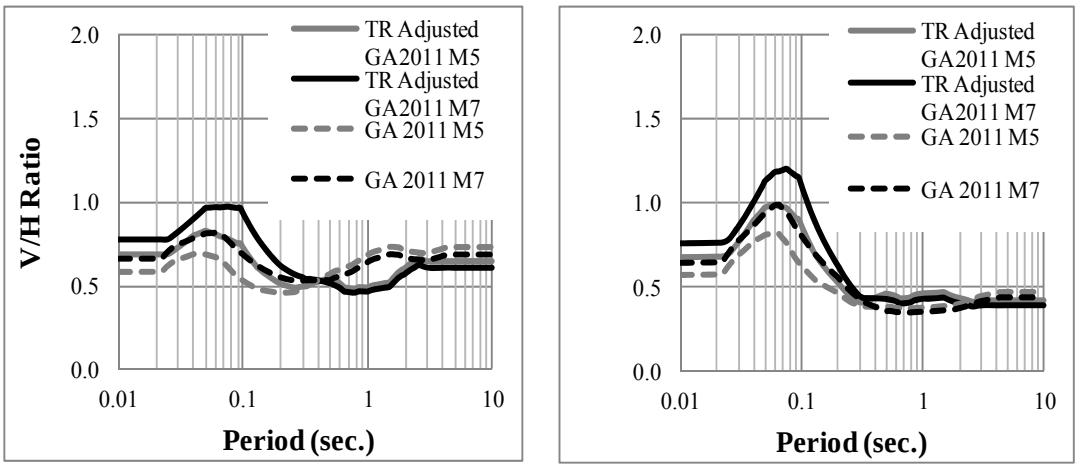

Figure 3.16 Comparison of median spectral acceleration from the proposed model with the median spectral acceleration from the GA2011 model for vertical strike-slip earthquakes for R_{rup}=30 km (a) for rock sites (V_{s30}=760 m/s), and (b) for soil sites (V_{s30}=270 m/s).

The median V/H ratio curves that shown in Figures 3.15 and 3.16 exhibits the well-known shape with a peak near spectral periods of 0.05 seconds and a trough near 0.3 seconds for rock sites and near 1.0 second for soil sites (Gülerce and Abrahamson, 2011). The magnitude dependence of the V/H ratio at short spectral periods is much stronger for soil sites (in Figures 3.15(a) and 3.16(a)) than for rock sites (Figures 3.15(b) and 3.16(b)) due to the non-linear site response for soil sites which leads to additional damping of short-period

horizontal ground motions. Median predictions from the Turkey-Adjusted GA2011 model are higher than the original GA2011 model predictions in the short periods but turn out to be smaller than those in the long period range due to the shape of the mean offset correction in the constant term.

The median response spectra of the TR-Adjusted GA2011 model and the Kalkan and Gülkan (2004) model for the same scenarios are shown in Figures 3.17 and 3.18, respectively. Please note that the period range of the KG2004 model is 0.1-2 seconds therefore this model misses the short-period peak in the V/H ratio. Predictions from both models are similar however; the current model is slightly higher than the KG2004 model in the short period range.

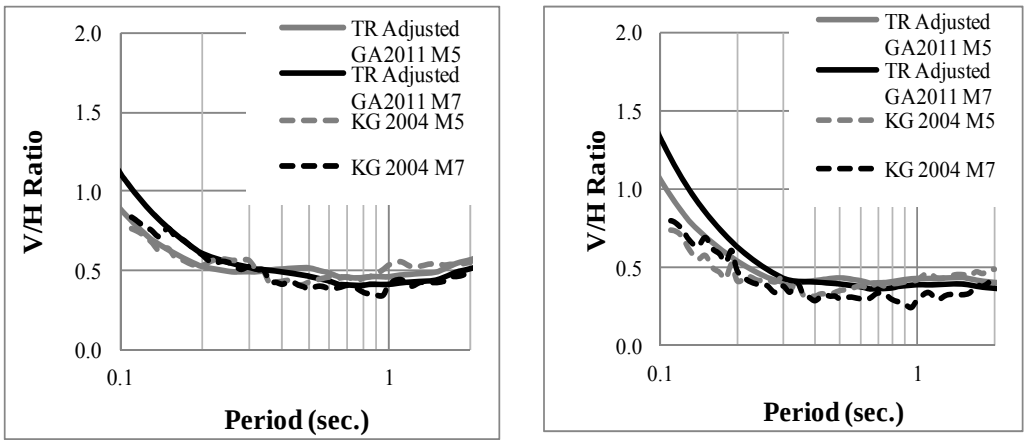

Figure 3.17 Comparison of median spectral acceleration from the proposed model with the median spectral acceleration from the Kalkan and Gülkan (2004) model for vertical strike-slip earthquakes for Mw=7 and Rrup=5 km. (a) for rock, and (b) for soil.

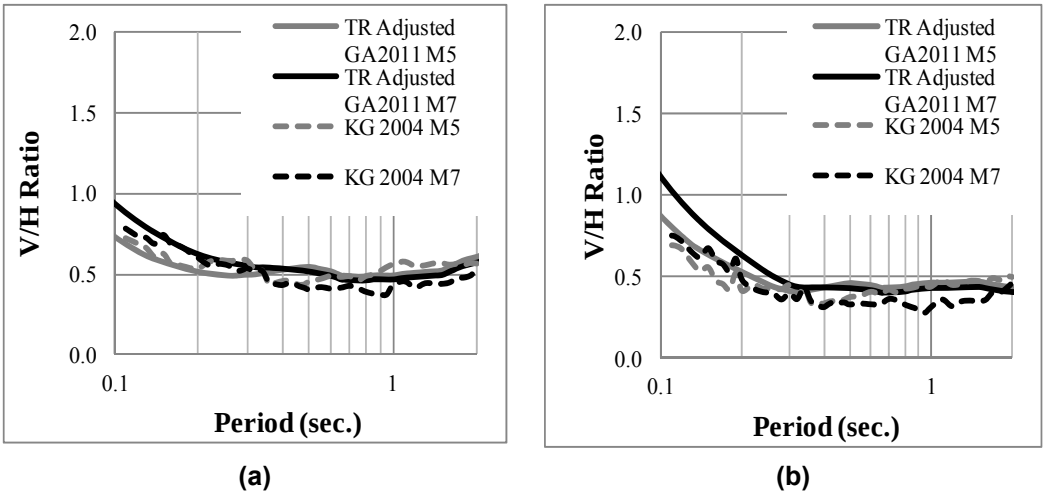

Figure 3.18 Comparison of median spectral acceleration from the proposed model with the median spectral acceleration from the Kalkan and Gülkan (2004) model for vertical strike-slip earthquakes for Mw=7 and Rrup=30 km. (a) for rock, and (b) for soil.

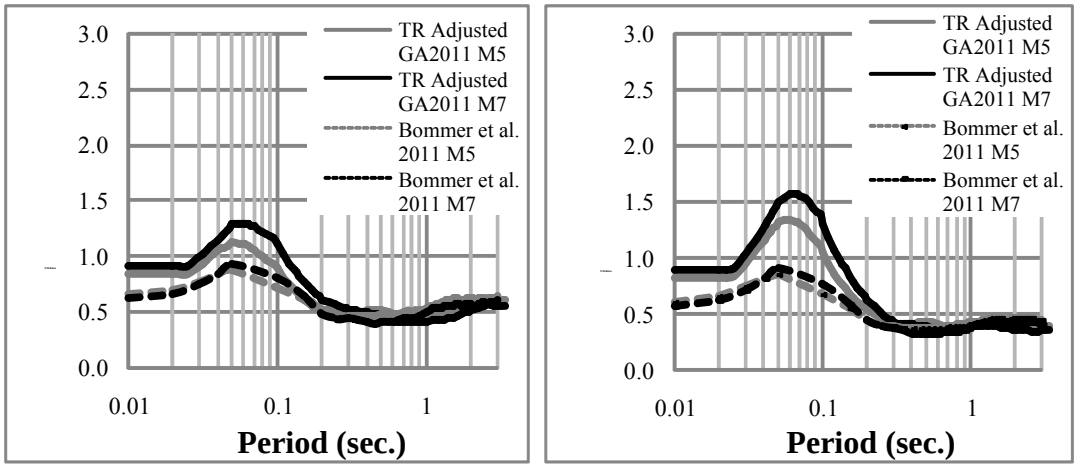

(a) **(b)**

Figure 3.19 Comparison of median spectral acceleration from the proposed model with the median spectral acceleration from the Bommer et al. (2011) model for vertical strike-slip earthquakes for Mw=7 and Rrup=5 km. (a) for rock, and (b) for soil.

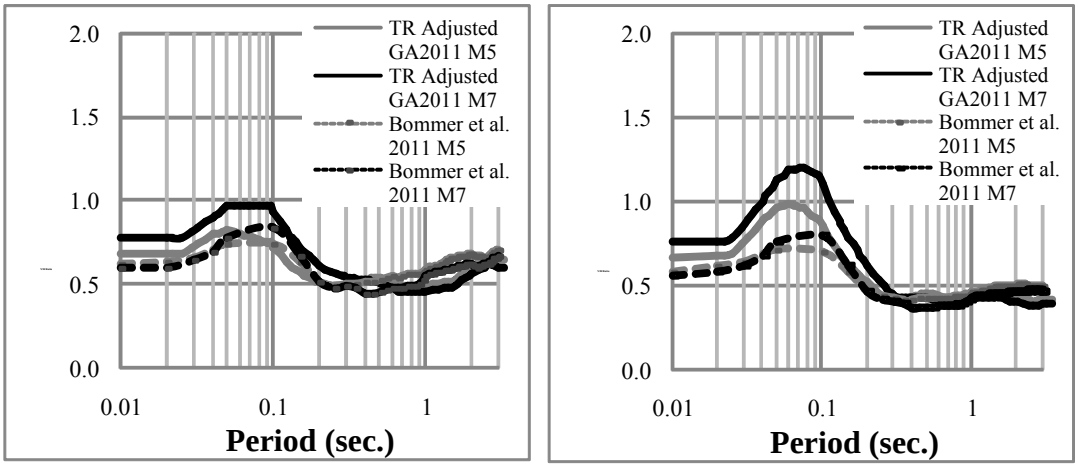

(a) **(b)**

Figure 3.20 Comparison of median spectral acceleration from the proposed model with the median spectral acceleration from the Bommer et al. (2011) model for vertical strike-slip earthquakes for Mw=7 and Rrup=30 km. (a) for rock, and (b) for soil.

The median response spectra of the TR-Adjusted GA2011 model are compared with the median response spectra of Bommer et al. (2011) model for the same scenarios as given in Figures 3.19 and 3.20, respectively. Predictions of the proposed mode is higher than the Bommer et al. (2011) model prediction for all scenarios, however the difference between both models increases at soil sites since the non-linear site response effects were not included in Bommer et al. (2011) model. Both models result in very similar V/H ratios for spectral periods longer than 0.3 seconds.

3.4 Recent Events in 2010 and 2011: Test Cases for Adjusted Model

An earthquake of M_W = 6.1 occurred in the Elazığ Region of Eastern Turkey on March 08, 2010. The earthquake was reported to be on the left-lateral strike-slip East Anatolian Fault, which is one of the two major active fault systems in Turkey. Table 3.3 presents the strong motion stations with the rupture distance of 200 km or smaller that recorded the mainshock. The closest station was 16 km away from the epicenter, while the remaining ones were at moderate to long distance away. The V_{S30} values of the recording stations and closest distance to co-seismic rupture plane (as given in Table 3.3) provided by Akkar et al. (2011) are adopted for calculating the model predictions of the Turkey-Adjusted GA2011 model.

Another destructive earthquake occurred on 20 kilometers north of Van City Center on October 23, 2011. The epicenter coordinates, depth and the moment magnitude of the earthquake disseminated by KOERI (Kandilli Observatory and Earthquake Research Institute), AFAD (General Directorate of Disaster Affairs), and USGS are slightly different, however with a moment magnitude larger than 7, Van-Tabanlı Earthquake is the third biggest magnitude earthquake recorded extensively in Turkey after the 1999 Kocaeli and Düzce Earthquakes. Focal mechanism solutions pointed out that the source of the activity is NE-SW oriented Van Fault with thrust fault mechanism (Emre et al., 2011). The strong motion stations with the rupture distance of 200 km or smaller that recorded the earthquake and V_{S30} values of the recording stations are provided in Table 3.3 (source: http://daphne.deprem.gov.tr). Again, the closest station was 20 kilometers away from the rupture plane therefore the near fault effects cannot be evaluated for this earthquake.

Table 3.3 Station ID numbers, rupture distances and VS30 values of the ground motion recording stations that recorded the mainshock of the recent 2010 Elazığ and 2011 Van Earthquakes.

EQ Name	Mw	SOF	Station ID	V_{S30} (m/s)	R_{JB} (km)	R_{RUP}(km)
Elazığ	6.1	Strike-Slip	3922	329	16	16
Elazığ	6.1	Strike-Slip	229	529	30	30
Elazığ	6.1	Strike-Slip	231	407	77	77
Elazığ	6.1	Strike-Slip	2540	356	89	89
Elazığ	6.1	Strike-Slip	3921	519	95	95
Elazığ	6.1	Strike-Slip	3923	709	171	171
Elazığ	6.1	Strike-Slip	2436	391	194	194
Van	7.1	Reverse	2912	293	0	20
Van	7.1	Reverse	3972	311	63	74
Van	7.1	Reverse	2541	652	75	77
Van	7.1	Reverse	2581	295	98	105
Van	7.1	Reverse	2514	315	130	135
Van	7.1	Reverse	3975	463	171	175
Van	7.1	Reverse	3974	450	186	188
Van	7.1	Reverse	2540	356	184	188

V/H ratios of the ground motions recorded during both earthquakes (only the mainshock) are computed for 6 spectral periods (0.01, 0.1, 0.2, 0.5, 1, and 2 seconds) using the processed records. The event terms of both earthquakes are shown in Figure 3.4 with grey squares for 2010-Elazığ and grey circles for 2011-Van events at PGA, T=0.2 and T=1 second spectral

periods. According to this figure, the event terms of both earthquakes are within reasonable limits when compared to the other earthquakes in the large magnitude range. The intra-event residuals at 0.2 seconds are plotted with respect to R_{RUP} and V_{S30} in Figure 3.21(a) and Figure 3.21(b), respectively. The distribution of intra-event residuals is also comparable with Figures 3.5 and 3.10, indicating no trend in the residuals of the Turkey-Adjusted GA2011 model. Finally, the distance scaling of the adjusted model is evaluated by plotting the model predictions (for both scenarios and V_{S30}=550 m/s) and actual V/H ratios of Elazığ and Van Earthquakes with respect to R_{RUP} at 0.01, 0.1, 0.2, 0.5, 1, and 2 seconds through Figure 3.22(a) to Figure 3.22(f).

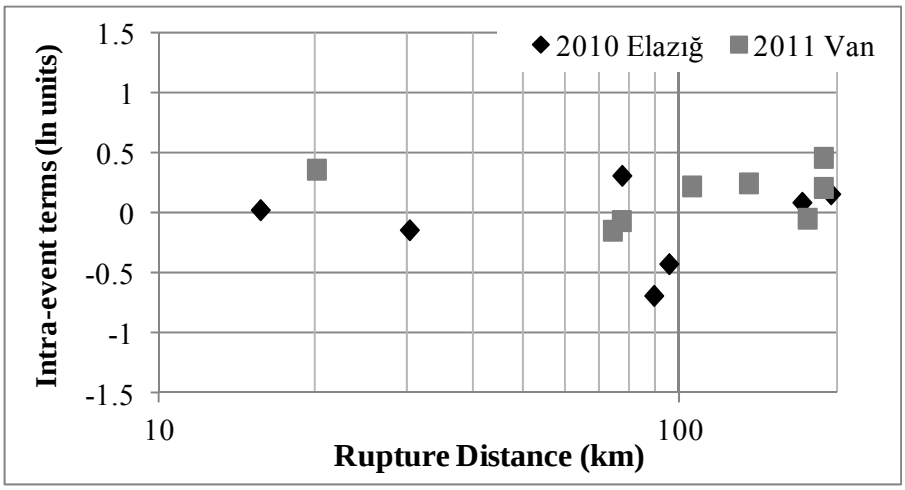

(a)

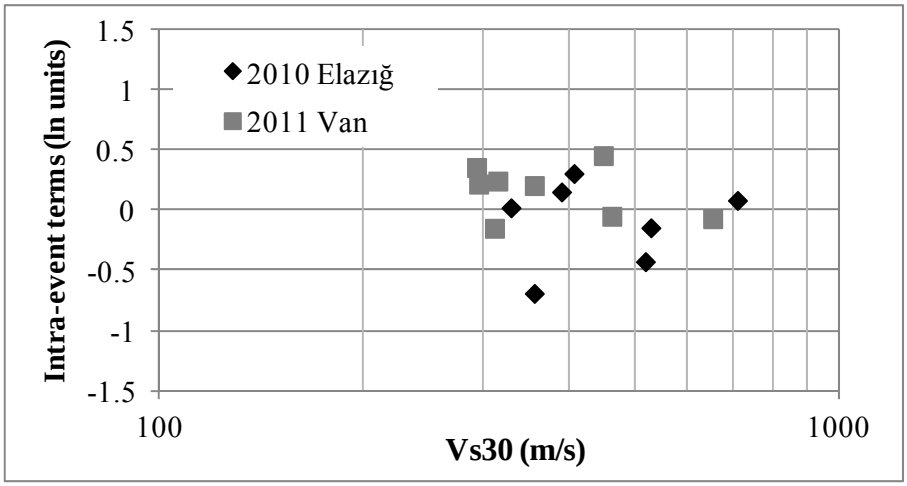

(b)

Figure 3.21 The intra-event residuals (in natural log units) of strong motions recorded in 2010 Elazığ and 2011 Van Earthquakes within 200 kilometers (a) with respect to rupture distance and (b) with respect to VS30.

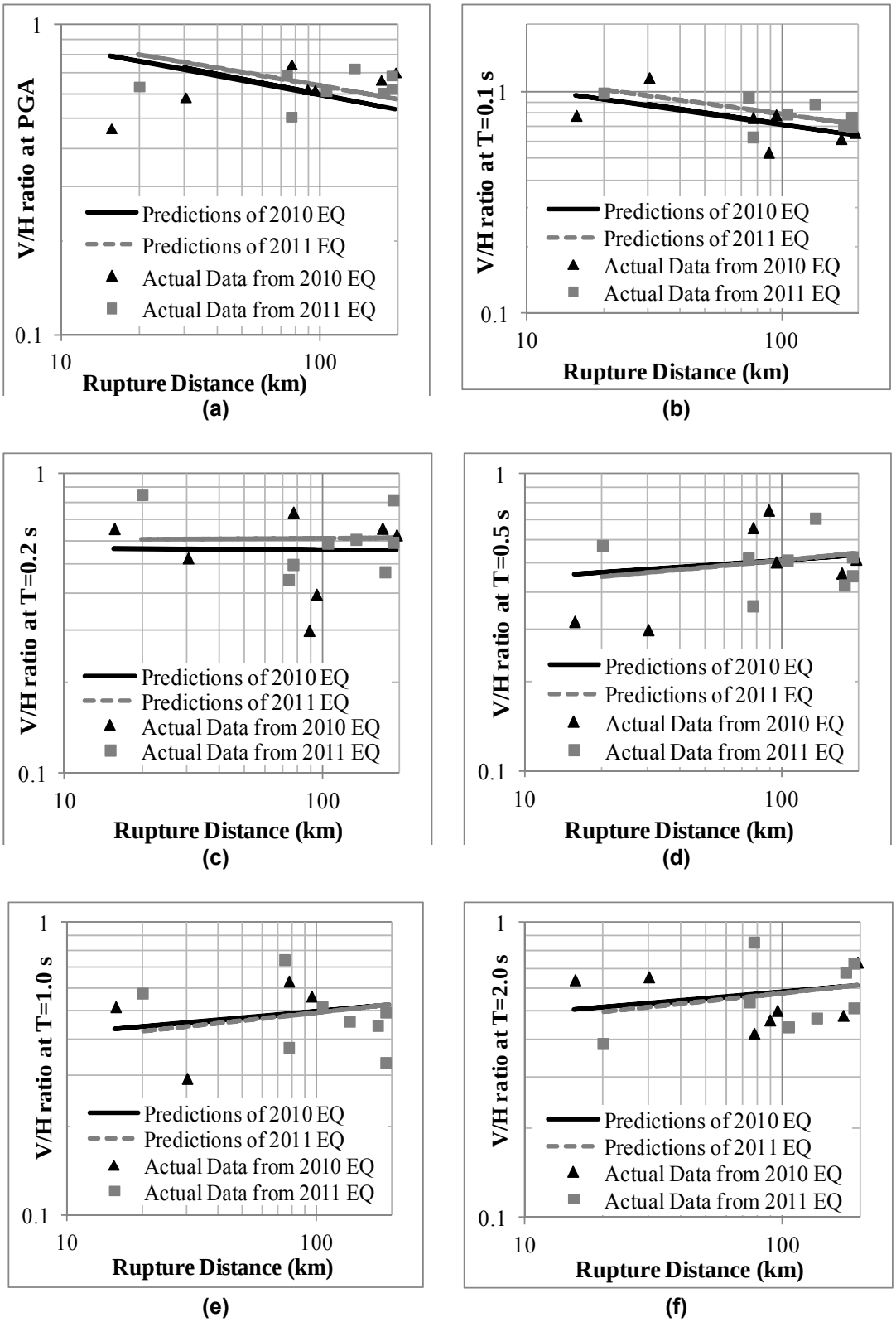

Figure 3.22 The normalized V/H ratio of the strong ground motions recorded during 2010 Elazığ and 2011 Van Earthquakes and TR-Adjusted GA2011 model predictions with respect to r at (a) PGA, (b) T=0.1 sec, (c) T=0.2 sec, (d) T=0.5 sec, (e) T=1 sec, and (f) T=2 sec.

The actual data shown in Figure 3.22 is centered at V_{S30}=550 m/s by the site effects scaling of the adjusted model and normalized by the event terms at that particular period. For short periods, there is a strong decrease in the V/H ratio predictions reflecting the more rapid attenuation of P-waves than S-waves. For long periods, the V/H ratio predictions are nearly independent of distance with slight increase at large distances. V/H ratio vs. R_{RUP} plots provided in Figure 3.22 show that the distance slope of the model is parallel to the distance slope of the actual data except for one case. The V/H ratios at PGA from 2010 Elazığ Earthquake (Figure 3.22(a)) increases with rupture distance as opposed to the model predictions, suggesting an error in the vertical component dataset since such trends were not observed in the horizontal component (Akkar et al., 2011).

CHAPTER 4

PRELIMINARY VERTICAL GROUND MOTION PREDICTION EQUATIONS FOR TURKEY

In addition to the regionalized V/H ratio model presented in Chapter 3, a preliminary vertical ground motion prediction equation for Turkey consistent with the preliminary vertical model based on NGA-W1 dataset developed by Yılmaz (2008) is developed for this study. Same dataset discussed at Chapter 3 is utilized; however the magnitudes are tentatively restricted to Mw ≥ 5.0 to emphasize the ground motions of engineering interests for the vertical ground motion component. The model is applicable to magnitudes 5-8.5, distances 0-200 km, and spectral periods of 0-10 sec. In place of generic site categories (soil and rock), the site is parameterized by average shear-wave velocity in the top 30 m (V_{S30}). Nonlinear site effects were not observed in the NGA-W1 vertical ground motion dataset (Yılmaz, 2008); therefore only linear site amplification is included for this preliminary effort. The standard deviation is magnitude dependent with smaller magnitudes leading to larger standard deviations. Within the contents of this chapter, the functional form of the attenuation model and the regression analysis are described in parallel to preliminary vertical model based on NGA-W1 dataset developed by Yılmaz (2008). Median predictions of the current model are compared the predictions of the only regional vertical model available, Kalkan and Gulkan (2004), in this chapter. Comparisons with Yilmaz (2008) model are not included since both models are in preliminary form and will be finalized at the end of this year. The vertical design spectra constructed by the models proposed in Chapter 3 and Chapter 4 is compared for the same scenarios in Chapter 5.

4.1 Model Form Development

While developing the functional form of the model, functional form used by preliminary vertical model developed by Yılmaz (2008) is taken as a starting point and is modified as needed based on the Turkish ground motion dataset. The general form of the model used by Yılmaz (2008) was given in Equation 4.1:

$$\ln Sa(g) = \begin{pmatrix} f_1(M, R_{rup}) + a_{12} \times F_{RV} + a_{13} \times F_N + a_{15} \times AS \\ + f_5(V_{s30}) + F_{HW} \times f_4(M, R_x, dip, Z_{top}, R_{JB}) \\ + F_{RV} \times f_6(Z_{top}) + (1 - F_{RV}) \times f_7(Z_{top}) + f_8(R_{rup}) \end{pmatrix} \quad (4.1)$$

Where:

- M = Moment magnitude,
- R_{rup} = rupture distance (km),
- R_{JB} = Joyner-Boore distance (km),
- R_x = horizontal distance from the top edge of the rupture on HW side (km) measured perpendicular to the strike of the fault,
- W = down-dip width of the rupture (km),
- Z_{top} = depth to the top of rupture (km),
- F_{RV} = 1 for reverse (150 > rake > 30) and 0 otherwise,
- F_N = 1 for normal (-120 < rake < 60) and 0 otherwise,
- F_{HW} = 1 for sites on the hanging wall side of the fault and 0 otherwise (the boundary between the FW and HW is defined by the vertical projection of the top of rupture. Dip = fault dip in degrees,

- V_{S30} = shear wave velocity over the top 30 m (m/s).

The tems f1, f4, f5, f6, f7, and f8 are provided through Equations 4.2-4.8:

$$f_1(M,R_{rup})=\begin{cases}a_1+a_4(M-c_1)+a_8(8.5-M)^2+\left[a_2+a_3(M-c_1)\right]\ln(R)\rightarrow for(M\le c_1)\\ a_1+a_5(M-c_1)+a_8(8.5-M)^2+\left[a_2+a_3(M-c_1)\right]\ln(R)\rightarrow for(M>c_1)\end{cases} \quad (4.2)$$

$$R=\sqrt{R_{rup}{}^2+c_4{}^2} \quad (4.3)$$

$$f_4(M,R_x,dip,Z_{top},R_{JB})=a_{14}\times T_1(R_{JB})\times T_2(R_x)\times T_3(R_x,Z_{top})\times T_4(M)\times T_5(dip) \quad (4.4)$$

$$f_5(V_{s30})=a_{10}\times\ln(\frac{V_{s30}}{V_{Lin}}) \quad (4.5)$$

$$f_6(Z_{top})=\begin{cases}0\rightarrow\ for(Z_{top}\le 2km)\\ a_{16}(\frac{Z_{top}-2}{3})\rightarrow\ for(2\le Z_{top}<5km)\\ a_{16}\rightarrow\ for(Z_{top}\ge 5km)\end{cases} \quad (4.6)$$

$$f_7(Z_{top})=\begin{cases}0\rightarrow\ for(Z_{top}\le 2km)\\ a_{17}(\frac{Z_{top}-2}{8})\rightarrow\ for(2\le Z_{top}<10km)\\ a_{17}\rightarrow\ for(Z_{top}\ge 10km)\end{cases} \quad (4.7)$$

$$f_8(R_{rup})=\begin{cases}0\rightarrow\ forR_{rup}<100km\\ a_{18}(R_{rup}-100)T_7(M)\rightarrow otherwise\end{cases} \quad (4.8)$$

The style-of-faulting factors for reverse and normal earthquakes were modeled by:

$$a_{12}\times F_{RV}+a_{13}\times F_{NM} \quad (4.9)$$

The data set includes a large number of aftershocks. A constant term is included for aftershocks where FAS is 1 for aftershocks and 0 otherwise:

$$f(AS)=a_{15}\times F_{AS} \quad (4.10)$$

Akkar et al. (2010) stated that nearly 60% of the records have strike-slip or normal type fault mechanisms and a small number, approximately 1% of the records have thrust or reverse-type fault mechanism in TSDM database. Since the number of ground motions recorded from reverse earthquakes is very small, the hanging wall term (f_4) cannot be constrained properly. Therefore, this term is removed and Equation 4.9 is modified into:

$$a_6\times F_{NM} \quad (4.11)$$

where F_N = 1 for normal (-120 < rake < 60) and 0 otherwise. Estimates of the depth to the top of the rupture in the Turkish ground motion dataset are not very reliable except for the 1999 Kocaeli and Düzce Earthquakes, therefore the terms represent the depth to top scaling

(f_6 and f_7) are removed from this preliminary model. Since the dataset is limited to distances up to 200 kilometers, the large distance (gamma) term (f_4) is not used. The final form of the preliminary vertical model is given by:

$$\ln Sa(g) = \left(f_1(M, R_{rup}) + f_5(V_{s30}) + a_6 \times F_N + a_9 \times AS \right) \quad (4.12)$$

where f_1 and f_5 are the base model and site amplification term as given in Equations 4.2 and 4.5.

4.2 Regression Methodology and Residuals

There are two commonly used regression methods to develop ground motion models that account for the correlation of the ground motions recorded in a single earthquake: two-step method and random-effects method. These two methods are described briefly below.

In the two-step method, the ground motions are first fit to a model in which each earthquake has its own constant term, ai:

$$\ln(Y_{ij}) = f_1(M_i, R_{ij}, V_{s30\,ij}) + \sum_{k=1}^{N_i} E_{ik} \times a_i + \varepsilon_{ij} \quad (4.13)$$

where Yij is the ground motion from the jth recording from the ith earthquake, Ni is the number of recordings from earthquake i, Eik is a dummy variable that equals 1 if i=k and zero otherwise. The ai's are the event terms and the εij are the intra-event residuals. The intra-event residuals represent the difference between the observed ground motion and the median ground motion at distance Rij for the ith event. In the second step, the event terms are then fit to a model that captures the additional magnitude dependence and any other dependence on the source properties such as style of faulting (F), depth to top (Ztop), and aftershock/mainshock class (AS):

$$a_i = f_2(M_i, F_i, Z_{top\,i}, AS_i) + \eta_i \quad (4.14)$$

where the ηi are the inter-event residuals. The inter-event residuals represent the difference between the average level of ground motion for an event and the expected level for that event given the M, F, Ztop and, AS.

In the random effects approach, the two error terms are considered at once:

$$\ln(Y_{ij}) = f_3(M_i, R_{ij}, V_{s30\,ij}, F_i, Z_{top\,i}, AS_i) + \eta_i + \varepsilon_{ij} \quad (4.15)$$

In this approach, there are no event terms, only inter-event residuals. Having two error terms precludes using ordinary least-squares, so the random-effects approach uses maximum likelihood. The regression is based on the random effect approach. The random-effects approach leads to two standard deviation terms: the inter-event standard deviation, □□, and the intra-event standard deviation, σ. The algorithm described in Abrahamson and Youngs (1992) is used for this study. This algorithm uses an iterative approach to finding the maximum likelihood solution. The steps are given below:

1. Set the inter-event residuals to zero: η_i=0
2. Subtract the estimate of the inter-event residual from the observed ground motion: $y_{ij}' = y_{ij} - \eta_i$
3. Estimate the coefficients, a_i, fitting the y_{ij}' using ordinary least-squares.
4. Compute the median ground motion, μ_{ij}, for each recording given the a_i
5. Given the median estimates (μ_{ij}), find the σ and τ by maximum likelihood (4.16)

6. Given the σ and τ, estimate the inter-event residuals, η_i (4.17)
7. Repeat steps 2-6 until the likelihood reaches a maximum.

The log likelihood function is given by:

$$LL=\left[\sum_{i=1}^{N_{eqk}}\sum_{j=1}^{N_i}\frac{(y_{i\,j}-\mu_{i\,j})}{2\sigma^2}\left((y_{i\,j}-\mu_{i\,j})-\frac{\rho S_i}{(1+N_i\rho)}\right)\right]-\left[\sum_{i=1}^{N_{eqk}}\sum_{j=1}^{N_i}\ln(\sigma^2+N_i\tau^2)+\ln(\sigma^2)(N_i-1\right] \quad (4.16)$$

Where $S_i=\sum_{i=1}^{N_i} y_{i\,j}-\mu_{i\,j}$ and $\rho=\frac{\tau^2}{\sigma^2}$.

Given the σ and τ, the maximum likelihood solution for the inter event residuals is given by:

$$\eta_i=\frac{\tau^2\sum_{j=1}^{N_i} y_{i\,j}-\mu_{i\,j}}{\sigma^2+N_i\tau^2} \quad (4.17)$$

If the standard deviations are not constant, then 4.16 is modified to use the mean value of σ and τ for each event. For just magnitude dependence, this is just σ(M) and τ(M).

To produce a model with a smooth spectrum, the coefficients were smoothed over several steps. This process is shown in Table 4.1. To avoid having poorly recorded earthquakes impacting the scaling with magnitude, depth and distance, only earthquakes with 3 or more recordings were used in the initial steps. In later steps, when these scaling parameters held fixed, the dataset used in the regression was expanded to include the poorly recorded earthquakes. The minimum number of recordings per event used in each step is indicated in the third column of Table 4.1.

In the first run, the linear magnitude scaling is determined just using the PGA. With my subset of data, which includes large magnitude events from Turkey, the available larger magnitude data lead to over-saturation if allowed. It was imposed a full saturation limit on the regression to be consistent with the horizontal component. In this run, only earthquakes with at least 5 recordings are used. This was done to allow the better recorded earthquakes to define the basic magnitude and distance. The three linear magnitude terms were estimated, with a break in the magnitude scaling at c_1=6.75 and c_4 = 6.8 which are same as that used by Yılmaz (2008). This constrained regression resulted in the following estimates of the coefficients for PGA:

a_3 = 0.2876; a_4 = 0.1066; a_5 = -0.5514

Table 4.1 Summary of Regression Analysis

Step No	N_{min}	Coefficients Estimated	Coefficients Held Fixed	σ, τ	Use of Results
1	3	a_1, a_2, a_3, a_4, a_5, a_6, a_7, a_8, a_9, a_{10}	c_1=6.75, c_4=6.8, a_5= -a_3 ln(c_4), a_8=0, a_6=0, a_7=0, a_9=0	constant	Fix a_3, a_4, a_5 (linear magnitude Scaling terms)
2	3	a_1, a_2, a_6, a_7, a_8, a_9, a_{10}	c_1=6.75, c_4=6.8, a_3, a_4, a_5 (fixed)	constant	Smooth a_8 and a_2
3	1	a_1, a_6, a_7, a_9, a_{10}	c_1=6.75, c_4=6.8, a_3, a_4, a_5, a_2, a_8(fixed)	constant	Smooth a_9
4	1	a_1, a_6, a_7, a_{10}	c_1=6.75, c_4=6.8, a_3, a_4, a_5, a_2, a_8,a_9(fixed)	constant	Smooth a_6
5	1	a_1, a_{10}	c_1=6.75, c_4=6.8, a_3, a_4, a_5, a_2, a_8,a_9, a_6(fixed)	constant	Smooth a_{10}
6	1	a_1	c_1=6.75, c_4=6.8, a_3, a_4, a_5, a_2, a_8,a_9, a_6,a_{10}(fixed)	constant	Smooth a_1
7	1	Standard Deviations	c_1=6.75, c_4=6.8, a_3, a_4, a_5, a_2, a_8,a_9, a_6, a_7, a_{10}, a_1(fixed)	magnitude dependent	Evaluate standard deviations and smooth s_1,s_2,s_3,s_4

After the first run, the quadratic magnitude scaling (a_8) and the logarithmic distance scaling coefficients (a_2) are then smoothed in second step. Two coefficients are smoothed in this step since they are not highly correlated. The a_2 and a_8 terms estimated from the regression are already fairly smooth, so very little smoothing is required. The period dependence of the estimated a_2 and a_8 terms are shown in Figures 4.1 and 4.2,respectively. The smoothed coefficients are shown also shown in Figures 4.1 and 4.2.

In the final steps (runs 3-7), the data set is expanded to include poorly recorded earthquakes by reducing the N_{min} from 3 to 1. The basic model for the magnitude and distance scaling is already fixed at this point. The distance scaling of aftershock events are smoothed at the end of run 3. The aftershock term, a_9, is also smoothed after Step 3 (Figure 4.3).

The style-of-faulting factor for normal earthquakes (a_6) is smoothed after Step 4. The period dependence of the estimated a_6 term is shown in Figure 4.4 and 4.5, respectively. For the normal earthquakes, the style-of-faulting factor (a_7) is fairly smooth and relatively small at short periods.

In Step 5, the linear site response term is smoothed. The period dependence of the a_{10} term and the smoothed values is shown in Figure 4.6. The estimates from the regression are very smooth so little smoothing is needed. The smoothed values are also shown below in Figure 4.6.

The period dependence of the resulting constant term, a_1, from the regression that included magnitude dependent standard deviations, is shown in Figure 4.7. By this stage, the constant term is very smooth. Minor smoothing is applied as shown in Figure 4.7.

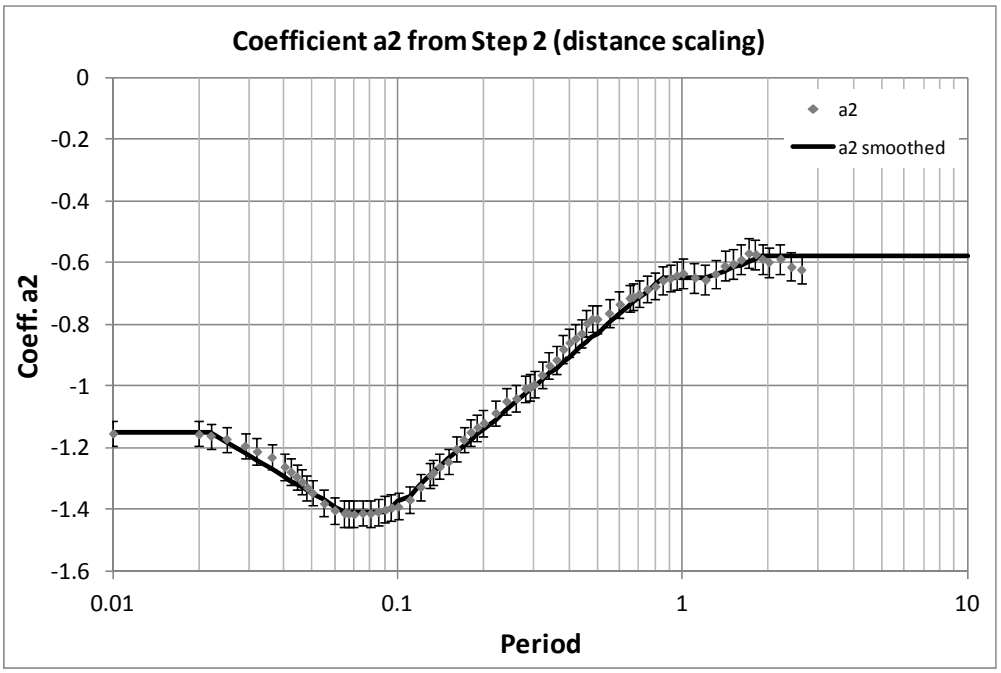

Figure 4.1 Smoothed a_2 from Step 2.

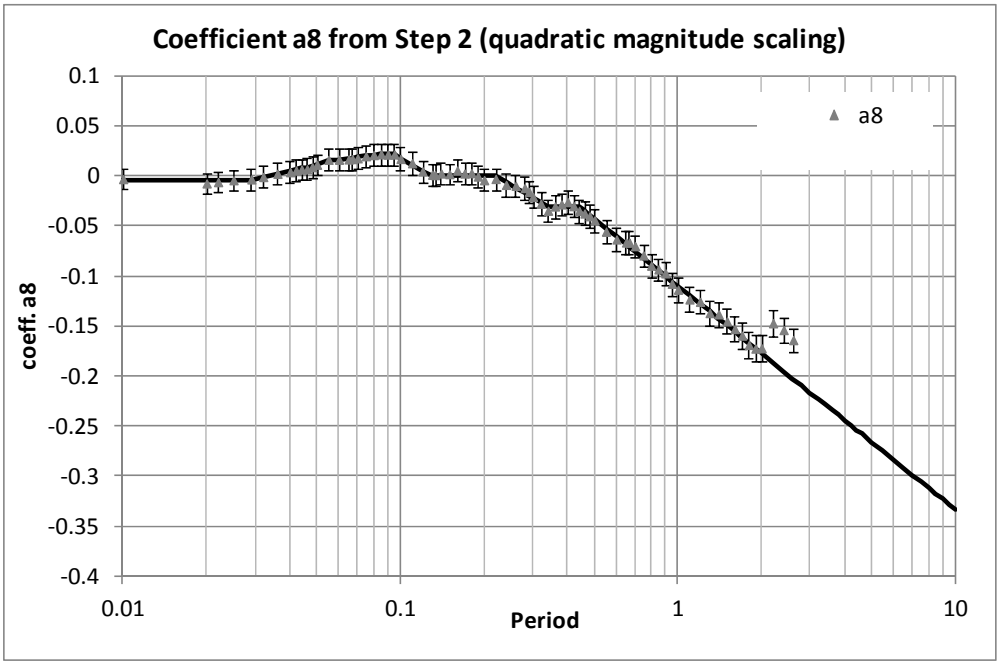

Figure 4.2 Smoothed a_8 from Step 2.

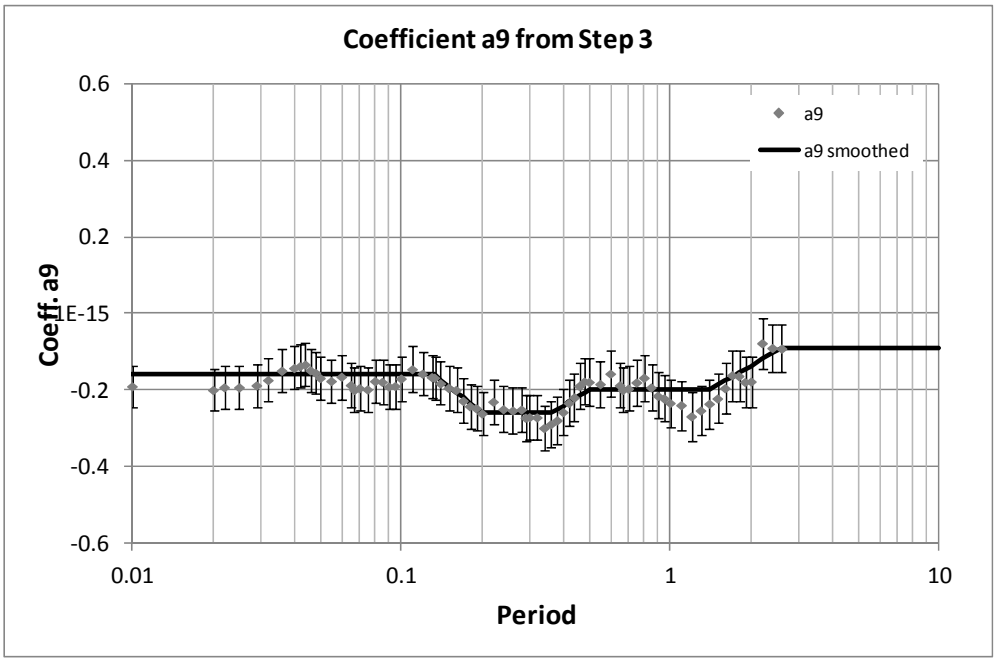

Figure 4.3 Smoothed a_9 from Step 3

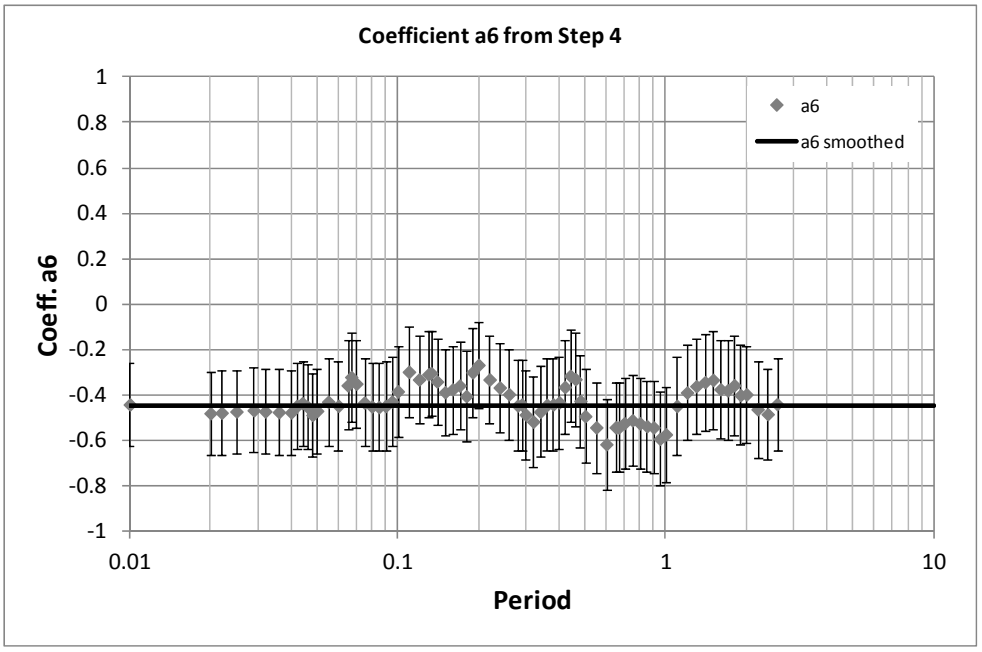

Figure 4.4 Smoothed a_6 from Step 4

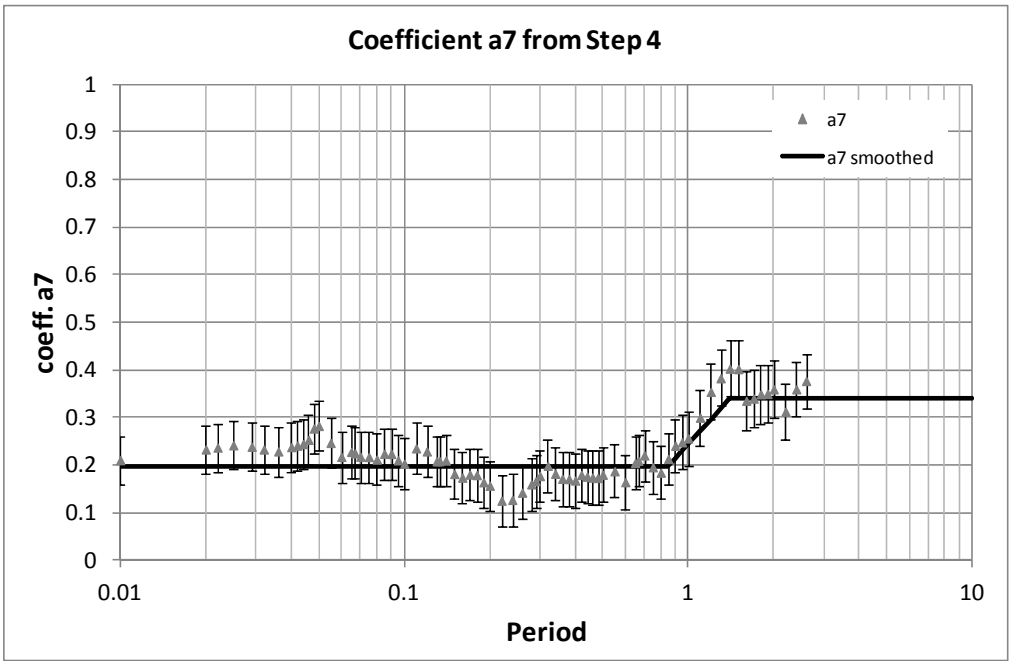

Figure 4.5 Smoothed a_6 from Step 4

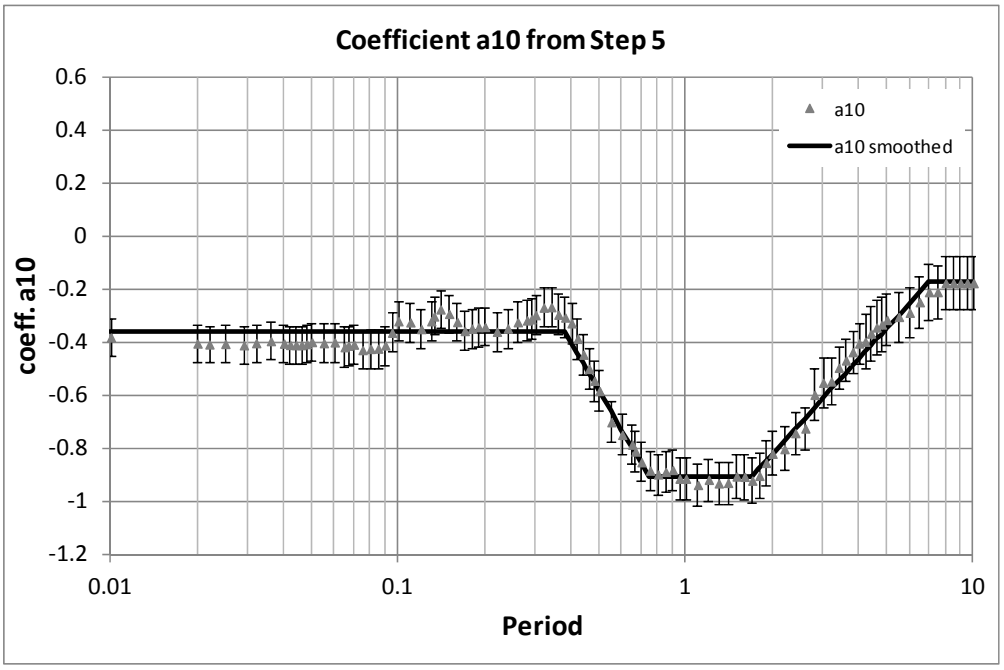

Figure 4.6 Smoothed a_{10} from Step 5

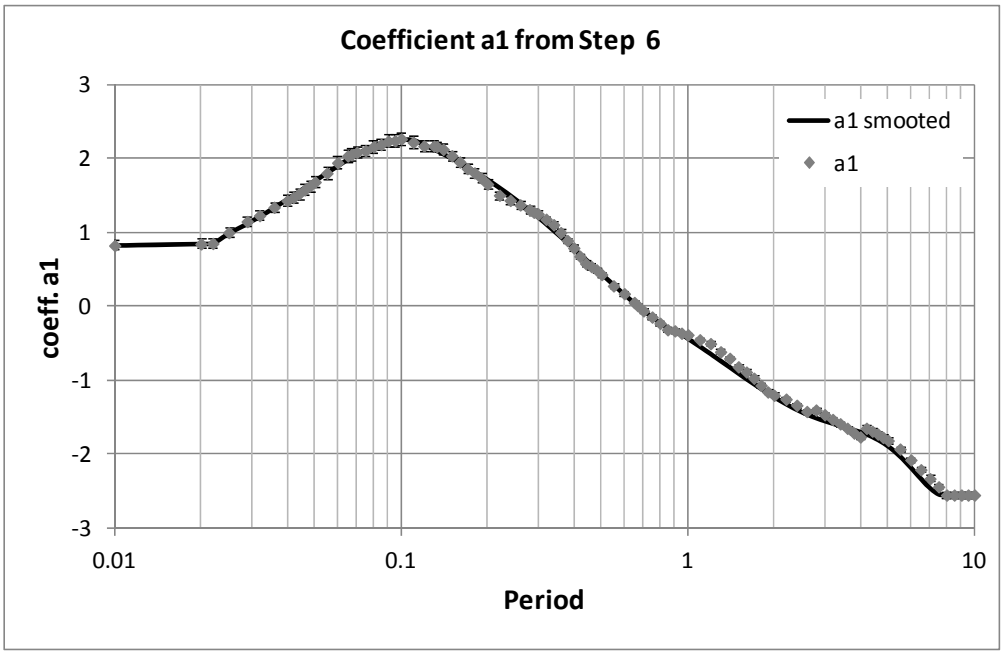

Figure 4.7 Smoothed a_1 from Step 6

The magnitude dependence of the standard deviation from the intra-event and inter-event residuals from Step 7 are evaluated for magnitude dependence by computing the standard deviation for 0.5 magnitude bins. The resulting magnitude dependence of the inter-event and intra-event standard deviations is shown in Figures 4.8 and 4.9, respectively. At short spectral periods, there is clear magnitude dependence for both the inter-event and intra-event standard deviations. This magnitude dependence was modeled by Yılmaz (2008) using a tri-linear model for both the intra-event standard deviation (σ) and the inter-event standard deviation (τ):

$$\sigma_0(M) = \begin{cases} s_1 \rightarrow for(M < 5) \\ s_1 + \dfrac{(s_2 - s_1)}{2} \times (M - 5) \rightarrow for(5 \le M \le 7) \\ s_2 \rightarrow for(M > 7) \end{cases} \quad (4.18)$$

$$\tau_0(M) = \begin{cases} s_3 \rightarrow for(M < 5) \\ s_3 + \dfrac{(s_4 - s_3)}{2} \times (M - 5) \rightarrow for(5 \le M \le 7) \\ s_4 \rightarrow for(M > 7) \end{cases} \quad (4.19)$$

In run 7, the regression is conducted using the magnitude dependent model of the inter-event and intra-event standard deviations given in Equations 4.18 and 4.19. The likelihood function given in Equation 4.16 is generalized to use a magnitude dependent σ and τ. In the final step, the intra-event and inter-event standard deviations are smoothed. The period dependence of the s_1 and s_2 terms for the intra-event standard deviation (equation 4.18) is shown in Figure 4.8. For short periods (T<1 sec), s_1 is larger than s_2, consistent with magnitude dependence seen in previous studies (e.g. Abrahamson and Silva, 1997). At periods greater than 1 seconds, the s_1 values are smaller than the s_2 values. Since there is a sharp drop in the number of recordings from small magnitude earthquakes with useable long periods beyond 1 seconds, it is considered that this trend seen at long periods is unreliable.

The period dependence of the s_3 and s_4 terms for the inter-event standard deviation (equation 4.13) is shown in Figure 4.9.

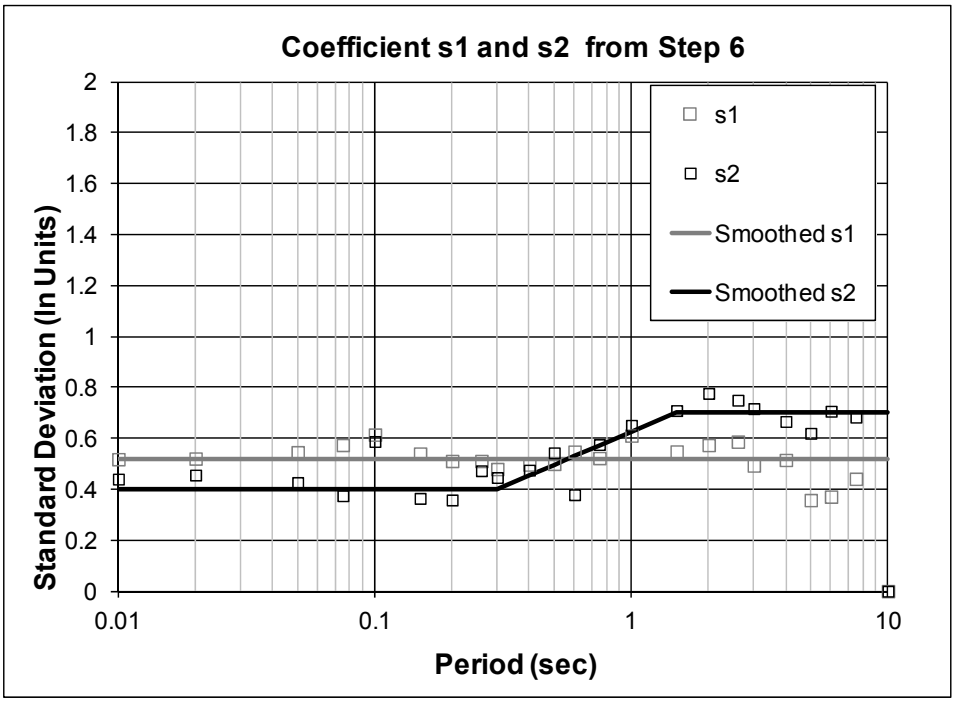

Figure 4.8 Smoothed Intra-event Standard Deviations from Step 7

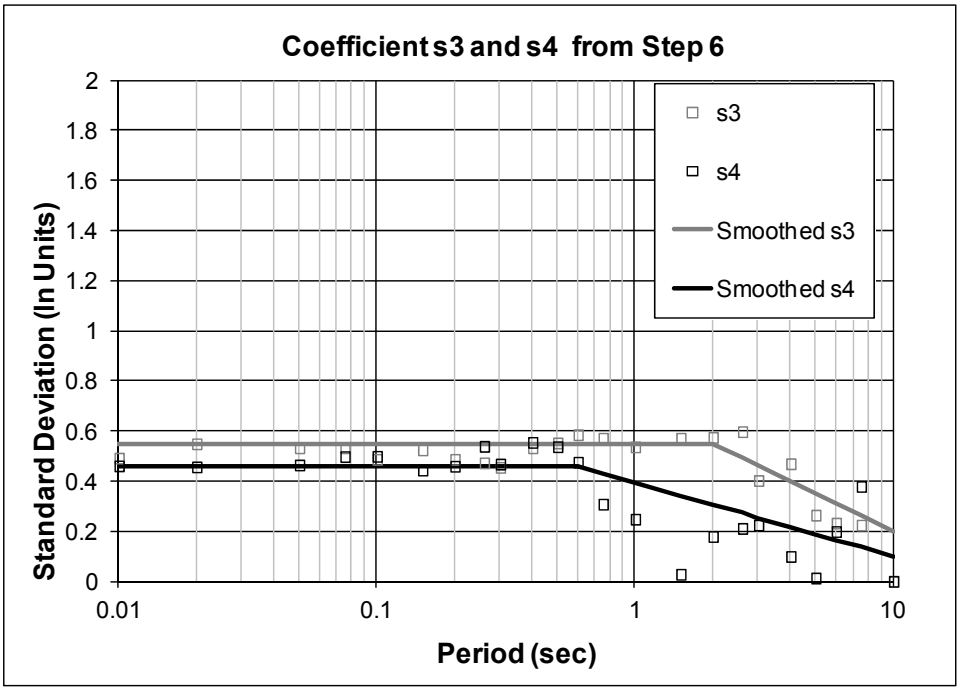

Figure 4.9 Smoothed Inter-event Standard Deviations from Step 7

4.3 Evaluation of Residuals

In this section, residuals from the regression analysis are shown as functions of all the main independent parameters to allow an evaluation of the model. The residuals are shown for PGA and spectral periods of 0.1, 0.2, 0.5, 1.0, and 2.0 seconds.

The inter-event and intra-event residuals are plotted as functions of magnitude, rupture distance and V_{S30} in Figure 4.10(a-c) to 4.15 (a-c) for PGA and spectral periods of 0.1, 0.2, 0.5, 1.0, and 2.0 seconds, respectively. At periods up to 5 seconds, the trends in the inter-event and intra-event residuals are similar. There is no magnitude, rupture distance and V_{S30} trend in the residuals.

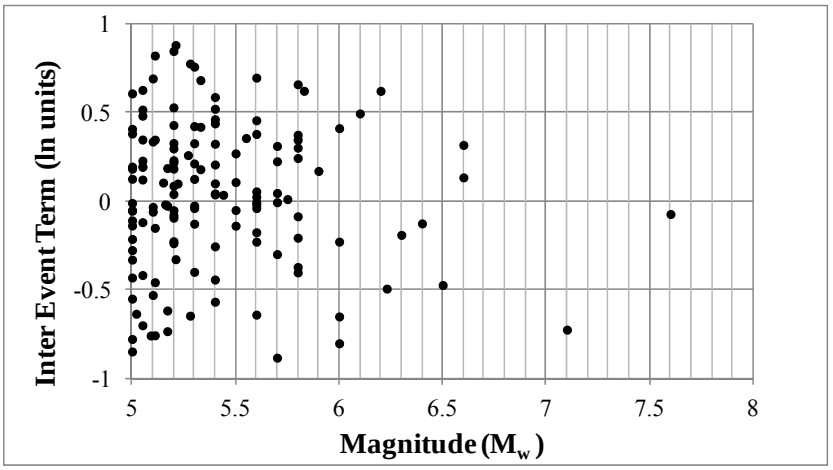

(a)

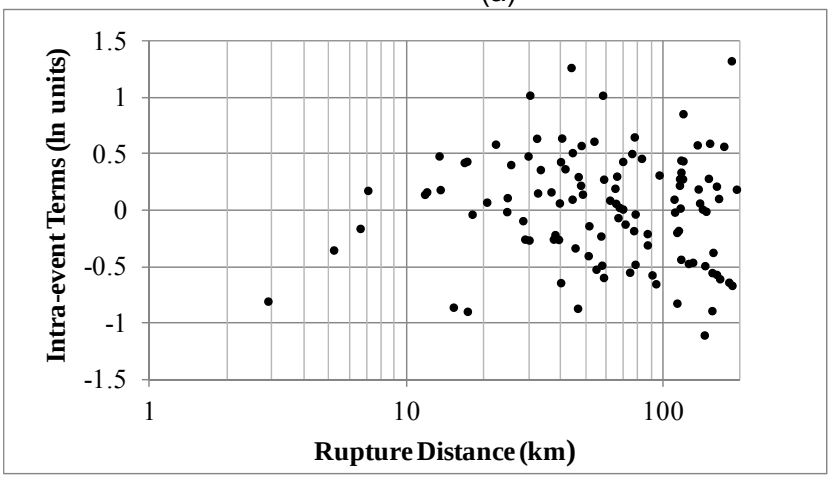

(b)

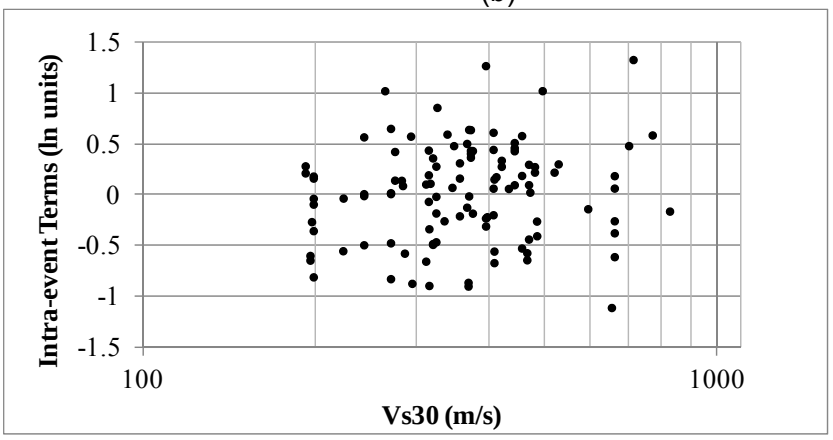

(c)

Figure 4.10 The model residuals in natural log units for PGA with respect to (a) magnitude (M_w), (b) rupture distance, and (c) average shear wave velocity at the top 30 meters.

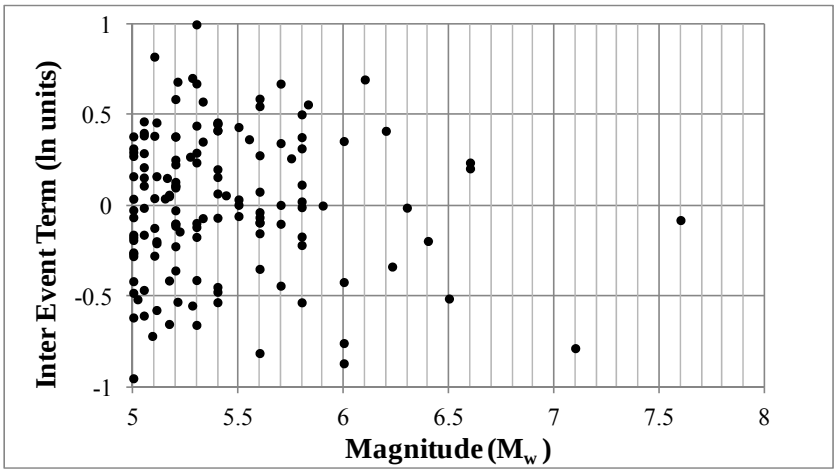

(a)

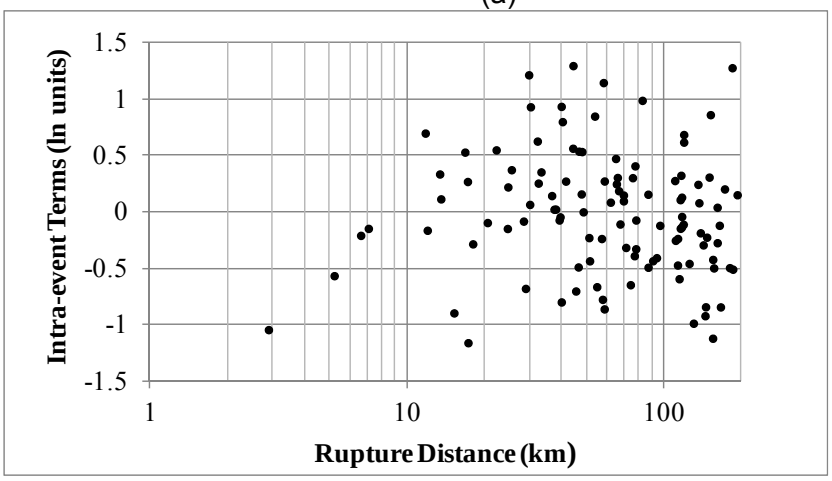

(b)

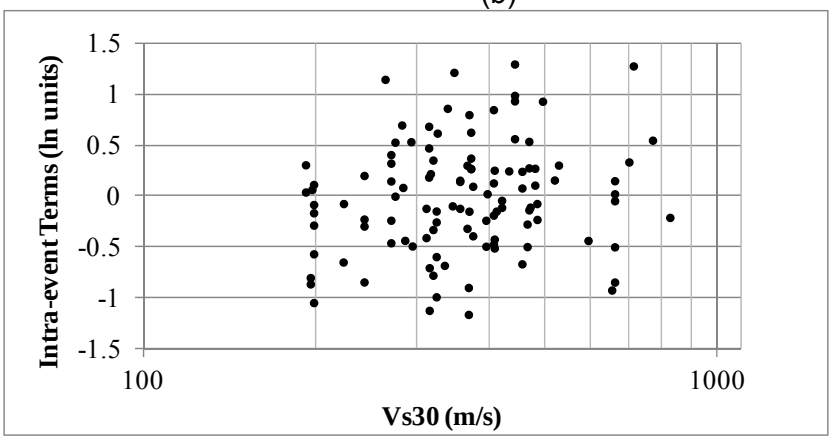

(c)

Figure 4.11 The model residuals in natural log units for 0.1 second spectral period with respect to (a) magnitude (M_w), (b) rupture distance, and (c) average shear wave velocity at the top 30 meters.

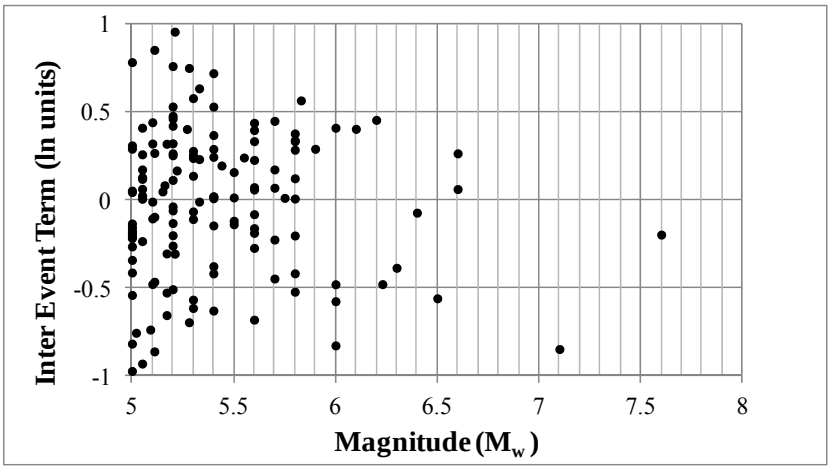

(a)

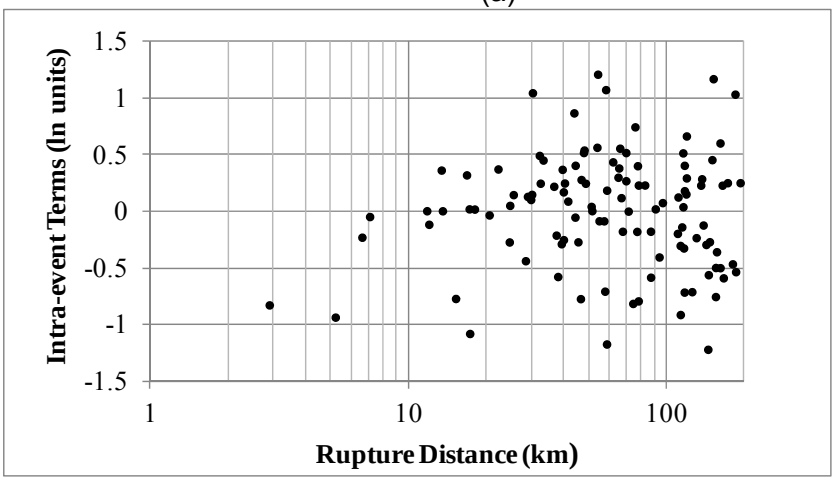

(b)

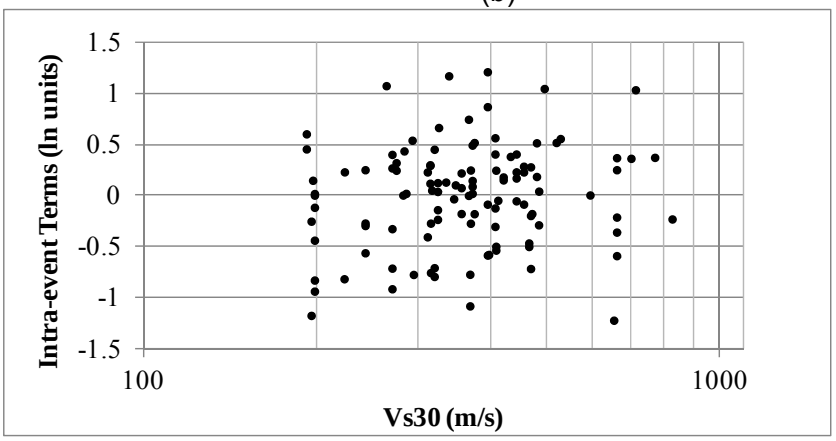

(c)

Figure 4.12 The model residuals in natural log units for 0.2 second spectral period with respect to (a) magnitude (M_w), (b) rupture distance, and (c) average shear wave velocity at the top 30 meters.

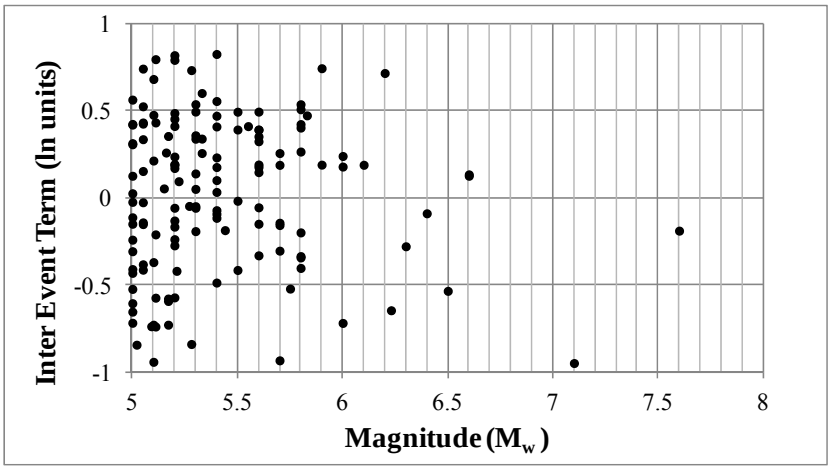

(a)

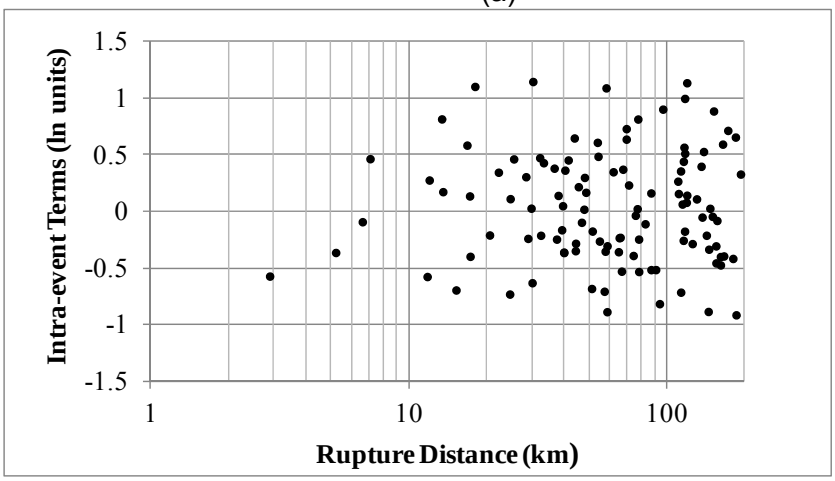

(b)

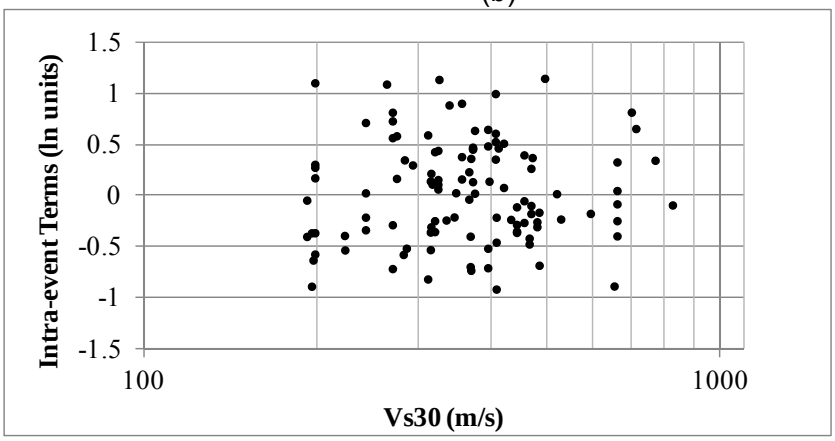

(c)

Figure 4.13 The model residuals in natural log units for 0.5 second spectral period with respect to (a) magnitude (M_w), (b) rupture distance, and (c) average shear wave velocity at the top 30 meters.

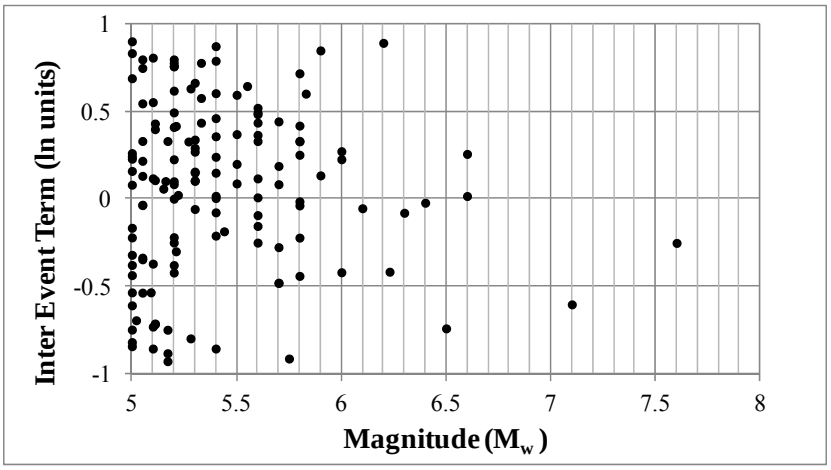

(a)

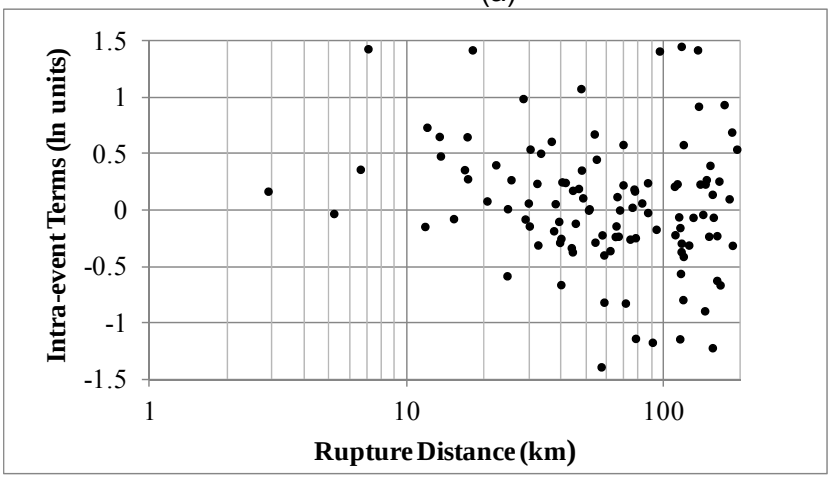

(b)

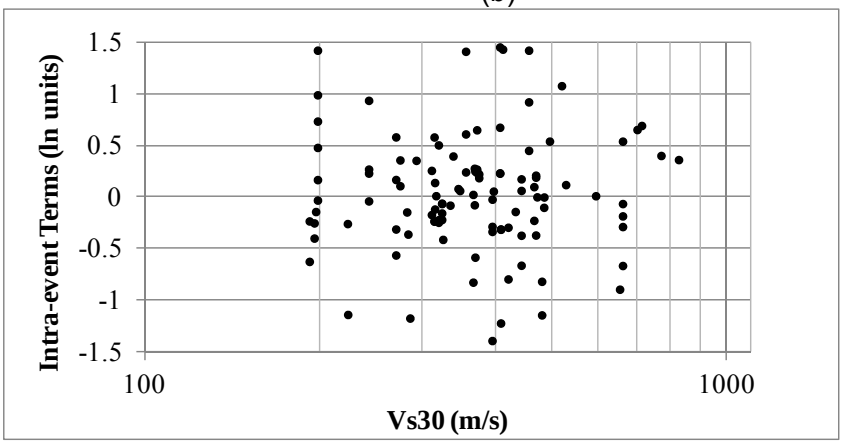

(c)

Figure 4.14 The model residuals in natural log units for 1.0 second spectral period with respect to (a) magnitude (M_w), (b) rupture distance, and (c) average shear wave velocity at the top 30 meters.

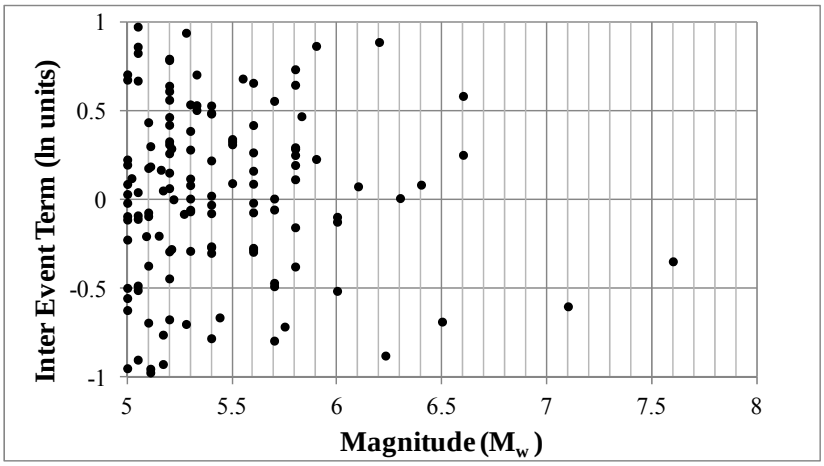

(a)

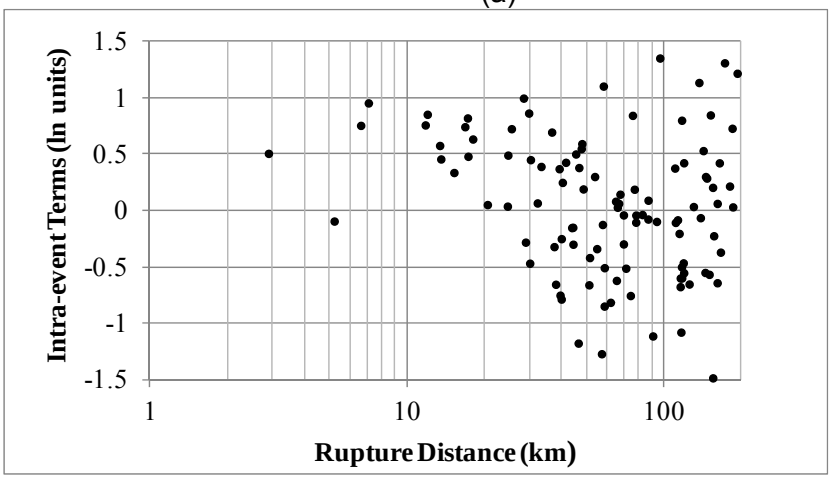

(b)

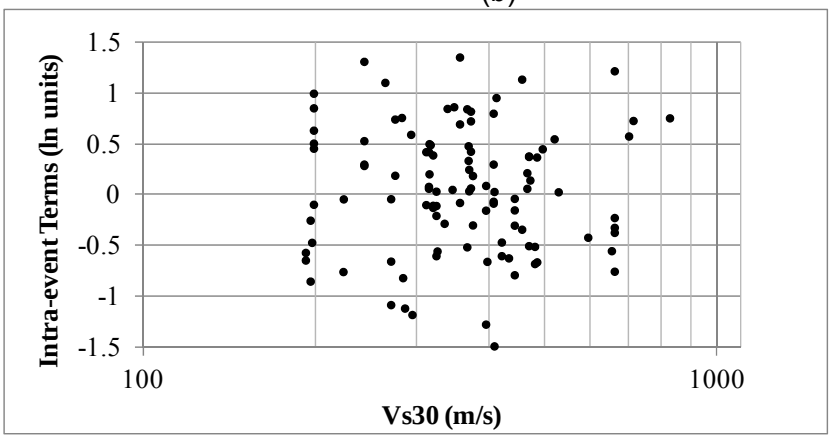

(c)

Figure 4.15 The model residuals in natural log units for 2.0 second spectral period with respect to (a) magnitude (M_w), (b) rupture distance, and (c) average shear wave velocity at the top 30 meters.

4.4 Final Model and Comparison with Kalkan and Gulkan (2004) Model

The resulting model for the median ground motion is given by:

$$\ln Sa(g) = \left(f_1(M, R_{rup}) + f_5(V_{s30}) + a_6 \times F_N + a_9 \times AS \right) \quad (4.20)$$

where M is moment magnitude, R_{rup} is rupture distance (km), F_N = 1 for normal (-120 < rake < 60) and 0 otherwise and V_{S30} is shear wave velocity over the top 30 m (m/s). The base form of the magnitude and distance dependence is given by:

$$f_1(M, R_{rup}) = \begin{cases} a_1 + a_4(M - c_1) + a_8(8.5 - M)^2 + \left[a_2 + a_3(M - c_1)\right] \ln(R) \rightarrow for(M \le c_1) \\ a_1 + a_5(M - c_1) + a_8(8.5 - M)^2 + \left[a_2 + a_3(M - c_1)\right] \ln(R) \rightarrow for(M > c_1) \end{cases} \quad (4.21)$$

Where $R = \sqrt{{R_{rup}}^2 + {c_4}^2}$

The V_{S30} dependence is given by:

$$f_5(V_{s30}) = a_{10} \times \ln\left(\frac{V_{s30}}{V_{Lin}}\right) \quad (4.22)$$

The intra-event standard deviation (σ) and the inter-event standard deviation (τ) are given by:

$$\sigma_0(M) = \begin{cases} s_1 \rightarrow for\,(M < 5) \\ s_1 + \dfrac{(s_2 - s_1)}{2} \times (M - 5) \rightarrow for\,(5 \le M \le 7) \\ s_2 \rightarrow for\,(M > 7) \end{cases} \quad (4.23)$$

$$\tau_0(M) = \begin{cases} s_3 \rightarrow for(M < 5) \\ s_3 + \dfrac{(s_4 - s_3)}{2} \times (M - 5) \rightarrow for(5 \le M \le 7) \\ s_4 \rightarrow for(M > 7) \end{cases} \quad (4.24)$$

$$\sigma = \sqrt{{\sigma_0}^2 + {\tau_0}^2} \quad (4.25)$$

The coefficients for the median ground motion models are listed in Table 4.2 and Table 4.3. The coefficients for the standard deviation model are listed in Table 4.4.

Table 4.2 Period Independent Coefficients for the Median Ground Motion

Coefficient	c_1	c_4	a_3	a_4	a_5
Value	6.75	6.8	0.2876	0.1066	-0.5515

Table 4.3 Coefficients for the Median Ground Motion

Period	a_1	a_2	a_6	a_7	a_8	a_9	a_{10}
0.01	0.827	-1.150	-0.450	0.195	-0.004	-0.160	-0.360
0.02	0.849	-1.150	-0.450	0.195	-0.004	-0.160	-0.360
0.022	0.855	-1.150	-0.450	0.195	-0.004	-0.160	-0.360
0.025	0.990	-1.181	-0.450	0.195	-0.004	-0.160	-0.360
0.029	1.123	-1.216	-0.450	0.195	-0.004	-0.160	-0.360
0.032	1.218	-1.240	-0.450	0.195	-0.001	-0.160	-0.360
0.036	1.338	-1.268	-0.450	0.195	0.003	-0.160	-0.360
0.04	1.451	-1.294	-0.450	0.195	0.006	-0.160	-0.360
0.042	1.505	-1.305	-0.450	0.195	0.008	-0.160	-0.360
0.044	1.557	-1.316	-0.450	0.195	0.009	-0.160	-0.360
0.046	1.607	-1.327	-0.450	0.195	0.011	-0.160	-0.360
0.048	1.655	-1.337	-0.450	0.195	0.012	-0.160	-0.360
0.05	1.701	-1.347	-0.450	0.195	0.013	-0.160	-0.360
0.055	1.809	-1.370	-0.450	0.195	0.016	-0.160	-0.360
0.06	1.905	-1.391	-0.450	0.195	0.016	-0.160	-0.360
0.065	1.989	-1.410	-0.450	0.195	0.018	-0.160	-0.360
0.067	2.020	-1.410	-0.450	0.195	0.018	-0.160	-0.360
0.07	2.062	-1.410	-0.450	0.195	0.019	-0.160	-0.360
0.075	2.124	-1.410	-0.450	0.195	0.020	-0.160	-0.360
0.08	2.174	-1.410	-0.450	0.195	0.021	-0.160	-0.360
0.085	2.212	-1.410	-0.450	0.195	0.022	-0.160	-0.360
0.09	2.239	-1.410	-0.450	0.195	0.022	-0.160	-0.360
0.095	2.254	-1.392	-0.450	0.195	0.022	-0.160	-0.360
0.1	2.258	-1.374	-0.450	0.195	0.018	-0.160	-0.360
0.11	2.254	-1.360	-0.450	0.195	0.012	-0.160	-0.360
0.12	2.190	-1.320	-0.450	0.195	0.006	-0.160	-0.360
0.13	2.127	-1.286	-0.450	0.195	0.000	-0.160	-0.360
0.133	2.109	-1.278	-0.450	0.195	0.000	-0.160	-0.360
0.14	2.066	-1.261	-0.450	0.195	0.000	-0.173	-0.360
0.15	2.005	-1.237	-0.450	0.195	0.000	-0.190	-0.360
0.16	1.946	-1.215	-0.450	0.195	0.000	-0.205	-0.360
0.17	1.887	-1.195	-0.450	0.195	0.000	-0.220	-0.360
0.18	1.830	-1.175	-0.450	0.195	0.000	-0.234	-0.360
0.19	1.773	-1.157	-0.450	0.195	0.000	-0.247	-0.360
0.2	1.717	-1.140	-0.450	0.195	0.000	-0.260	-0.360
0.22	1.608	-1.108	-0.450	0.195	0.000	-0.260	-0.360
0.24	1.503	-1.078	-0.450	0.195	-0.006	-0.260	-0.360
0.26	1.402	-1.051	-0.450	0.195	-0.012	-0.260	-0.360
0.28	1.304	-1.026	-0.450	0.195	-0.017	-0.260	-0.360
0.29	1.257	-1.014	-0.450	0.195	-0.019	-0.260	-0.360

Table 4.3 (continued) Coefficients for the Median Ground Motion

Period	a_1	a_2	a_6	a_7	a_8	a_9	a_{10}
0.3	1.210	-1.003	-0.450	0.195	-0.021	-0.260	-0.360
0.32	1.119	-0.981	-0.450	0.195	-0.026	-0.260	-0.360
0.34	1.031	-0.960	-0.450	0.195	-0.030	-0.260	-0.360
0.36	0.947	-0.941	-0.450	0.195	-0.030	-0.260	-0.360
0.38	0.865	-0.923	-0.450	0.195	-0.030	-0.250	-0.360
0.4	0.787	-0.905	-0.450	0.195	-0.030	-0.241	-0.401
0.42	0.712	-0.889	-0.450	0.195	-0.030	-0.232	-0.441
0.44	0.640	-0.873	-0.450	0.195	-0.030	-0.223	-0.479
0.46	0.571	-0.858	-0.450	0.195	-0.034	-0.215	-0.515
0.48	0.505	-0.843	-0.450	0.195	-0.038	-0.208	-0.549
0.5	0.442	-0.830	-0.450	0.195	-0.042	-0.200	-0.582
0.55	0.295	-0.797	-0.450	0.195	-0.052	-0.200	-0.659
0.6	0.164	-0.768	-0.450	0.195	-0.060	-0.200	-0.729
0.65	0.048	-0.741	-0.450	0.195	-0.068	-0.200	-0.794
0.667	0.012	-0.732	-0.450	0.195	-0.070	-0.200	-0.815
0.7	-0.054	-0.716	-0.450	0.195	-0.075	-0.200	-0.854
0.75	-0.143	-0.692	-0.450	0.195	-0.082	-0.200	-0.910
0.8	-0.221	-0.671	-0.450	0.195	-0.088	-0.200	-0.910
0.85	-0.287	-0.650	-0.450	0.195	-0.094	-0.200	-0.910
0.9	-0.344	-0.650	-0.450	0.212	-0.099	-0.200	-0.910
0.95	-0.375	-0.650	-0.450	0.227	-0.105	-0.200	-0.910
1	-0.431	-0.650	-0.450	0.242	-0.110	-0.200	-0.910
1.1	-0.538	-0.650	-0.450	0.270	-0.119	-0.200	-0.910
1.2	-0.639	-0.650	-0.450	0.295	-0.127	-0.200	-0.910
1.3	-0.733	-0.638	-0.450	0.319	-0.135	-0.200	-0.910
1.4	-0.820	-0.627	-0.450	0.340	-0.142	-0.200	-0.910
1.5	-0.902	-0.616	-0.450	0.340	-0.149	-0.188	-0.910
1.6	-0.977	-0.606	-0.450	0.340	-0.155	-0.176	-0.910
1.7	-1.047	-0.597	-0.450	0.340	-0.161	-0.166	-0.910
1.8	-1.111	-0.588	-0.450	0.340	-0.167	-0.155	-0.880
1.9	-1.170	-0.580	-0.450	0.340	-0.172	-0.146	-0.852
2	-1.223	-0.580	-0.450	0.340	-0.177	-0.137	-0.826
2.2	-1.317	-0.580	-0.450	0.340	-0.186	-0.120	-0.776
2.4	-1.394	-0.580	-0.450	0.340	-0.195	-0.104	-0.731
2.6	-1.456	-0.580	-0.450	0.340	-0.202	-0.090	-0.689
2.8	-1.507	-0.580	-0.450	0.340	-0.210	-0.090	-0.651
3	-1.549	-0.580	-0.450	0.340	-0.216	-0.090	-0.615
3.2	-1.584	-0.580	-0.450	0.340	-0.223	-0.090	-0.582
3.4	-1.614	-0.580	-0.450	0.340	-0.228	-0.090	-0.550
3.6	-1.642	-0.580	-0.450	0.340	-0.234	-0.090	-0.520

Table 4.3 (continued) Coefficients for the Median Ground Motion

Period	a_1	a_2	a_6	a_7	a_8	a_9	a_{10}
3.8	-1.669	-0.580	-0.450	0.340	-0.239	-0.090	-0.492
4	-1.697	-0.580	-0.450	0.340	-0.244	-0.090	-0.466
4.2	-1.728	-0.580	-0.450	0.340	-0.249	-0.090	-0.440
4.4	-1.762	-0.580	-0.450	0.340	-0.253	-0.090	-0.416
4.6	-1.799	-0.580	-0.450	0.340	-0.258	-0.090	-0.393
4.8	-1.842	-0.580	-0.450	0.340	-0.262	-0.090	-0.371
5	-1.889	-0.580	-0.450	0.340	-0.266	-0.090	-0.350
5.5	-2.025	-0.580	-0.450	0.340	-0.275	-0.090	-0.300
6	-2.177	-0.580	-0.450	0.340	-0.283	-0.090	-0.255
6.5	-2.328	-0.580	-0.450	0.340	-0.291	-0.090	-0.213
7	-2.455	-0.580	-0.450	0.340	-0.298	-0.090	-0.175
7.5	-2.538	-0.580	-0.450	0.340	-0.305	-0.090	-0.175
8	-2.550	-0.580	-0.450	0.340	-0.311	-0.090	-0.175
8.5	-2.550	-0.580	-0.450	0.340	-0.311	-0.090	-0.175
9	-2.550	-0.580	-0.450	0.340	-0.311	-0.090	-0.175
9.5	-2.550	-0.580	-0.450	0.340	-0.311	-0.090	-0.175
10	-2.550	-0.580	-0.450	0.340	-0.311	-0.090	-0.175

Table 4.4 Coefficients for the Standard Deviation

Period	s_1	s_2	s_3	s_4
0.01	0.450	0.330	0.230	0.150
0.02	0.450	0.330	0.230	0.150
0.022	0.450	0.330	0.230	0.150
0.025	0.450	0.330	0.230	0.150
0.029	0.450	0.330	0.230	0.150
0.032	0.450	0.330	0.230	0.150
0.036	0.450	0.336	0.230	0.150
0.04	0.450	0.341	0.230	0.150
0.042	0.450	0.343	0.230	0.150
0.044	0.450	0.345	0.230	0.150
0.046	0.450	0.347	0.230	0.150
0.048	0.450	0.349	0.230	0.150
0.05	0.450	0.351	0.230	0.150
0.055	0.450	0.356	0.230	0.150
0.06	0.450	0.360	0.230	0.150
0.065	0.450	0.363	0.230	0.150
0.067	0.450	0.365	0.230	0.150
0.07	0.450	0.367	0.230	0.150
0.075	0.450	0.370	0.230	0.150
0.08	0.450	0.373	0.230	0.150
0.085	0.450	0.376	0.230	0.150
0.09	0.450	0.379	0.230	0.150

Table 4.4 (continued) Coefficients for the Standard Deviation

0.095	0.450	0.381	0.230	0.150
0.1	0.450	0.384	0.230	0.150
0.11	0.450	0.388	0.230	0.150
0.12	0.450	0.392	0.230	0.150
0.13	0.450	0.396	0.230	0.150
0.133	0.450	0.397	0.230	0.150
0.14	0.450	0.400	0.230	0.150
0.15	0.450	0.403	0.230	0.150
0.16	0.450	0.406	0.230	0.150
0.17	0.450	0.409	0.230	0.150
0.18	0.450	0.411	0.230	0.150
0.19	0.450	0.414	0.230	0.150
0.2	0.450	0.416	0.230	0.150
0.22	0.450	0.421	0.230	0.150
0.24	0.450	0.425	0.230	0.150
0.26	0.450	0.429	0.230	0.150
0.28	0.450	0.432	0.230	0.150
0.29	0.450	0.434	0.230	0.150
0.3	0.450	0.436	0.230	0.150
0.32	0.450	0.439	0.230	0.150
0.34	0.450	0.441	0.230	0.150
0.36	0.450	0.444	0.230	0.150
0.38	0.450	0.447	0.230	0.150
0.4	0.450	0.449	0.230	0.150
0.42	0.450	0.451	0.230	0.150
0.44	0.450	0.454	0.230	0.150
0.46	0.450	0.456	0.230	0.150
0.48	0.450	0.458	0.230	0.150
0.5	0.450	0.460	0.230	0.150
0.55	0.450	0.464	0.230	0.150
0.6	0.450	0.468	0.230	0.150
0.65	0.450	0.472	0.230	0.150
0.667	0.450	0.473	0.230	0.150
0.7	0.450	0.475	0.230	0.150
0.75	0.450	0.479	0.237	0.150
0.8	0.450	0.482	0.244	0.150
0.85	0.450	0.485	0.250	0.150
0.9	0.450	0.487	0.256	0.150
0.95	0.450	0.490	0.261	0.150
1	0.450	0.492	0.266	0.150
1.1	0.450	0.497	0.276	0.150
1.2	0.450	0.501	0.285	0.150
1.3	0.450	0.505	0.293	0.150
1.4	0.450	0.508	0.300	0.150
1.5	0.450	0.511	0.307	0.150
1.6	0.468	0.514	0.314	0.150
1.7	0.486	0.517	0.320	0.150
1.8	0.502	0.520	0.326	0.150

Table 4.4 (continue) Coefficients for the Standard Deviation

1.9	0.518	0.520	0.331	0.150
2	0.532	0.520	0.337	0.150
2.2	0.559	0.520	0.346	0.165
2.4	0.584	0.520	0.355	0.178
2.6	0.607	0.520	0.363	0.191
2.8	0.628	0.520	0.371	0.202
3	0.648	0.520	0.378	0.213
3.2	0.666	0.520	0.384	0.223
3.4	0.684	0.520	0.390	0.232
3.6	0.700	0.520	0.396	0.241
3.8	0.700	0.520	0.402	0.250
4	0.700	0.520	0.407	0.258
4.2	0.700	0.520	0.412	0.265
4.4	0.700	0.520	0.417	0.272
4.6	0.700	0.520	0.421	0.279
4.8	0.700	0.520	0.425	0.286
5	0.700	0.520	0.430	0.292
5.5	0.700	0.520	0.439	0.307
6	0.700	0.520	0.448	0.321
6.5	0.700	0.520	0.456	0.333
7	0.700	0.520	0.464	0.345
7.5	0.700	0.520	0.471	0.355
8	0.700	0.520	0.477	0.365
8.5	0.700	0.520	0.483	0.375
9	0.700	0.520	0.489	0.384
9.5	0.700	0.520	0.495	0.392
10	0.700	0.520	0.500	0.400

The median spectral shapes of the proposed regional model are compared with the median spectral accelerations from Kalkan and Gulkan (2004) model for M5, M6, M7 and M8 strike slip earthquakes at rupture distance of 5 km for V_{S30}=760 m/s and V_{S30}=270 m/s in Figures 4.17 and 4.18, respectively. Similarly, median spectral acceleration of the same earthquake scenarios at a rupture distance of 30 km for V_{S30}=760 m/s and V_{S30}=270 m/s are presented in Figures 4.17 and 4.18, respectively. For all magnitude values, rock site curves are smaller than the soil site curves; however this difference is not very large since the non-linear site effects are not included in this preliminary model. In Figure 4.16, the models are in close agreement except for M7 curve, partly due to the full saturation of magnitude scaling in the proposed model. The model predictions are close to each other in Figure 4.17; a comprehensive evaluation of the misfit is hard to make since the full spectra of Kalkan Gulkan (2004) model is not available. Figures 4.18 and 4.19 indicates that the current model leads to smaller ground motions for M5 and M6, but almost equal to the Kalkan and Gulkan (2004) model predictions for M7 and M7. This difference can be explained by the bi-linear magnitude scaling applied in the current model with a hinge magnitude at 6.75.

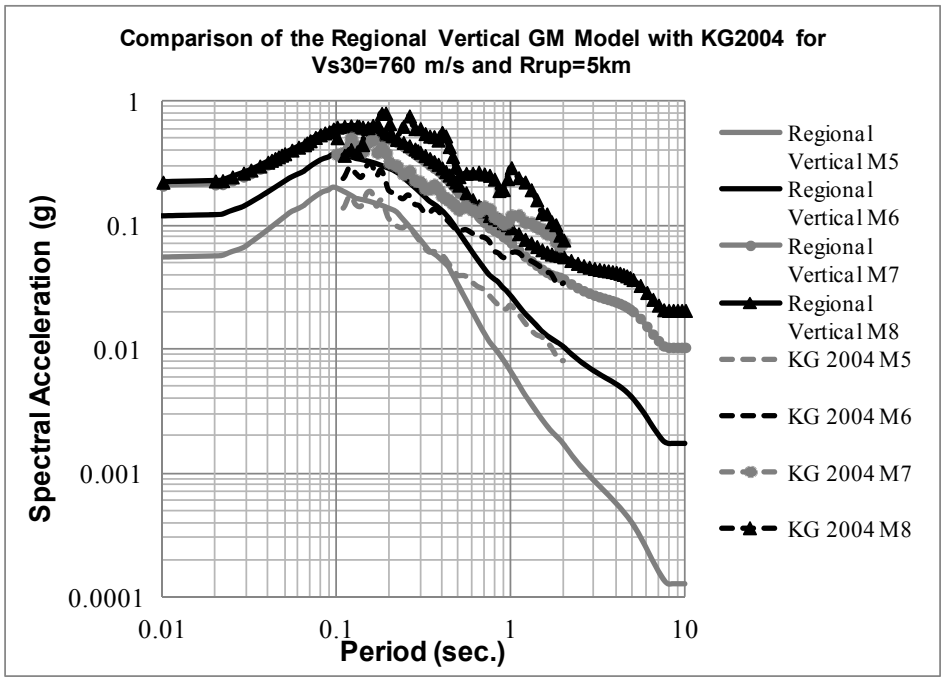

Figure 4.16 Comparison of the Median Spectral Acceleration for VS30=760 m/s from the Current Model with the Median from the Kalkan and Gülkan (2004) Model for Vertical Earthquakes at a Rupture Distance of 5 km.

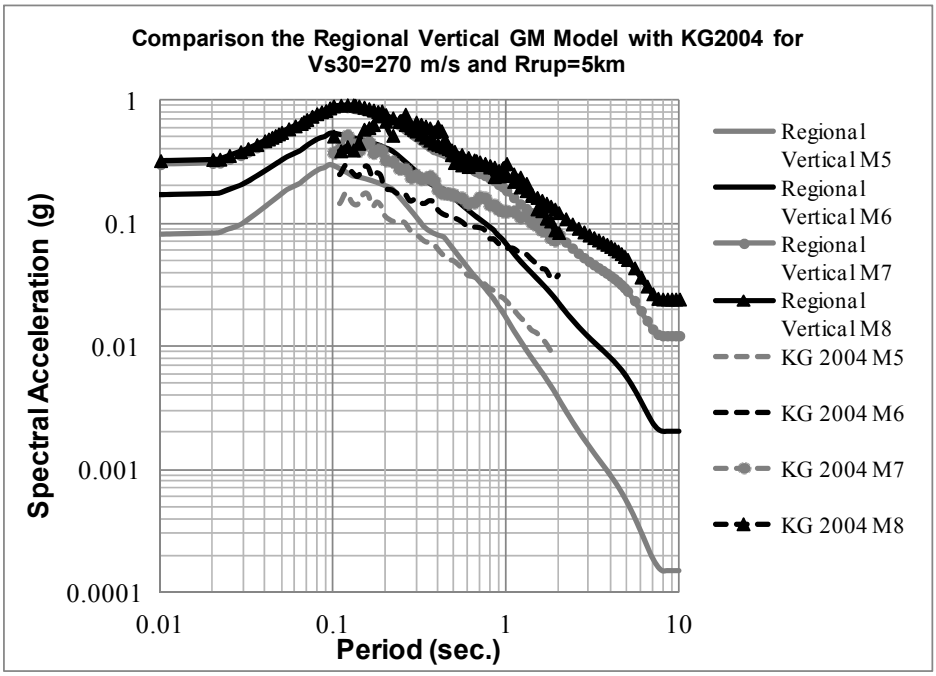

Figure 4.17 Comparison of the Median Spectral Acceleration for V_{S30}=270 m/s from the Current Model with the Median from the Kalkan and Gülkan (2004) Model for Vertical Earthquakes at a Rupture Distance of 5 km.

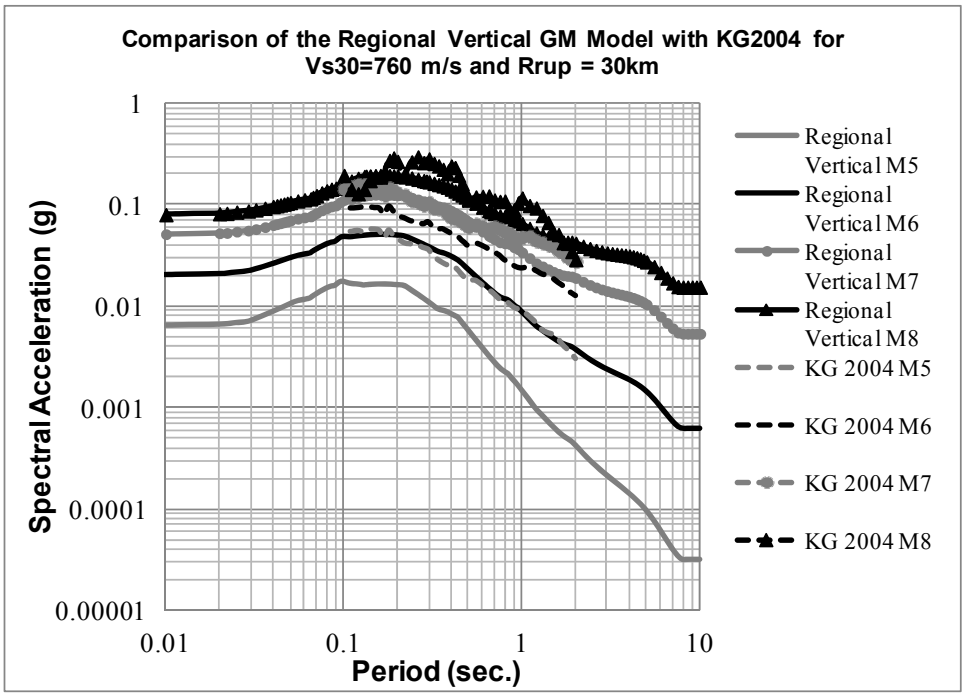

Figure 4.18 Comparison of the Median Spectral Acceleration for V_{S30}=760 m/s from the Current Model with the Median from the Kalkan and Gülkan (2004) Model for Vertical Earthquakes at a Rupture Distance of 30 km.

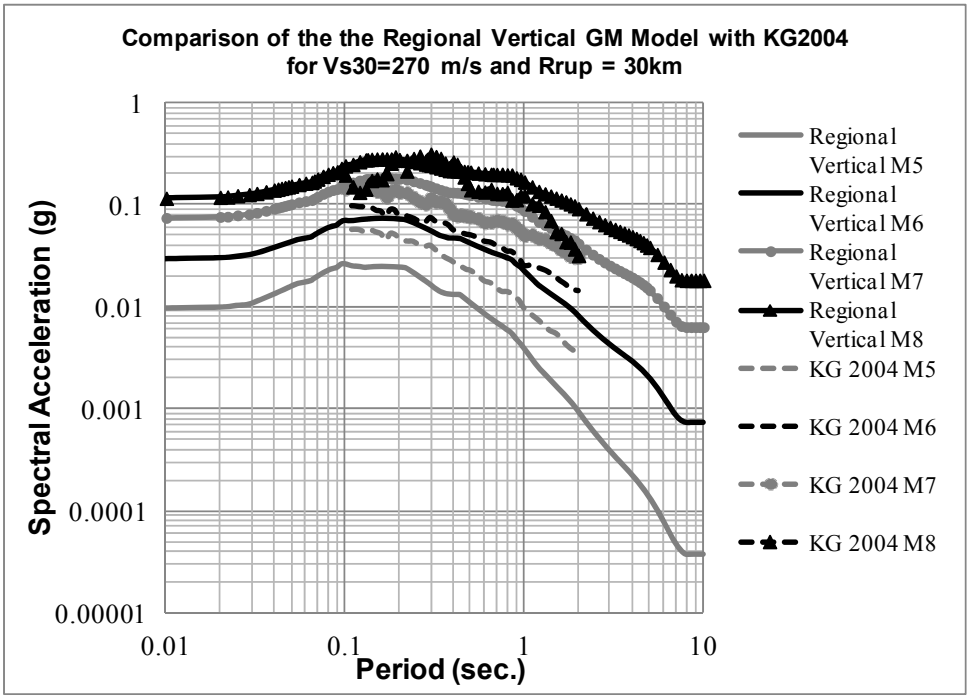

Figure 4.19 Comparison of the Median Spectral Acceleration for V_{S30}=270 m/s from the Current Model with the Median from the Kalkan and Gülkan (2004) Model for Vertical Earthquakes at a Rupture Distance of 30 km.

CHAPTER 5

SUMMARY AND CONCLUSION

The influence of the vertical component of an earthquake on the overall seismic response of regular structures is usually not considered. Some engineering guidelines in the United States recommend the use of a constant value of vertical to horizontal response ratio over the entire period range of engineering interest as V/H=2/3. In 1993, the Commission of the European Communities allowed V/H to vary with period in the European Building Code (EC8). The 1997 Uniform Building Code (UBC-97) recognized the fact that V/H is dependent on source-to-site distance at relatively short distances and recommended using site-specific vertical response spectra for sites located close to active faults; however, neither the UBC-97 nor the 2000 International Building Code (IBC-2000) offers guidance on how a general vertical design spectrum should be developed. The effect of vertical ground motions are not considered in the Turkish Earthquake Code (2007).

Site-specific vertical design spectra may be developed by computing the hazard independently for the vertical ground motion component in the probabilistic seismic hazard assessment (PSHA) environment. Evidently, performing PSHA for vertical design spectrum requires accurate prediction of vertical component ground motion intensity measures. However; new and updated vertical ground motion prediction equations (GMPEs) are not available for Western US or other active tectonic regions like Turkey. Along with the increase in the national strong motion network and acceleometric data, it has been attempted to develop regional attenuation models of horizontal ground motion component by several researchers for Turkey (Gülkan and Kalkan 2002, Ulusay et al. 2004, Özbey et al. 2004, Akkar and Cagnan 2010). Only one of these studies, the Gülkan and Kalkan (2002) model, has a consistent set of empirical attenuation relationships for predicting the vertical ground motion and the V/H ratio. Even after the comprehensive efforts on compiling the Turkish Strong Motion Database (Akkar et al., 2010), Kalkan and Gülkan (2004) model was not updated by its developers or any alternative regional vertical and V/H ratio ground motion prediction model were not proposed for Turkey.

In the first stage of this study, compatibility of recently proposed V/H ratio prediction equations by Gülerce and Abrahamson (2011) with the Turkish strong ground motion characteristics is evaluated using the comparison dataset of Gülerce et al. (2013) and an up-to-date alternative to the regional V/H ratio model by Kalkan and Gülkan (2004) is offered. The V/H ratio model developed by Gulerce and Abrahamson (2011) (GA2011) was based on the NGA-W1 database. Turkish strong ground motions may show a divergence from the V/H ratio model predictions, since only three earthquakes occurred in Turkey and 19 ground motions from these earthquakes were included in the GA2011 dataset. A vertical and V/H ratio strong motion database consistent with the prediction model parameters is developed by including the strong motion data from earthquakes occurred in Turkey with at least three recordings per earthquake. Final comparison dataset includes 1142 recordings from 288 events with the earthquake metadata, source to site distance metrics for the recordings, V_{s30} values for the recording stations, and spectral accelerations of the horizontal and vertical ground motion component.

The preferred methodology is the analysis of model residuals. Trends of the event terms with respect to moment magnitude and intra-event residuals with respect to rupture distance, V_{s30} and PGA_{1100} values are checked to evaluate the differences in the magnitude, distance, site amplification scaling between the Turkish V/H ratio comparison dataset and the GA2011 prediction model. Observations on the residual plots pointed out that:

- the magnitude scaling and distance scaling of the model is compatible with the comparison dataset,
- site amplification model is generally suitable (especially the non-linear effects piece), however the V/H ratios for stiff soil/rock sites in the comparison dataset are slightly miscalculated for a period range of 0.4-3 seconds,
- An average misfit from the actual data is present along the periods even after the V_{S30} adjustment.

The prediction model coefficients in the linear site amplification term (a_{10}) and the constant term (a_1) are modified by adding adjustment functions to the original model. The standard deviation model coefficients of the original GA2011 are found to be compatible with the standard deviations of the Turkey-Adjusted GA2011 model predictions and these values are not modified. Adjusting the global GA2011 model due to the regional tectonic characteristics instead of developing new model allowed us to keep the well-constrained features of the global datasets such as large magnitude - short distance scaling and non-linear site amplification effects while reflecting the regional ground motion characteristics.

The median response spectra of the TR-Adjusted GA2011 model are compared with the median predictions from the original GA2011 model and regional model for Turkey (KG 2004 model) for a range of scenarios. Median predictions from the Turkey-Adjusted GA2011 model are similar to the KG2004 curves but quite different than the original GA2011 model predictions, especially in the short period range due to the adjustments in the site effects and constant term parameters. This result is expected since the applicability range of KG2004 model is 0.1-2 seconds and the median curves are almost flatten out at these spectral periods. The performance of the adjusted model for predicting the ground motions from the recent events (2010 Elazığ and 2012 Van Earthquakes, which were not included in the comparison dataset) verified that; (i) the distance scaling of the model does not need any modifications, and (ii) the modified site amplification scaling of the model is compatible. Turkey-Adjusted GA2011 model is a suitable candidate V/H ratio model for probabilistic seismic hazard assessment studies conducted for vertical ground motions in Turkey.

In the second stage of this study, a set of preliminary regional vertical ground motion prediction equations consistent with the preliminary vertical model based on NGA-W1 dataset developed by Yılmaz (2008) is developed for Turkey. Same dataset used in adjusting the GA2011 V/H model is utilized; however the magnitudes are tentatively restricted to Mw ≥ 5.0 to emphasize the ground motions of engineering interests for the vertical ground motion component. The functional form used by preliminary vertical model developed by Yılmaz (2008) is taken as a starting point and modified as needed based on the Turkish ground motion dataset Following changes are made:

- Nearly 95% of the records have strike-slip or normal type fault mechanisms and a small number, approximately 1% of the records have thrust or reverse-type fault mechanism in Gulerce et al. (2013) database. Since the number of ground motions recorded from reverse earthquakes is very small, the hanging wall term cannot be constrained properly. Therefore this term is removed and the style of faulting piece of the Yilmaz (2008) model is modified.
- Estimates of the depth to the top of the rupture in the Turkish ground motion dataset are not very reliable except for the 1999 Kocaeli and Düzce Earthquakes, therefore the terms represent the depth to top scaling are removed from this preliminary model.
- Since the dataset is limited to distances up to 200 kilometers, the large distance (gamma) term is not used.

Proposed model is applicable to magnitudes 5-8.5, distances 0-200 km, and spectral periods of 0-10 sec. In place of generic site categories (soil and rock), the site is parameterized by average shear-wave velocity in the top 30 m (V_{S30}). Nonlinear site effects were not observed in the NGA-W1 vertical ground motion dataset (Yılmaz, 2008); therefore only linear site

amplification is included for this preliminary effort. The standard deviation is magnitude dependent with smaller magnitudes leading to larger standard deviations. The median spectral shapes of the proposed regional model are compared with the median spectral accelerations from Kalkan and Gulkan (2004) model however; comparisons with Yilmaz (2008) model are not included since both models are in preliminary form and will be finalized at the end of this year.

Finally, the site specific vertical design spectra constructed using the models proposed in Chapter 3 and Chapter 4 are compared for the scenarios listed in Table 5.1. To develop the site specific vertical design spectra, the TR-Adjusted GA2011 V/H median predictions are multiplied by the median predictions of equally weighted TR-Adjusted horizontal NGA-W1 models (Gulerce et al., 2013) (denoted by dashed lines in Figure 5.1 and 5.2). Solid lines represent the median predictions from the preliminary vertical model proposed in Chapter 4 for these scenarios.

Table 5.1 Different scenarios for the comparison of regional vertical and TR-Adjusted V/H ratio models

Scenario No	Magnitude	Distance (km)	V_{s30} (m/s)
1	5.0	5.0 km	270 m/s
2	5.0	5.0 km	760 m/s
3	5.0	30.0 km	270 m/s
4	5.0	30.0 km	760 m/s
5	7.0	5.0 km	270 m/s
6	7.0	5.0 km	760 m/s
7	7.0	30.0 km	270 m/s
8	7.0	30.0 km	760 m/s

Following interpretations are made based on Figures 5.1 and 5.2:

- For small magnitudes, the vertical spectral accelerations are small (almost negligible) as expected (Figure 5.1).
- Peak of the spectral acceleration curves is observed around 0.1 second whereas the peak is at 0.2 second for the horizontal ground motions. This difference shifts the peak of vertical spectral acceleration estimated using V/H ratio model between the periods of 0.1s and 0.2s (e.g. Scenario 5).
- For the soil sites, there is a small difference between the estimated spectral accelerations using the proposed vertical model directly and estimated accelerations using TR-Adjusted GA2011 V/H ratio model (e.g. Scenario 1 and 2). The reason for this small difference might be the site effects scaling adjustment applied to the V/H ratio model. Also, the preliminary vertical model does not include non-linear soil effects which might be updated in the final form.
- Both spectral shapes estimated using the proposed vertical model directly and estimated using the TR-Adjusted GA 2011 V/H ratio model are in good agreement at periods longer than 1 second.
- The largest differences are observed at 0.08s – 0.8s period range (e.g. Scenario 1)

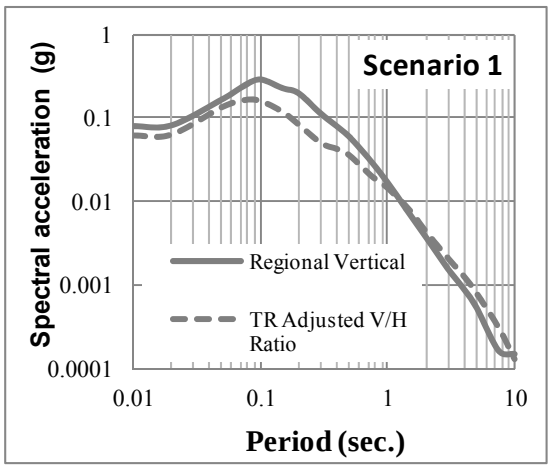

Scenario 1 : Magnitude **:** 5.0
Distance **:** 5.0 km
V_{s30} **:** 270 m/s

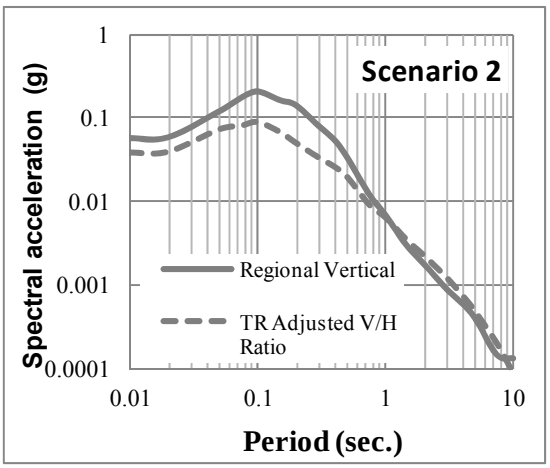

Scenario 2 : Magnitude **:** 5.0
Distance **:** 5.0 km
V_{s30} **:** 760 m/s

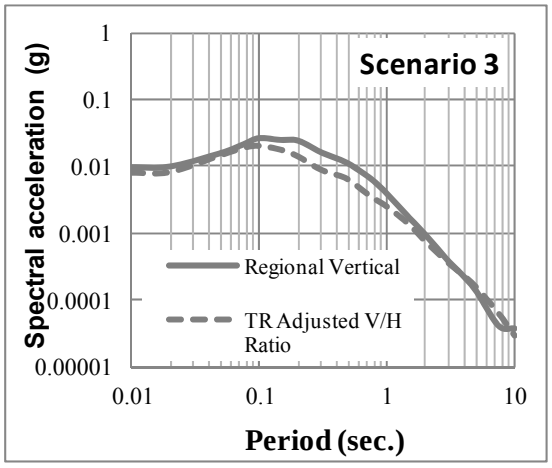

Scenario 3 : Magnitude **:** 5.0
Distance **:** 30.0 km
V_{s30} **:** 270 m/s

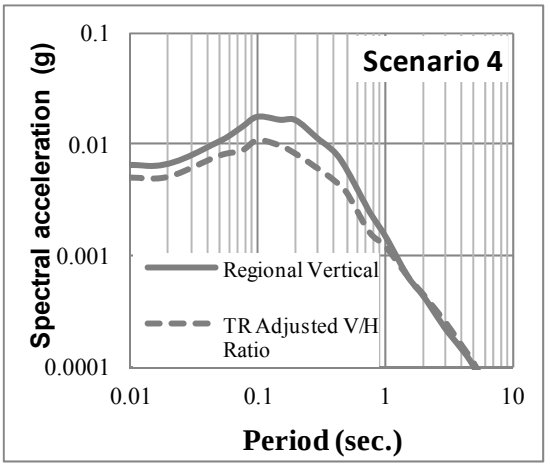

Scenario 4 : Magnitude **:** 5.0
Distance **:** 30.0 km
V_{s30} **:** 760 m/s

Figure 5.1 Comparisons of the median predictions of the preliminary vertical model and TR-Adjusted GA2011 V/H model from Scenarios 1 to 4.

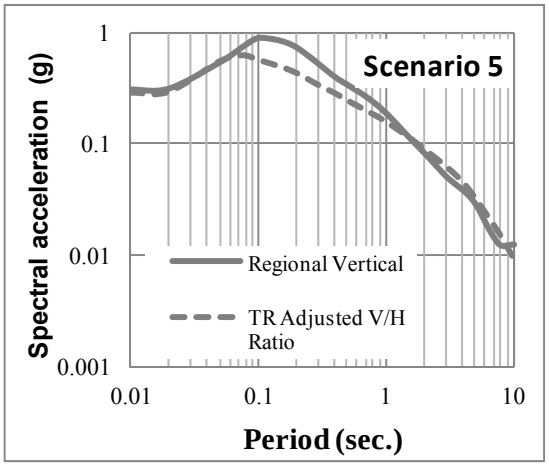

Scenario 5 : Magnitude : 7.0
Distance : 5.0 km
V_{s30} : 270 m/s

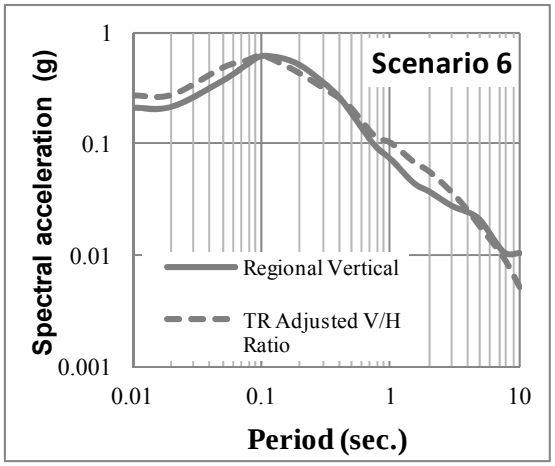

Scenario 6 : Magnitude : 7.0
Distance : 5.0 km
V_{s30} : 760 m/s

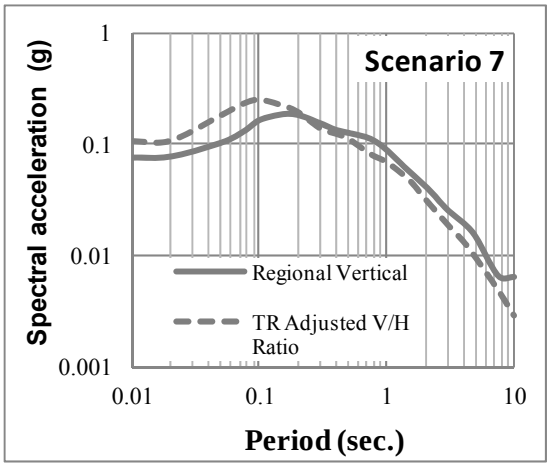

Scenario 7 : Magnitude : 7.0
Distance : 30.0 km
V_{s30} : 270 m/s

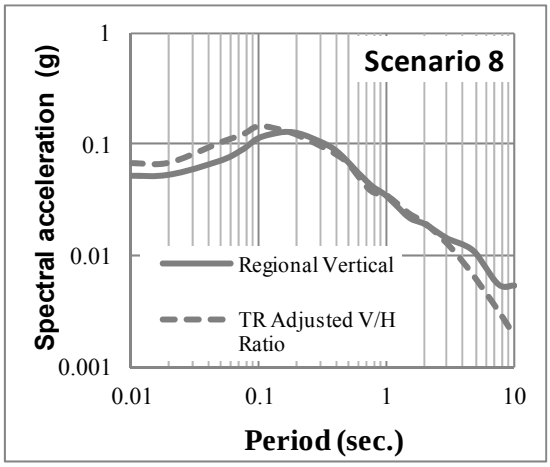

Scenario 8 : Magnitude : 7.0
Distance : 30.0 km
V_{s30} : 760 m/s

Figure 5.2 Comparisons of the median predictions of the preliminary vertical model and TR-Adjusted GA2011 V/H model from Scenarios 5 to 8.

The preliminary vertical model based on the Turkish dataset will be finalized in the short term in accordance with the NGA-W2 project vertical ground motion tasks. As first step toward this goal, a small magnitude piece will be added to the magnitude scaling by changing the base function into a tri-linear form. After this modification, the magnitude limit for the model will be lowered and the amount of the ground motions in the dataset will increase significantly. Recent efforts of NGA-W2 project vertical ground motion on the site amplification of vertical ground motions will be finalized soon. If a site amplification model for NGA-W2 vertical ground motion database is proposed, that model might also be included in the regional model after testing. Finally, the depth to top of the rupture effects was found to be significant by Yilmaz (2008) and adding a depth to the top of rupture function should be reconsidered.

After completing, both of these models will be incorporated in the hazard code HAZ39 (PG&E, 2010) for future scalar and vector-valued PSHA applications.

REFERENCES

Abrahamson, N. A. (2012). Personal communication.

Abrahamson, N. A., and Youngs, R. R., 1992. A stable algorithm for regression analyses using the random effects model, Bulletin of Seismological Society of America 82, 505-510.

Abrahamson, N. A., and Silva, W. J., (1997). Empirical response spectral attenuation relations for shallow crustal earthquakes, Seismological Research Letters 68, 94-127.

Abrahamson, N. A. and Silva, W. J. (2008). Summary of the Abrahamson & Silva NGA ground-motion relations. Earthquake Spectra. 24: 1, 67-97.

Akkar, S. and Cagnan, Z. (2010). A local ground-motion predictive model for Turkey and its comparison with other regional and global ground-motion models. Bulletin of the Seismological Society of America, 100, 2978-2995.

Akkar, S., Çağnan, Z., Yenier, E., Erdoğan, Ö., Sandıkkaya, A., Gülkan, P. (2010). The recently compiled Turkish strong motion database: preliminary investigation for seismological parameters. Journal of Seismology. 14, 457– 479.

Akkar, S., Aldemir, A., Askan, A., Bakır, S., Canbay, E., Demirel, İ. O., Erberik, M. A., Gülerce, Z., Gülkan, P., Kalkan, E., Prakash, S., Sandıkkaya, M. A., Sevilgen, V., Ugurhan, B., Yenier, E. (2011). 8 March 2010 Elazığ (Turkey) Earthquake: Observations on ground motions and building damage. Seismological Research Letters 82, 42-58.

Ambraseys, N. N., and Douglas, J., 2003. Near field horizontal and vertical earthquake ground motions, Soil Dynamics and Earthquake Engineering 23, 1-18.

Ambraseys, N. N., Douglas, J., Sarma, S. K., and Smit, P. M., 2005. Equations for the estimation of strong ground motions from shallow crustal earthquakes using data from Europe and the Middle East: vertical peak ground acceleration and spectral acceleration, Bulletin of Earthquake Engineering 3, 55-73.

Bindi, D., Luzi, L., Massa, M. and Pacor, F. (2009). Horizontal and Vertical Ground Motion Prediction Equations derived from the Italian Accelerometric Archive (ITACA). Bull Earthquake Engineering. 8: 6, 1209-1230.

Bommer, J.J., Akkar, S. and Kale, O. (2011). A Model for vertical-to-horizontal response spectral ratios for Europe and the Middle East. Bulletin of the Seismological Society of America. 101, 1783-1806.

Bozorgnia, Y. M., and Campbell, K. W. (2004). The vertical-to-horizontal response spectral ratio and tentative procedures for developing simplified V/H and vertical design spectra. Journal of Earthquake Engineering, 8, 175-207.

Campbell, K. W., 1997. Empirical near-source attenuation relationships for horizontal and vertical components of peak ground acceleration, peak ground velocity, and pseudo-absolute acceleration response spectra, Seismological Research Letters 68, 154–179.

Campbell, K. W., and Bozorgnia, Y., 2008. NGA ground motion model for the geometric mean horizontal component of PGA, PGV, PGD and 5% damped linear elastic response spectra for periods ranging from 0.01 to 10 s, Earthquake Spectra 24, 139–173.

Chiou, B., Darragh, R., Gregor, N. and Silva, W. (2008). NGA project strong motion database. Earthquake Spectra, 24, 23–44.

Edwards, B., Poggi, V. and Fäh, D. (2011). A predictive equation for the vertical-to-horizontal ratio of ground motion at rock sites based on shear-wave velocity profiles from Japan and Switzerland. Bulletin of the Seismological Society of America. 101, 2998–301.

Emre, Ö., Duman, T.Y., Özalp, S., and Elmacı, H. (2011). 23 Ekim 2011 Van Depremi saha gözlemleri ve kaynak faya ilişkin ön değerlendirmeler (in Turkish), MTA, Ankara.

Gülerce, Z. and Abrahamson, N. A. (2010). Vector-valued probabilistic seismic hazard assessment for the effects of vertical ground motions on the seismic response of highway bridges. Earthquake Spectra. 26, 999-1016.

Gülerce, Z., and Abrahamson, N.A. (2011). Site-specific design spectra for vertical ground motion. Earthquake Spectra. 27, 1023-1047.

Gülerce, Z., Erduran, E., Kunnath, S., and Abrahamson, N.A. (2012). Seismic demand models for probabilistic risk analysis of near fault vertical ground motion effects on ordinary highway bridges. Earthquake Engineering and Structural Dynamics, 41, 159-175.

Gülerce, Z., Kargioglu, B., and Abrahamson, N. A. (2013). Turkey-Adjusted NGA-W1 ground motion prediction models. In preparation for Earthquake Spectra.

Gülkan, P., Kalkan, E. (2002). Attenuation modelling of recent earthquakes in Turkey. Journal of Seismology, 6, 397 – 409.

Kalkan, E. and Gülkan, P. (2004). Site-dependent spectra derived from ground motion records in Turkey. *Earthquake Spectra*, 20, 1111–1138.

Newmark, N. M., and Hall, W. J. (1978). "Development of Criteria for Seismic Review of Selected Nuclear Power Plants," Report NUREG/ CR-0098, U.S. Nuclear Regulatory Commission, Rockville, MD.

Özbey C., Sari A., Manuel L., Erdik M., Fahjan Y. (2004). An empirical attenuation relationship for Northwestern Turkey ground motion using a random effects approach. Soil Dynamics and Earthquake Engineering, 24,115–25.

Sadigh, C. -Y., Chang, J., Egan, A., Makdisi, F., and Youngs, R. R., 1997. Attenuation relationships for shallow crustal earthquakes based on California strong motion data, Bulletin of the Seismological Society of America 68, 180-189.

Scasserra, G., Stewart, J. P., Bazzurro, P. Lanzo, G. and Mollaioli, F. (2009) A comparison of NGA ground-motion prediction equations to Italian data. *Bulletin of the Seis. Society of America. 99, 2961-2978.*

Stafford, P.J., Strasser, O. and Bommer, J.J. (2008). An evaluation of the applicability of the NGA models to ground-motion prediction in the Euro-Mediterranean region. Bulletin of Earthquake Engineering, 6, 149-177.

Yılmaz, Z., 2008 "Probailistic Seismic Hazard Assessment of the Effects of Vertical Ground Motions on the Seismic Response of Highway Bridges," Ph.D. Thesis, Department of Civil and Environmental Engineering, University of California Davis.